Mechanisms of retrograde transport from Golgi apparatus to endoplasmic reticulum

Yen-Ling Lian

▶ **To cite this version:**

Yen-Ling Lian. Mechanisms of retrograde transport from Golgi apparatus to endoplasmic reticulum. Cellular Biology. Université Paris sciences et lettres, 2022. English. NNT : 2022UPSLS067 . tel-04080838

HAL Id: tel-04080838

https://theses.hal.science/tel-04080838v1

Submitted on 25 Apr 2023

HAL is a multi-disciplinary open access archive for the deposit and dissemination of scientific research documents, whether they are published or not. The documents may come from teaching and research institutions in France or abroad, or from public or private research centers.

L'archive ouverte pluridisciplinaire **HAL**, est destinée au dépôt et à la diffusion de documents scientifiques de niveau recherche, publiés ou non, émanant des établissements d'enseignement et de recherche français ou étrangers, des laboratoires publics ou privés.

PSL
UNIVERSITÉ PARIS

THÈSE DE DOCTORAT
DE L'UNIVERSITÉ PSL

Laboratoire Biologie Cellulaire et Cancer, CNRS-UMR144, Institut Curie (Paris)
Équipe Dynamique de l'Organisation Intracellulaire

Mechanisms of retrograde transport from Golgi apparatus to endoplasmic reticulum
(Mécanismes du transport rétrograde entre l'appareil de Golgi et le reticulum endoplasmique)

Soutenue par
Yen-Ling LIAN
Le 20 Septembre 2022

Ecole doctorale n° 515
Complexité du vivant

Spécialité
Biologie Cellulaire

Composition du jury :

Frederic PINCET Professeur, ENS, Université PSL	*Président*
Francis BARR Professeur, Université d'Oxford	*Rapporteur*
Frederic BARD Directeur de recherche, CNRS, Aix-Marseille Université	*Rapporteur*
Stéphanie LEBRETON Chargée de recherche, Institut Pasteur	*Examinateur*
Franck PEREZ Directeur de recherche, CNRS, Institut Curie	*Membre Invité*
Gaëlle BONCOMPAIN Chargée de recherche, CNRS, Institut Curie	*Directeur de thèse*

institutCurie | PSL

Content

Abbreviation

RNA	Ribonucleic Acid
COPI/II	Coat Protein Complex I/II
DNA	Deoxyribonucleic Acid
ERGIC	Endoplasmic Reticulum-Golgi Intermediate Compartment
ER	Endoplasmic Reticulum
ERES	Endoplasmic Reticulum Exit Site
B4GalT1 (GalT)	β-1,4-Galactosyltransferase 1
GalNAc-T1 (GalNT1)	Polypeptide N-Acetylgalactosaminyltransferase 1
GDP	Guanosine Diphosphate
GEF	Guanine Exchange Factor
GFP	Green Fluorescent Protein
Glc	Glucose
GlcNAc	N-Acetylglucosamine
GPCR	G protein-coupled Receptor
GPI	Glycosylphosphatidyl Inositol
GTP	Guanosine TriPhosphate
Man:	Mannose
Man2A1 (ManII)	Mannosidase α-Class 2A Member 1
MHC	Major Histocompatibility Complex
MPR	Mannose-6-Phosphate Receptor
PA	Phosphatidic Acid
PI	Phosphatidylinositol
PI4P	Phosphatidylinositol 4-Phosphate
PS	Phosphatidylserine
RUSH	Retention Using Selective Hooks
SM	Sphingomyelin
SNARE	Soluble N-ethylmaleimide-sensitive Factor Attachment Proteins Receptor
ST6Gal1 (ST)	ST6 β-Galactoside α-2,6-Sialyltransferase 1
TGN	Trans-Golgi Network

Introduction

1. Cells are the fundamental units of life

Thanks to the development of glass lenses in the 17th century, Robert Hooke visualized the detailed structures of a piece of cork slices from a primitive microscope. In his book *Micrographia* published in 1665, he described the formation of tiny chambers within the cork, which he termed “cells” (Hooke and Jo. Martyn and Ja. Allestry., 1665). In the following 200 years, developments in light microscopy enabled the visualization of cells in ever greater details. The birth of cell biology (a.k.a cell theory) as a recognized subject emerges from two publications by Matthias Schleiden in 1838 and Theodor Schwann in 1839 (Schleiden, 1838; Schwann and Hünseler, 1839). Rudolf Virchow also added one of the tenets to cell theory and in 1855 concluded: 1) All living organisms are composed of one or more cells. 2) The cell is a basic unit of structure, physiology, and organization. 3) All cells come from the pre-existing cells. To date, high-end technology allows us to observe the fundamental unit of life – cells in a nanoscopic scale.

1.1 Cell membranes

In the 1930s, Max Knoll and Ernst Ruska built the first electron microscope, and the improvements in higher resolution in turn overcame the limitations of visible light. David Robertson revealed the first micrograph of the lipid bilayer in the cell membrane in 1957 (Robertson, 1960). Not until 1972, Seymour Singer and Garth Nicolson proposed the fluid mosaic model to elucidate the functional cell membrane, in which lipids, proteins and carbohydrates together constitute the structures of biological membranes (Singer and Nicolson, 1972). The phospholipid bilayer provides fluidity and elasticity, with the mobile proteins partially or totally embedded in the membranes. A typical eukaryotic cell carries out billions of chemical reactions in one second. Membrane structure is essential to serve as a barrier, which protects the substances from escaping and mixing with the surroundings. It is worth noting that most of the chemical reactions take place in the solution of water. The hydrophobic tails of the phospholipids assemble together to exclude water and the hydrophilic head groups allow them to face towards the aqueous environment. On the other hand, the cell membrane, and the membrane embedded proteins act as the gatekeepers, which selectively restrict the exchange between the interior and exterior environment. The characteristics of semi-permeable cell membranes enable the cells to control the passage of molecules and further to permit cellular communication.

1.2 Membrane transport

Membrane transport plays a vital role for living cells as delivery of newly synthetized molecules to their destination is essential for cell homeostasis including nutrients uptake and mobilization, or intra- or trans-organelle communication, for instance. To ensure and regulate the specialized functions inside the cells, cells possess two different types of membrane transport: passive and active transport.

1.2.1 Passive Transport

Passive transport refers to the movement of substances across cell membranes without energy expenditure. There are two types of passive transport: 1) simple diffusion, 2) facilitated diffusion. The direction of the transport relies on the concentration gradient due to compartmentalization of the cell membrane. Particles will spontaneously flow from the areas with higher concentration to lower concentration, such as CO_2 and O_2, until two areas reach equilibrium concentration. However, large uncharged polar molecules and ions are unable to cross the membrane, owing to their size and solubility. To achieve their entry into the cells, solutes require specific channels or transporters to facilitate the diffusion. A classic example of transporter-mediated transport is glucose transporter 2 (GLUT2), which undergoes conformational changes upon the binding of glucose (Loo et al., 1998). Since the binding site of GLUT2 is only exposed to one side of the cell membrane at a time, the transition between the on- and off-state is reversible to transport glucose inward to the cell or outward to the extracellular space, which is dependent on concentration of glucose across cell membranes.

1.2.2 Active Transport

Despite the fact that passive transport offers an effective way to transfer molecules, it is of importance to ensure the homeostasis of certain molecules or ions across the membrane, which may not follow the concentration or electrochemical gradient. An active transport allows the movement of molecules against the concentration gradient with the need of energy consumption, namely ATP. Primary active transport depends on the transmembrane pumps, with which ATP hydrolysis powers the direct transport of the molecules (Chen and Lui, 2022). Over 100 years, studies have demonstrated that maintaining the membrane potential is critical in cell cycle, cell volume, muscle contraction and neuronal system (Abdul Kadir et al., 2018). Na+/K+ ATPase drives K+ influx together with Na+ outflux across the membrane, keeping the cytosolic concentration of K+ high and Na+ low (Lin and Tang, 1997).

1.3 Intracellular compartments and protein transport

1.3.1 Endomembrane system and membrane-enclosed organelles

Prokaryotic and eukaryotic cells are classified according to the presence of a nucleus enclosed with a nuclear envelope. A prokaryotic cell consists of a single plasma membrane and all the chemical reactions take place in the cytoplasm. In contrast, a eukaryotic cell has internal membrane structures leading to elaborate cellular compartmentalization. As mentioned above, the differential permeability of cell membranes provides the barriers and allows the specialized subcellular processes to perform in a confined space.

From the evolutionary perspectives, it is possible that the plasma membrane was invaginated together with the DNA in an ancient prokaryotic cell, and in turn contributed to the early formation of a nucleus and a nuclear envelope (Cavalier-Smith, 1988). Other portions of the invaginated membrane later extended and gave rise to the endoplasmic reticulum (ER), Golgi apparatus, endosomes, lysosomes and so on (Martin et al., 2015). Contrarily, it is believed that mitochondria and chloroplasts have originated from engulfed pre-existing prokaryotes, which used to be free-living organisms. This theory may explain why these two organelles contain two lipid bilayer membranes, their own genome, ribosomes, and can perform protein synthesis.

1.3.2 Protein synthesis and transport

By the 1920s, it has been intensely debated that the biological basis of heredity relies on DNA or protein, while the latter shows more chemical diversity than the former. Not until Frederick Griffith in 1928, Oswald Avery, Colin MacLeod and Maclyn McCarty in 1944, reported the astonishing findings did the scientific community generally reach an agreement that DNA is the genetic material. Followed by Robert Roeder in 1969 with the landmark discovery of 3 nuclear RNA polymerases, Roger Kornberg in 1974 revealed the eukaryotic transcription machinery from DNA to RNA with the regulation of certain proteins (Kornberg, 2007; Roeder, 2019). George Palade in 1955 used the newly developed electron microscope to examine subcellular structures, and his identification of ribosomes as the protein-synthesizing organelles unveiled the translation mechanisms from RNA to protein (Palade, 1955). His contribution, together with Philip Siekevitz in 1956, revealed that secretory protein was primarily synthesized in the cisternal membranes of rough ER (Palade and Siekevitz, 1956a; Palade and Siekevitz, 1956b) (Figure 1). These findings provide sufficient evidence for the subsequent studies by Jim Jamieson and George Palade in 1967 that the

secretory proteins are further transported to the Golgi apparatus through small vesicles located in the periphery of the complex (Jamieson and Palade, 1967). In sum, the central dogma of molecular biology summarized the genetic information flow is transferred from DNA, RNA and finally proteins, firstly illustrated by Francis Crick in 1957 (Crick, 1958).

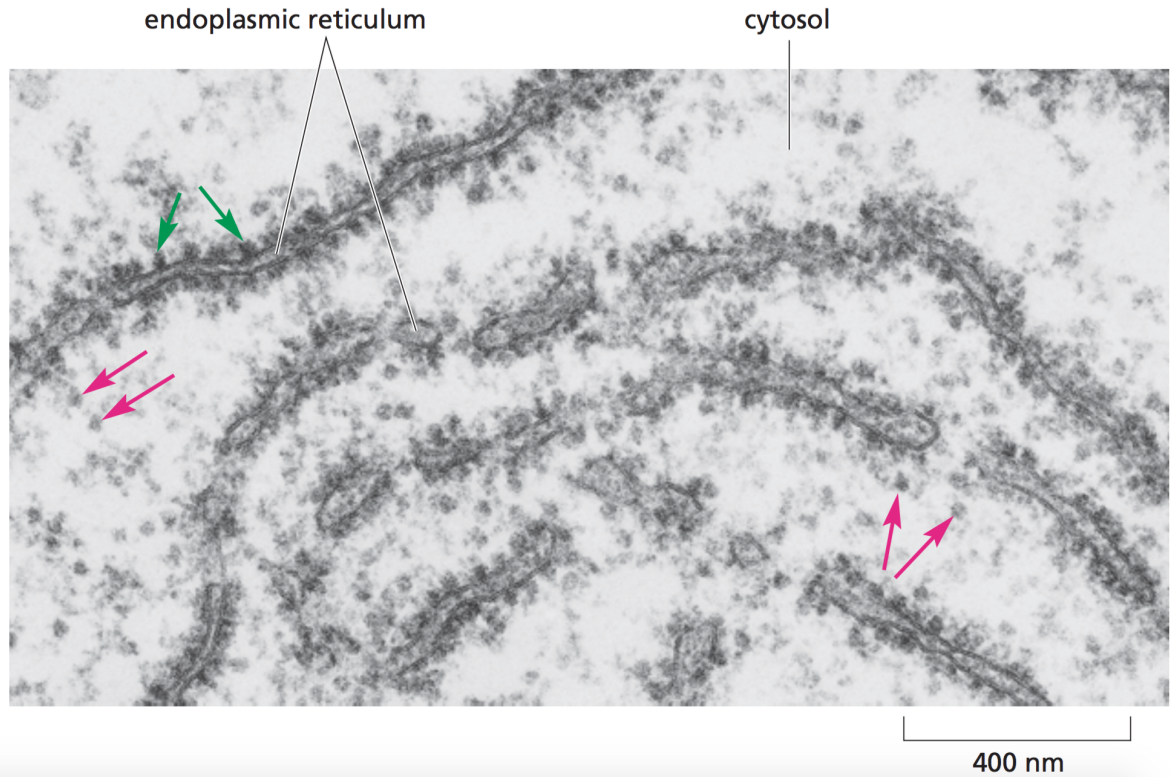

Figure 1. Micrograph of ER ribosomes through electron microscopy. A thin layer of a region at the cytoplasm is shown. Pink arrows indicate the free ribosomes in the cytosol, and green arrows reveal the ribosomes attached to the ER membrane. (Wells, 2005)

Despite the remarkable biodiversity on earth, all the living creatures share a similar and basic chemistry. In eukaryotic cells, the transcription of a target gene takes place firstly in the nucleus, and RNA molecules are then exported to the cytoplasm, where protein translation occurs. Proteins are indispensable components in the cells, the mechanisms of which governing specification and transmission are elegantly controlled by their signal sequences. Sorted proteins contain some typical signal sequences, ranging from 15 to 60 amino acids, to direct the proteins to certain membrane-bounded organelles, such as mitochondria, chloroplasts and peroxisomes.

2. Anterograde transport from Endoplasmic Reticulum to Golgi apparatus

Mammalian cells are characterized by the co-existence of multiple trafficking pathways, including anterograde and retrograde protein transport. In the anterograde direction, newly synthesized proteins are processed firstly in the ER, then eventually post-translationally modified by Golgi-resident enzymes, and finally sorted to their final destinations, including endosomes, lysosomes or plasma membrane.

2.1 Endoplasmic reticulum

2.1.1 Structure and function of endoplasmic reticulum

The architecture of endoplasmic reticulum is composed of a range of interconnected sheets and tubules, and is continuous with the nuclear envelope. A recent study has shown that ER is indeed made almost exclusively of tubules, sheets being dense tubular matrices, as demonstrated by advanced spatiotemporal analysis (Nixon-Abell et al., 2016). Two types of endoplasmic reticulum are present in the plant and animal cells, including smooth endoplasmic reticulum (SER) and rough endoplasmic reticulum (RER), particularly studded with ribosomes on the cytosolic surface. Both SER and RER ensure several functions depending on the cell type. In eukaryotic cells, SER is involved in lipid biosynthesis and RER is associated with protein production, folding and post-translational modifications. The dynamic ER network is constantly rearranging its structure and position through cytoskeleton, motor proteins and membrane-shaping proteins. The ER tubules are pulled out from the membrane reservoirs through the attachment of microtubules (MT) to ER-resident proteins, such as cytoskeleton-associated protein 4 (CKAP4 or CLIMP-63), and stromal interaction molecule 1 (STIM1) (Grigoriev et al., 2008; Vedrenne et al., 2005). Three types of ER movement are categorized: 1) Sliding: ER tubules undergo motor-dependent tracking along acetylated MT toward plus end with dynein and minus end with kinesin-1 (Woźniak et al., 2009). Inhibition of kinesin-1 impairs the ER tubule extension (Friedman et al., 2010). 2) Tip attachment complex (TAC)-mediated movement: TAC dynamics depends on the tethering of a plus-end-tracking protein – EB1 and STIM1. Membrane sliding and TAC-driven mechanisms account for 68.6% and 31.4% of the newly formed ER tubules (Waterman-Storer and Salmon, 1998). 3) Ring rearrangement: simultaneous imaging has revealed that tubular ER membranes wrap around endosomes or mitochondria (Friedman et al., 2011). This interorgenelle contact forms the ER ring structures, which often leads to the endosome fission and mitochondrial division (Rowland et al., 2014). ER has been shown to establish contact with several cellular membrane compartments, namely mitochondria, peroxisomes, lipid

droplets, lysosomes, and the Golgi apparatus (Valm et al., 2017). Many studies show that ER-organelle membrane contacts are functionally important, which may in turn explains the wide distribution of ER networks.

ER serves as a major site of protein synthesis and transport of a variety of molecules. To ensure the protein quality, ER-resident chaperone proteins, containing ER retention signal, assist the newly synthesized proteins to achieve correct three-dimensional conformations. There are several categories of ER proteins and folding enzymes: ER chaperones (e.g. calreticulin, calnexin…), the heat shock family (e.g. BiP, GRP94…), the protein disulfide isomerase (PDI) family, etc (Halperin et al., 2014). Most of the proteins are covalently modified to glycoproteins in the ER through glycosylation, processed by an oligosaccharyltransferase, the central enzyme of the N-linked glycosylation pathway (Aebi, 2013). This glycosylation-fold-reglycosylation cycle continues until a functional product is produced, released by the chaperones, and transported to the final destinations. Otherwise, the misfolded or aggregated proteins can either remain in the ER or enter ER-associated protein degradation (ERAD) pathway, mediated by the proteasome (Meusser et al., 2005).

The homeostasis of calcium has profound influence on fertilization, muscle contraction, and synaptic transmission in neurons. ER is a primary storage site for intracellular calcium. The cytosolic concentration of free calcium in an unstimulated cell is extremely low (around 100nM), while its concentration in the ER lumen and in the extracellular fluid is around 100-800 uM and 2mM, respectively (Schwarz and Blower, 2016). Upon the stimulation of G-protein coupled receptors (GPCR), the cleavage of phosphatidylinositol 4,5 bisphosphate (PIP2) into diacyl-glycerol (DAG) and IP3, which can then bind to IP3R in the ER, leads to calcium release and induces muscle contraction and neuronal activity. Studies have indicated that the binding affinity of unfolded proteins and lectin-like chaperones is significantly higher at high concentrations of calcium in the ER (Corbett and Michalak, 2000).

The maintenance of ER homeostasis is of importance to regulate the intracellular calcium release, the biogenesis and function of many organelles, and protein maturation. The disruption of normal ER conditions can occur due to the microenvironmental changes (starvation, low pH or hypoxia), the alteration of intrinsic metabolism (ROS overproduction or low ATP), the oncogenic stress (growth or hormone receptors activation, high transcription

and translation rates, or augmented secretory capacity), and therapy (cytotoxic drugs or radiation treatment), which consequently induce the ER stress (Chen and Cubillos-Ruiz, 2021). ER stress activates the unfolded protein response (UPR) and downstream signaling cascades, which is controlled by 3 ER-localized transmembrane sensors, inositol-requiring protein 1α (IRE1α), protein kinase RNA-like endoplasmic reticulum (ER) kinase (PERK) and activating transcription factor 6 (ATF6) (Li et al., 2020) (Figure 2). Downstream target genes, activated by X-Box binding protein 1 (XBP1) and activating transcription factor 4 (ATF4), are involved in protein synthesis, folding, quality control and phospholipid synthesis. As for activating transcription factor 6 (ATF6) is transported to Golgi apparatus with the interaction of COPII, and controls the expression of genes, associated with autophagy, apoptosis and ERAD (Almanza et al., 2019; Hetz, 2012). Although detailed mechanisms of UPR have been extensively discussed in many reviews, it remains still puzzling how UPR provides effects in many different cell types, and how the information of ER stress, such as stimulus, intensity and duration, is translated into particular cell fate programs, including cell death, differentiation and tumorigenesis.

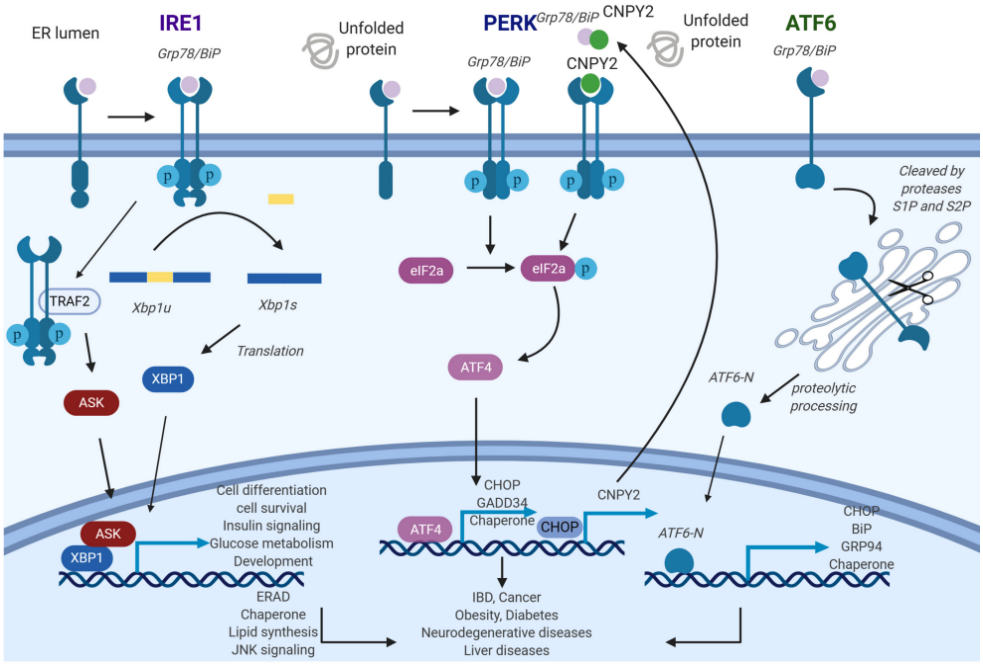

Figure 2. Overview of UPR signaling pathway. 3 UPR stress sensors: inositol-requiring enzyme 1 (IRE1), protein kinase RNA-like endoplasmic reticulum (ER) kinase (PERK) and activating transcription factor 6 (ATF6). (Li et al., 2020)

2.1.2 Protein transport from endoplasmic reticulum

Over the years, great advances towards tracking the proteins and vesicles allowed the biologists to visualize and examine the intracellular transport. Conditional temperature-sensitive mutant yeast is a powerful tool to identify the genes involved in the protein secretion. The phenotype of a mutant gene resembles that of wild type at 25°C, whereas the function of the protein is substantially reduced or inactivated at the temperature shift to 35°C (Novick and Schekman, 1979). This approach allows us to dissect the protein secretory pathway in yeast. In 2008, Osamu Shimomura, Martin Chalfie and Roger Tsien were awarded the Nobel Prize in Chemistry for their discovery and development of the green fluorescent protein, GFP. In the 1990s, membrane protein biogenesis can be monitored by synchronizing the protein transport of the temperature-sensitive mutant of viral glycoprotein (VSVtsO45) tagged with GFP. Upon the temperature shift from 40°C to 32°C, VSVGtsO45 oligomerizes and the translocation of VSVGtsO45-GFP could be observed from ER to pre-Golgi structures and then from the Golgi apparatus to plasma membrane (Bergmann, 1989; Kreis and Lodish, 1986; Presley et al., 1997). Together with the identification of many fluorescent proteins in various spectral regions (Kremers et al., 2011), the approach of fluorescence recovery after photobleaching (FRAP) and fluorescence resonance energy transfer (FRET) allows us to study and examine the protein subcellular structures and dynamics.

2.1.3 Formation of COPII complex at ER exit sites

Vesicular transport between various membrane-enclosed compartments is regulated in a highly ordered manner. Each vesicle budding off from the donor membrane is usually facilitated via coated proteins on the cytosolic surface. In the late 1970s, Randy Schekman and James Rothman pioneered the genetic and biochemical techniques to initially identify 23 *sec* genes and proteins, uncovering the fundamental machinery for vesicle transport (Balch et al., 1984; Novick and Schekman, 1979). The ER-to-Golgi anterograde transport is mediated by the production of COPII-coated vesicles, ranging from 60-90 nm in diameter, at the ER exit site (ERES). Components responsible for the assembly of the COPII complex include a small GTPase Sar1, along with its specific guanine exchange factor (GEF) Sec12, inner coat complex Sec23/24 and outer coat complex Sec13/31. Upon the activation of Sar1 through Sec12, the cargo can be captured by sec23/24 and the cage-like structure of sec13/31 is recruited to the ER membrane (Figure 3) (Budnik and Stephens, 2009).

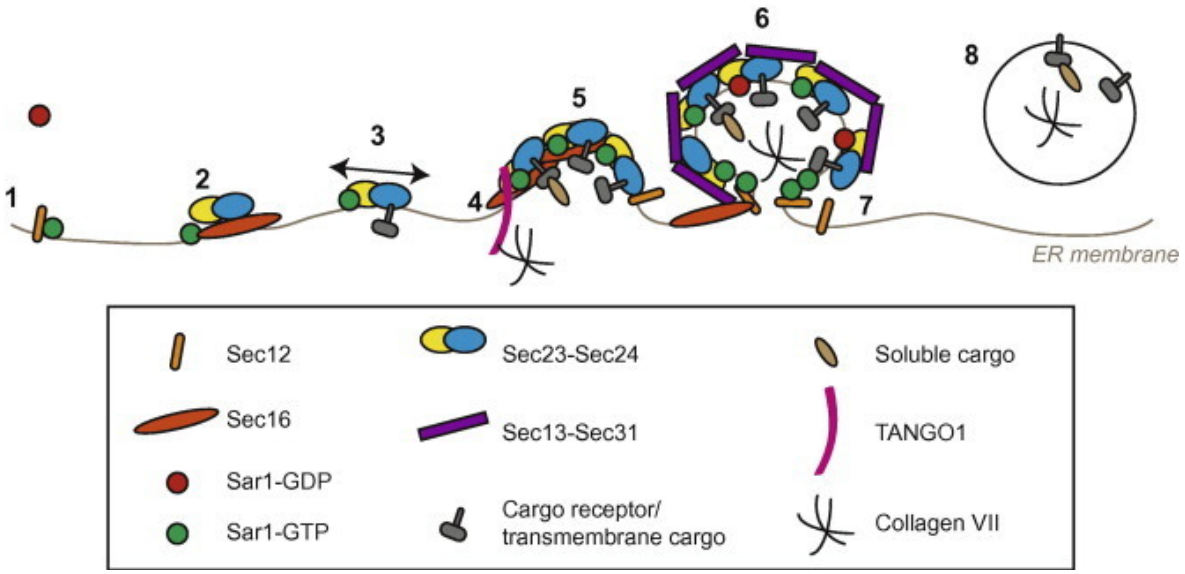

Figure 3. Scheme of COPII vesicle formation. Step 1-2: The activation of Sar1 through Sec12 directs the recruitment of Sec23/24. Step 3-5: Propagation of the COPII coat is facilitated by the interaction of soluble cargoes and cargo receptors/transmembrane cargo, as well as other adaptors such as TANGO1. Step 6-8: Recruitment of Sec13/31 results in the assembly of the COPII coat complex, and Sec12 and TANGO1 are then excluded from the final structure. (Budnik and Stephens, 2009)

One of the best characterized cargo receptors is ERGIC-53, a type I transmembrane mannose-specific lectin, continuously cycling between ER and ER-Golgi intermediate compartment. ERGIC-53 captures soluble lumenal glycoproteins, interacts directly with Sec23, and results in the engagement of ERGIC-53/cargo complexes into COPII vesicles, which is necessary for the maintenance of structural integrity. Functional ERGIC-53 is required for the package ability of such cargos as coagulation factors V and VIII, cathepsin C and Z, and α1-antitrypsin (Appenzeller et al., 1999; Nichols et al., 1998; Nyfeler et al., 2008; Vollenweider et al., 1998).

Another known transmembrane cargo receptor, Surfeit locus protein 4 (SURF4) in human or Erv29p homolog in yeast, can also promote the COPII complex assembly at ERES. SURF4 binds directly to the terminal tripeptide motifs of soluble cargo proteins, namely the amino-terminal peptide-encoding motif (ER-ESCAPE motif) (Yin et al., 2018). A recent paper identifies the physical interaction of SURF4 and Sec12, together with the binding of SURF4 and proinsulin cargo, regulates the COPII-driven ER export (Saegusa et al., 2022). Another publication also indicates that the luminal domain of SURF4 directly binds to sonic hedgehog (Shh) proteins with N-terminal KRRHPKK motifs, facilitating the package of Shh

into COPII-coated vesicles (Tang et al., 2022). In addition, the results also provide the evidence that the proteoglycans compete with SURF4 to bind to Shh, facilitating the dissociation of SURF and Shh at the Golgi, and therefore mediating the Golgi-to-ER retrograde transport (Tang et al., 2022). Aside from proinsulin secretion and Hedgehog signaling pathway, SURF4 (Erv29p in yeast; SFT-4 in C. elegans) has been documented to form complexes with various cargos, including pheromone precursor prepro-alpha factor (gpαF) in yeast, yolk lipoproteins in C. elegans, apolipoprotein B, proprotein convertase subtilisin/kexin type 9 (PCSK9), progranulin and prosaposin in human (Belden and Barlowe, 2001; Devireddy and Ferguson, 2021; Emmer et al., 2018; Saegusa et al., 2018).

Despite the predominant capture mechanism of ERGIC-53, certain large protein complexes may encounter the limitation to be loaded into the COPII carriers. It has been demonstrated that the size of an icosidodecahedron COPII-coated vesicles is ranged around 60-80 nm in diameter, whereas the structures with such large cargos as procollagen shows around 300-400 nm in length (Bonfanti et al., 1998; Fromme and Schekman, 2005). Through a genome-wide screen in Drosophila, a transmembrane cargo receptor, TANGO1, has been identified for the direct interaction of a bulky cargo collagen VII (Saito et al., 2009). The finding of TANGO1 SH3 domain - Hsp47, a collagen-specific chaperone, complex formation may explain the loading of collagen onto the COPII carriers (Ishikawa et al., 2016). The recruitment of collagen at the ERES is mediated by cutaneous T-cell lymphoma-associated antigen 5 (cTAGE5), a binding partner of TANGO1, and then Sec12 is localized at the ERES through the interaction with cTAGE5 (Saito et al., 2011, 2014). TANGO1/cTAGE5 can also bind directly to Sec23 for the assembly of large COPII carriers, and then TANGO1 recruits ERGIC-53-containing membranes for ER export of procollagen II (Ma and Goldberg, 2016; Raote et al., 2018). It is of note that TANGO1 directs the cargo loading in the COPII carriers, whereas TANGO1 itself is not incorporated into the budding vesicle, distinct from ERGIC-53-mediated mechanism (Budnik and Stephens, 2009). By analyzing the division of mouse embryonic stem cell, another report also demonstrated that complex of ubiquitin ligase CUL3–KLHL12 monoubiquitinated Sec31 and drove the assembly of large COPII complex for collagen secretion (Jin et al., 2012).

2.1.4 Formation of COPI complex

The better characterized function of COPI is to mediate the transport of cargo within the Golgi apparatus, as well as the Golgi-to-ER retrograde transport. The formation of the coat carriers was firstly purified *in vitro* in presence of a non-hydrolyzable GTP analog, GTPγS, which in turn inhibited the vesicle fusion (Malhotra et al., 1989; Melançon et al., 1987). The detailed analysis of heteroheptameric COPI complex were later identified as 7 large protein subunits, including α-, β-, β'-, γ-, δ-, ε- and ζ-COP (Beck et al., 2009).

The principle of COPI coat assembly is similar to that of COPII (Figure 4). The formation of COPI-coated vesicles involves the activation and insertion of Arf1 into the Golgi membrane, through the only known cis-Golgi-localized GEF, GBF1 (D'Souza-Schorey and Chavrier, 2006; Kawamoto et al., 2002). Interestingly, unlike the COPII complex, COPI complex forms a stable coat en bloc in the cytosol and docks on the vesicle budding site (Hara-Kuge, 1994). The initial recruitment of ArfI is mediated by the binding of p23 with its cytoplasmic tail, and the recruitment of COPI complex is facilitated by Arf1-COPI, together with p24-γ-COP interaction (Beck et al., 2009; Béthune and Wieland, 2018).

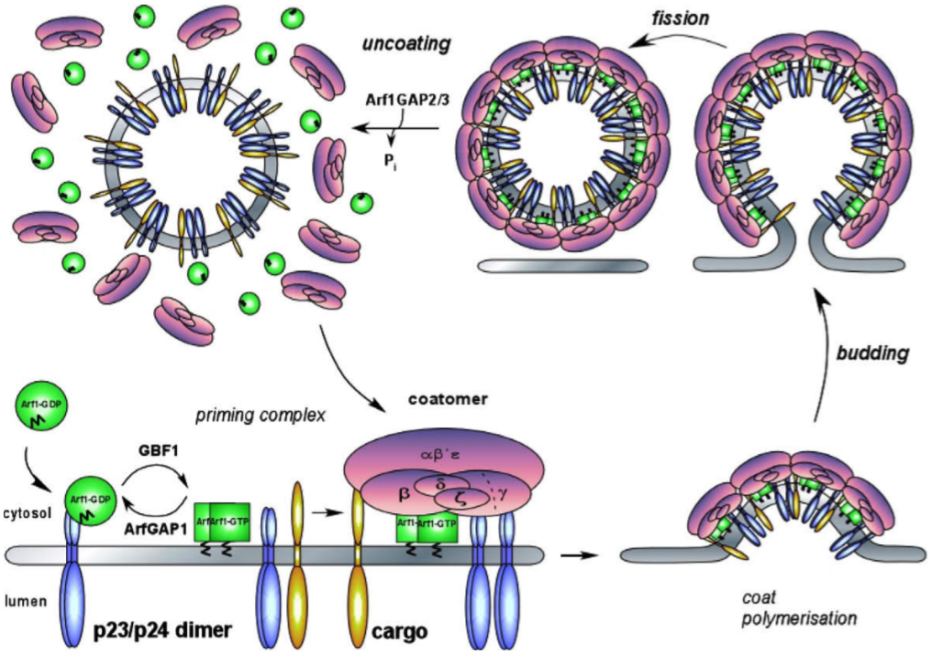

Figure 4. Scheme of COPI vesicle formation. The activation of Arf1 through GBF1 directs the insertion of Arf1 onto Golgi membranes. Propagation of the COPII coat is facilitated by the interaction of ArfI, COPI and the cargo receptors p23/24. (Beck et al., 2009)

However, the role of COPI complex in Golgi-to-ER retrograde transport is accepted by the community, whereas its association with anterograde transport carriers is less clear. A very recent study has shown that COPI complex is participating at ERES, revealed by cryo-structured illumination microscopy and whole-cell focused ion beam scanning electron microscopy (FIB-SEM) (Weigel et al., 2021).

2.2 Golgi Apparatus

2.2.1 Structure and function of Golgi apparatus

The discovery of Golgi the apparatus was firstly reported by Camillo Golgi in 1898, which he termed as an "internal reticular apparatus" in the Purkinje neurons with silver nitrate staining. In the early 1950s, the Golgi apparatus as a distinctive organelle became an accepted concept owing to the development of electron microscopy (Sjöstrand and Hanzon, 1954). Evidences were further provided that secretory proteins were exported from the ER to the Golgi apparatus through small vesicles (Jamieson and Palade, 1966). Over the past 20 years, remarkable data of high-resolution images have reconstructed the morphology of Golgi through electron tomography and correlative microscopy (CLEM) (Ladinsky et al., 2002; Trucco et al., 2004; Polishchuk et al., 2000). Golgi apparatus consists of a series of 3-20 stacks, with around 10 μm in the long axis and about 6 μm in the short axis of the Golgi apparatus in the epithelial cells, but number varies among different organisms and cell types (Koga and Ushiki, 2006). Each cisternal membrane of the Golgi apparatus aligns on top of each other, piling up closely opposed and flattened membranes, with each cisterna ranging from 0.7 to 1.1 μm (Pelletier et al., 2002) (Figure 5).

The Golgi complex is comprised of 4 distinct regions: *cis-, medial-*, *trans*-Golgi cisternae, and *trans*-Golgi network (TGN). The differential distribution of lipids and proteins bear a *cis*-to-*trans* gradient within the stacks (Holthuis et al., 2001; Orci et al., 1981; Rabouille et al., 1995; Roth et al., 1986). Most mammalian cells contain multiple Golgi stacks, interconnected by tubules. Each cisterna is anchored through the intervention of the Golgi reassembly and stacking protein 55 (GRASP55) and GRASP65. The myristoylation of GRASP55 and GRASP65 mediates their association with the Golgi membrane, and the oligomerization of GRASP55/65 interconnects one cisternae to another (Rabouille and Linstedt, 2016). In addition, the cytosolic face of the Golgi apparatus has a dense network of proteins, the Golgi matrix, which will be discussed later in the context. Knockdown of Giantin, the longest golgin in cells, increases the connectivity among Golgi cisterna and

stacks, suggesting its role in the generation of the non-compact throughout Golgi complex (Satoh et al., 2019).

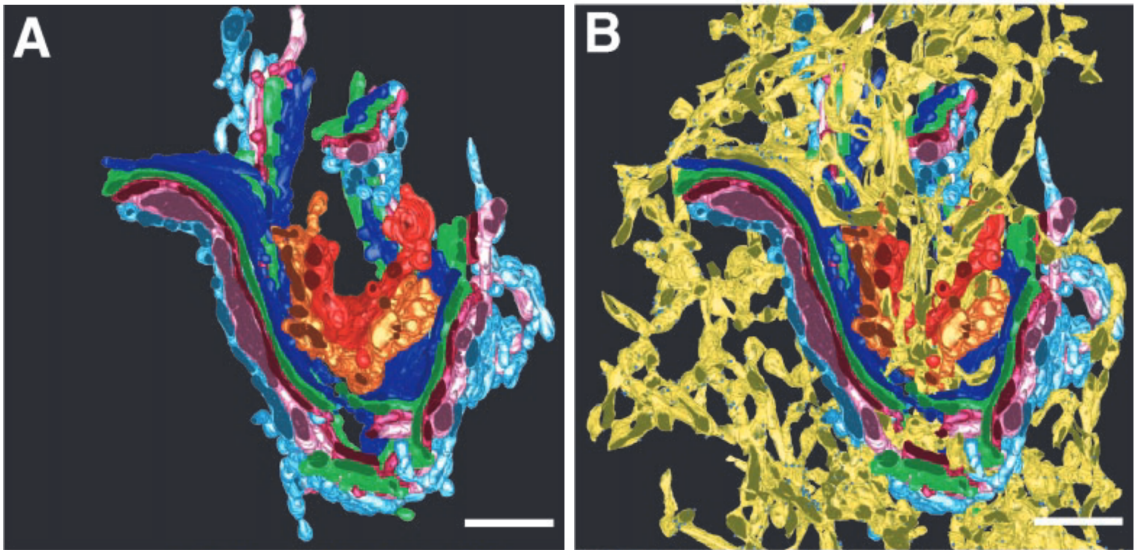

Figure 5. 3D reconstruction of the Golgi apparatus. (A) 3D reconstructions were generated from HIT-T15 cells (hamster pancreatic beta cells). The seven cisternae comprise the Golgi from C1-C7. C1, light blue; C2, pink; C3, cherry red; C4, green; C5, dark blue; C6, gold; C7, bright red. (B) The ER (yellow) traverses the Golgi stack and extends from Golgi to the opposite directions. Scale bar = 500 nm. (Marsh et al., 2001)

2.2.1.1 Non-centrosomal microtubule organizing center (MTOC)

The Golgi apparatus is localized at the cell center in various cell types, due to the action of microtubule cytoskeleton. Microtubules are built by α- and β-tubulin subunits through noncovalent interaction. Inside cells, microtubules extend from the centrosomes, made of γ-tubulin. The αβ-tubulin dimer attachs to each γ-tubulin ring complexes (γ-TuRC) and initiates the growing of microtubules. The recruitment of γ-tubulin ring complexes (γ-TuRC) was found also associated with isolated Golgi membrane, indicating the role of Golgi apparatus as a non-centrosomal microtubule organizing center (MTOC) (Chabin-Brion et al., 2001).

First, the recruitment of γ-TuRC initiated the MT outgrowth at the *cis*-Golgi face, requiring the association of AKAP450 (A-kinase anchoring protein of 450 kDa) and GM130, which allow the MT nucleation and in turn regulate the transport of specific cargos to the cell surface (Rivero et al., 2009). Golgi-derived microtubules formation is also controlled by the interaction of γ-TuRC, CDK5RAP2 and myomegalin (Rios, 2014; Roubin et al., 2013). Second, the nucleation of MT provides a secure template for the MT polymerization, which

includes a known MT stabilizer, CLASP. CLASPs are MT plus-end interacting proteins (+TIPs) and both CLASP1 and CLASP2 are targeted to *trans*-Golgi and TGN, recruited by the scaffolding golgin GCC185 (Efimov et al., 2007). The interaction of AKAP450 and CLASPs can enhance the microtubule-stabilizing activity through the binding of MT cross-linking factor 1 (MTCL1) (Sato et al., 2014). Lastly, to stabilize the MT structure, recent work has indicated that the clustered CAMSAP2 and CAMSAP3 at the minus-end of non-centrosomal MTs prevent MT depolymerization (Jiang et al., 2014).

Intriguingly, despite the importance of Golgi-derived MTs in organelle positioning and cargo trafficking, microtubules are dispensable for an efficient ER-to-Golgi and post-Golgi protein transport. Studies have demonstrated that nocodazole-induced Golgi mini-stacks maintain the *cis*-to-*trans* internal polarity adjacent to ERES, which in turn facilitates the normal ER-to-Golgi transport, and that post-Golgi trafficking requires the maturation of functional Golgi mini-stacks, but not the presence of microtubules (Cole et al., 1996; Fourriere et al., 2016; Presley et al., 1997).

2.2.1.2 Lipid metabolism

Lipids play fundamental structural and signaling roles in the eukaryotic endomembrane system and membrane composition, and regulate the cellular functions such as cell migration, recognition and polarity (Krahn and Wodarz, 2012). Based on their distinct structures and functions, lipids can be divided into various subtypes, including glycerophospholipids, sphingomyelin (SM), and glycosphingolipids, cholesterol. Glycerophospholipids account for approximately 70% of lipid species in mammalian cells, among which phosphatidylcholine (PC) is the most prevalent and accounts for 40%–50% of the total. Phosphatidylethanolamine (PE), which ranges from 20% to 45% of the total phospholipids, depending on the tissue, is the next most abundant (Murphy et al., 1993). Phosphatidylinositol (PI; 3%), phosphatidylserine (PS), phosphatidic acid (PA), and sphingomyelin (SM, 1%) are present in lesser amounts (Vance, 2008). Lipid composition also differs among intracellular organelles within the cell, showing a gradual increase in the concentration of SM from ER (3%), Golgi (8%) to plasma membrane (16%) (van Meer, 1998). Glycerophospholipids, cholesterol and ceramide are mainly synthesized in the ER, whereas Golgi serves as the principal site for the synthesis of SM and glycolipids. Many studies have shown the localization of SM synthase 1 (SMS1) in the *cis*- and *medial*-Golgi and that of SMS2 mainly at the plasma membrane (Futerman et al., 1990; Huitema et al.,

2004). Defects of SMSs result in the mis-localization of the secreted proteins away from the glycosylation enzymes at TGN, attenuated subcellular localization of DAG and its binding protein kinase D (PKD), delayed maturation and retarded trafficking of virus glycoproteins from Golgi to plasma membrane (Subathra et al., 2011; Tafesse et al., 2013; Villani et al., 2008; van Galen et al., 2014).

Studies of PIs, such as phosphatidylinositol-(4,5)-bisphosphate (PIP_2) and phosphatidylinositol-4-phosphate (PI4P), have demonstrated their functions in a remarkable number of crucial cellular processes, even though they occupy a relatively small proportion of the total phospholipids. Distinct classes of lipid transfer proteins (e.g. ceramide-transfer protein, or CERT), lipid kinases (e.g. PI4K and PIP5K), phosphatases (e.g. SAC1, OCRL1, INPP5B) and protein kinases (e.g. PKD) are present at Golgi apparatus, often recruited selectively through small GTPases of the Rab or Arf families. Four PI4Ks, PI4KIIα and β, PI4KIIIα and β, in mammalian cells distribute unevenly throughout the cell, whereas PI4KIIIβ is mainly associated with the Golgi complex (Godi et al., 1999). The Arf1-induced PI4KIIIβ complex, together with NCS-1, can be stabilized by the phosphorylation of PKD at Golgi. Inhibition of this complex formation leads to failure of the tubule fission the post-Golgi carriers (Mayinger, 2011; Valente et al., 2012). ER-to-Golgi translocation of SAC1 requires the oligomerization of SAC1 and the recruitment of the COPII complex, upon the stimulation of growth factor in mammalian cells. The up-regulation of SAC1 in the Golgi decreases the levels of PI4P and inhibits protein secretion (Blagoveshchenskaya et al., 2008; De Matteis et al., 2013).

2.2.1.3 Cargo sorting

Secretory proteins depart from the ERES, enter the *cis* face of the Golgi apparatus, and exit at the TGN to the plasma membrane. Protein and lipid sorting is most likely to occur at the TGN, whereas it has been demonstrated that cargos can be distributed at the main Golgi complex in both polarized and non-polarized cells (Beznoussenko et al., 2014; Cao et al., 2012; Chen et al., 2017; Simons and Fuller, 1985). Cargo adaptors at the TGN can recognize the sorting signals in the cytoplasmic tail of the secretory protein and recruit coat proteins, such as clathrin. In polarized epithelial cells, export from the TGN can be categorized into 2 main directions: basolateral and apical cargo sorting (Di Martino et al., 2019; Weisz and Rodriguez-Boulan, 2009).

Basolateral cargo is characterized through cytoplasmic motifs, including tyrosine-based YXXØ, and di-leucine-based (D/E)XXL(L/I) and DXXLL siganls, and is largely a clathrin-mediated process (Gonzalez and Rodriguez-Boulan, 2009). Transport from TGN to the endolysosomal compartments involves the adaptor protein 1 (AP-1), AP-3, AP-4 and the 3 Golgi-localized γ-adaptin ear homology Arf-binding (GGA) proteins. Cargos with tyrosine-based signal and di-leucine-based signal (D/E)XXL(L/I) can bind to APs, and the proteins bearing di-leucine-based signal DXXLL is recognized by GGAs (Janvier et al., 2003; Misra et al., 2002; Ohno et al., 1995). Through two-color stochastic optical reconstruction microscopy (STORM), a recent paper demonstrated the TGN- and endosome-localized adaptors AP-1, AP-3, GGA2 and epsin-related proteins (epsinR) form elongated structures (over 250 nm in length) at the juxtanuclear Golgi apparatus (Huang et al., 2019). Interestingly, a fraction of punctae with AP-1, GGA2 and epsinR is spatially segregated from AP-3, and over 40% of the structures with AP-1/GGA2/epsinR are enriched with clathrin (Huang et al., 2019).

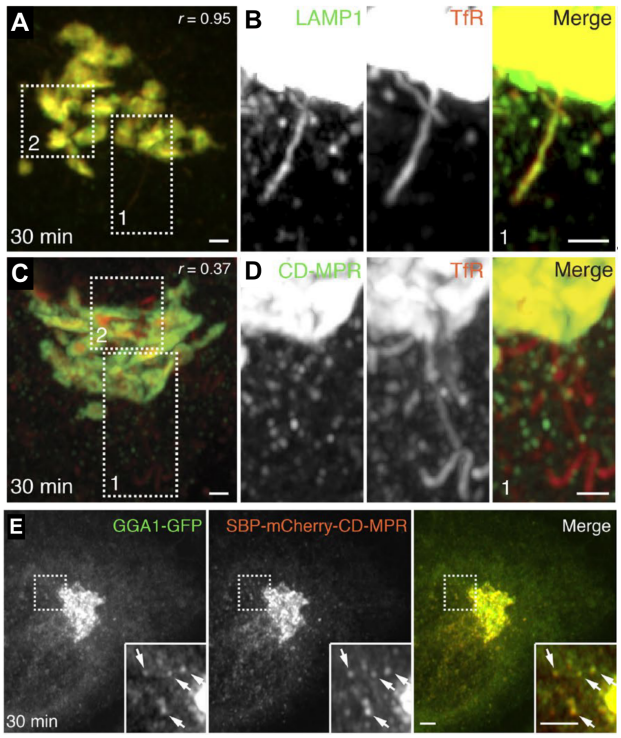

Figure 6. Segregation of endolysosomal proteins in the Golgi complex. (A-D) HeLa cells, coexpressing streptavidin–KDEL with combinations of the indicated reporter proteins were fixed 30 min after the addition of biotin and imaged by Airyscan microscopy. (B) Magnified views of box 1 in figure A. (D) Magnified views of box 1 in figure C. Scale bar = 1 µm. (E) HeLa cells coexpressing streptavidin–KDEL together with GGA1–GFP and CD-MPR reporter proteins were fixed 30 min after the addition of biotin and imaged by Airyscan microscopy. Arrows indicate carriers containing GGA1–GFP. Scale bar = 2 µm.

The trafficking routes between TGN to endolysosomes have been long described for the transport of lysosomal hydrolases via mannose 6-phosphate receptors (MPR) (Ghosh et al., 2003). Two types of MPR, the cation-dependent MPR (CD-MPR, 46 kDa) and cation-independent MPR (CI-MPR, 300 kDa), are both type I transmembrane receptors. Many soluble lysosomal enzymes, displaying with mannose 6-phosphate glycans, are recognized and sorted from TGN to endosomes by MPRs, and then released from MPRs due to the acidic PH in the endosomes (Olson et al., 2008). Another publication also provides an example of cargo segregation using retention using selective hooks (RUSH) assay. The export of cation-dependent mannose-6-phosphate receptor (CD-MPR) forms vesicular carriers with clathrin-associated GGA adaptors, whereas that of transferrin receptor (TfR) and lysosomal-associated membrane protein 1 (LAMP1) predominantly interacts with AP-2 complex in tubular carriers (Figure 6). Collectively, these data indicate that cargo adaptors can cooperatively regulate a specific sorting process at the TGN (Chen et al., 2017).

2.2.1.4 Glycosylation

More than 50% of all the proteins are found glycosylated in eukaryotes and archaea (Apweiler, 1999; Dell et al., 2010). Glycosylation can be categorized into 4 major classes according to the chemical linkage and the glycosylated residues of acceptor proteins: N-linked, O-linked, C-mannosylation and glycosylphosphatidylinositol (GPI) anchors (Schjoldager et al., 2020). The synthesis and modification of sugar on proteins or lipids can vary from a single residue or a complex polymer with more than 200 sugars (Figure 7). Glycosylation serves as a critical feature of many proteins and lipids. In the secretory pathway, newly synthesized proteins are processed post-translationally by Golgi-resident enzymes and sorted to their final destinations.

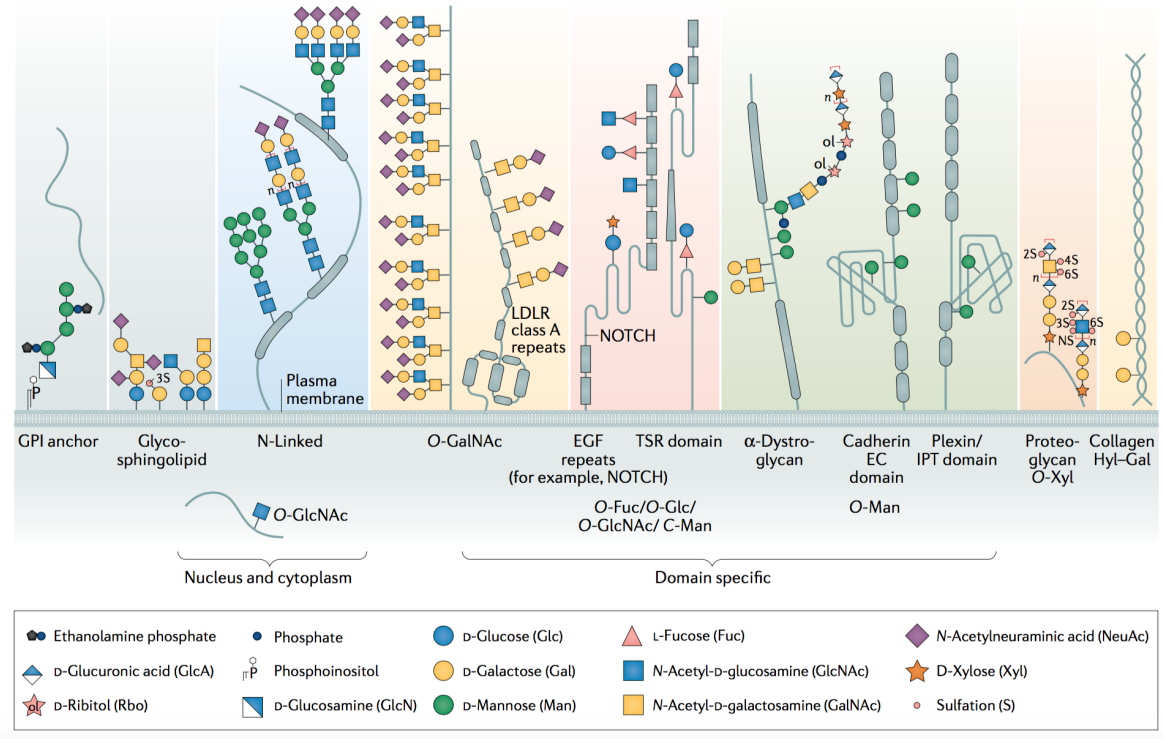

Figure 7. Main classes of human glycans. Scheme of the key components of the cellular glycome, highlighting glycosylation types for specific protein classes or protein domains. N-glycans and most O-glycans are widely found on most protein secretory pathways. The initial attachment of the first monosaccharide for N-glycosylation determines what proteins and their positions become glycosylated. Glycan symbols are depicted according to the Symbol Nomenclature for Glycans (SNFG) format. Sugar repeat units are shown with 'n' to indicate the number of repeats. EC: extracellular cadherin; EGF: epidermal growth factor; Hyl: hydroxylysine; IPT: immunoglobulin-like plexin transcription factor; LDLR: low-density lipoprotein receptor; NS: non-specific; TSR: thrombospondin type 1 repeat. (Schjoldager et al., 2020)

Among the 4 glycosylation groups, N-linked glycosylation serves as the most abundant type (Apweiler, 1999). N-linked glycosylation predominantly occurs at the asparagine (Asn) residue of the sequons with Asn-X-Ser/Thr, or Asn-X-Cys (rare cases), where X can be any amino acid except proline (Zielinska et al., 2010). The initiation of N-linked glycosylation occurs through oligosaccharyltransferase in the ER, transferring a precursor branched-chain sugar from a specific lipid-linked oligosaccharide, Glc3Man9GlcNAc2-P-P-dolichol (G3M9-DLO), to an asparagine residue of a protein (Reily et al., 2019). Synthesis of the precursor G3M9-DLO comprises 7 reactions, in which the key intermediate Man5GlcNAc2-PP-dolichol (M5-DLO) is firstly produced from the sugar donors of UDP-GlcNAc and GDP-Man on the ER cytoplasmic face. M5-DLO is translocated via scramblase to the ER lumen, where G3M9-DLO is finally generated (Verchère et al.,

2020) (Figure 8). The modification, including addition or trimming, of the sugars is processed in the ER and then in Golgi apparatus, which will be discussed in the later section. All N-linked glycans share a common pentasaccharide core (GlcNAc2Man3), which can be recognized by lectins, including Concanavalin A (Con A) and Phytohemagglutinin (PHA) (Cummings and Etzler, 2009).

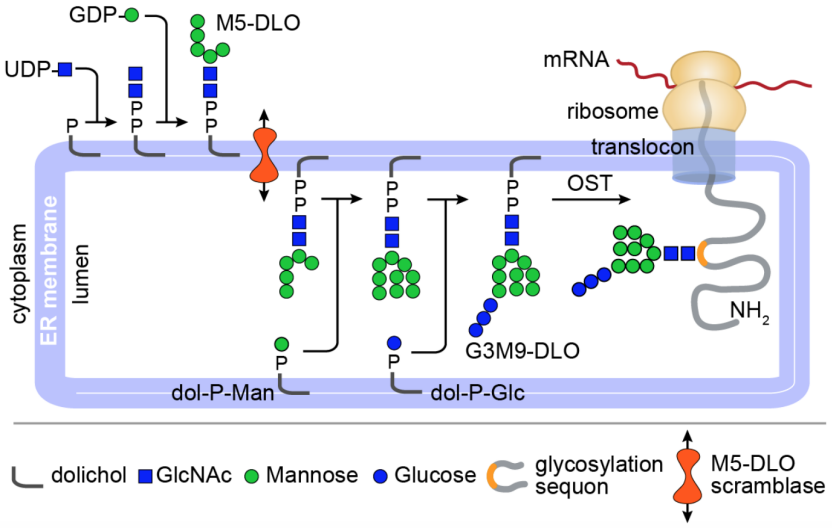

Figure 8. Transbilayer movement and synthesis of Glc3Man9GlcNAc2-PP-dolichol (G3M9-DLO) in seven steps. The first stage occurs on the ER cytoplasmic side to generate M5-DLO from UDP-GlcNAc and GDP-mannose. The remaining seven glycosyltransfer reactions occur in the ER lumen, adding 4 mannose and 3 glucose residues to generate G3M9-DLO. The movement of M5-DLO from cytosolic face to ER lumen is facilitated by M5-DLO scramblase. The final step shows the oligosaccharyltransferase (OST)-mediated transfer of the Glc3Man9GlcNAc2 oligosaccharide from G3M9-DLO to an asparagine residue within a glycosylation sequon in a nascent protein.

While the biosynthesis of O-glycans can be initiated in the ER, O-linked glycosylation mainly takes place in the Golgi apparatus. The O-linked glycosylation involves a monosaccharide linkage of mannose, galactose, fucose, glucose, xylose, or N-acetylglucosamine, onto the hydroxyl of either serine or threonine. The most prevalent form of O-linked glycosylation involves N-acetylgalactosamine (GalNAc) (Hang and Bertozzi, 2005). The initial glycan with GalNAc-α1- Ser/Thr is named Tn antigen, and can be elongated to form 8 core structures, which in turn form the mucin-type O-glycans (Brockhausen et al., 2022) (Figure 9). The transfer of GalNAc residues involves a glycosyltransferase family of up to 20 kinds of polypeptide GalNAc-transferases (GalNTs), as well as a series of glycosyltransferases to generate complex O-linked structures. The initial O-linked glycan chains are processed to form linear or branched O-glycans at Golgi

apparatus after protein folding (Tuccillo et al., 2014). It is of note that the oligosaccharides on proteins can increase their physical stability, protect them from proteolytic degradation, and may serve as a recognition signal with the O-glycan display on the cell surface (Cummings and Etzler, 2009; Stanley, 2011).

To characterize the protein glycan profiles, considerable efforts have advanced our understanding of protein glycosylation sites, occupancy, glycan heterogeneity levels, structures and so on. The analytical approaches include high-performance liquid chromatography (HPLC), mass spectrometry (MS), capillary electrophoresis (CE), isoelectric focusing (IEF), etc. With the development of the molecular tools, lectin-based microarray allows the direct measurement of various glycans in an intact protein, applicable for high throughput screening (Zhang et al., 2016a; Zhang et al., 2016b). The lectin and toxin ricin, first identified by Peter Stillmark in 1888, were extracted from the seed of castor bean. Ricin's lectin activity causes the agglutination of erythrocytes due to its binding affinity to terminal β-linked Gal or GalNAc of glycoproteins on the cell surface (Cummings et al., 2022; Van Damme, 2022). The online database of the Functional Glycomics Gateway (http://www.functionalglycomics.org/) provides a comprehensive analysis of glycan-binding proteins, glycan structures, and glycosyltransferases properties. Moreover, taking advantage of conjugated to fluorescent dyes, membrane trafficking of glycoproteins containing high-mannose N-glycans has been visualized in the pre-Golgi intermediates and post-ER structures (Morgan et al., 2013).

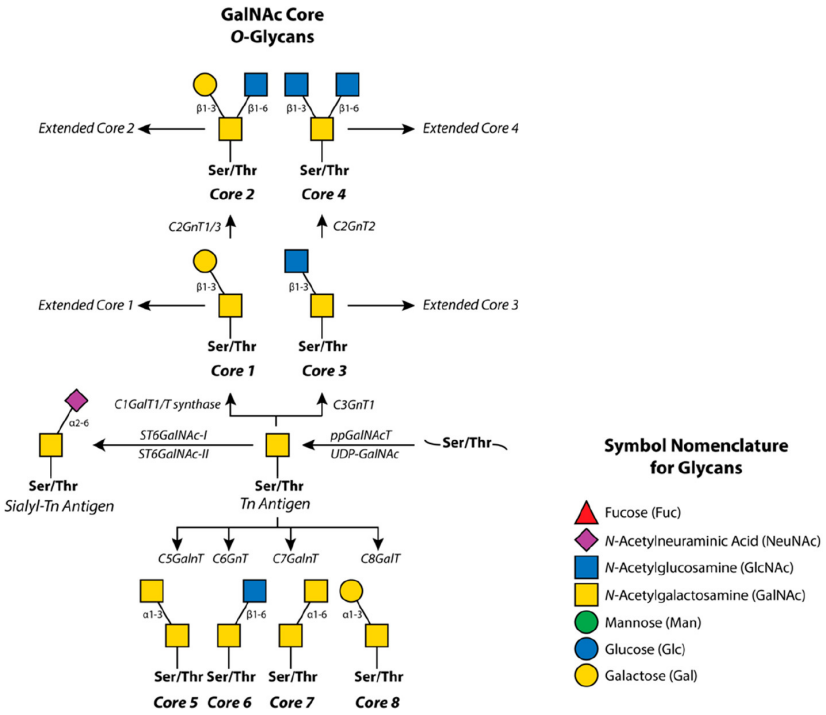

Figure 9. O-GalNAc glycan structures and their synthesis pathways. Glycan symbols are depicted according to the Symbol Nomenclature for Glycans (SNFG) format. (Wilkinson and Saldova, 2020)

Biochemical methods to study the intracellular trafficking of glycoproteins were pioneered by James Rothman in 1980 (Fries and Rothman, 1980). Glycoproteins in the ER or *cis*-Golgi acquire the N-glycans with high mannose are susceptible to Endoglycosidase H (Endo H) activity, as well as peptide N-glycosidase F (PNGase F), a glycoamidase cleaving the entire sugar chain. Once glycoprotein undergoes glycan modification in the *medial*- or *trans*-Golgi, the complex N-glycan structure becomes Endo H-resistant, but remains sensitive to PNGase F (Figure 10). EndoH-resistance thus provides the evidence for the transfer of a glycoprotein from ER to Golgi or post-Golgi compartments.

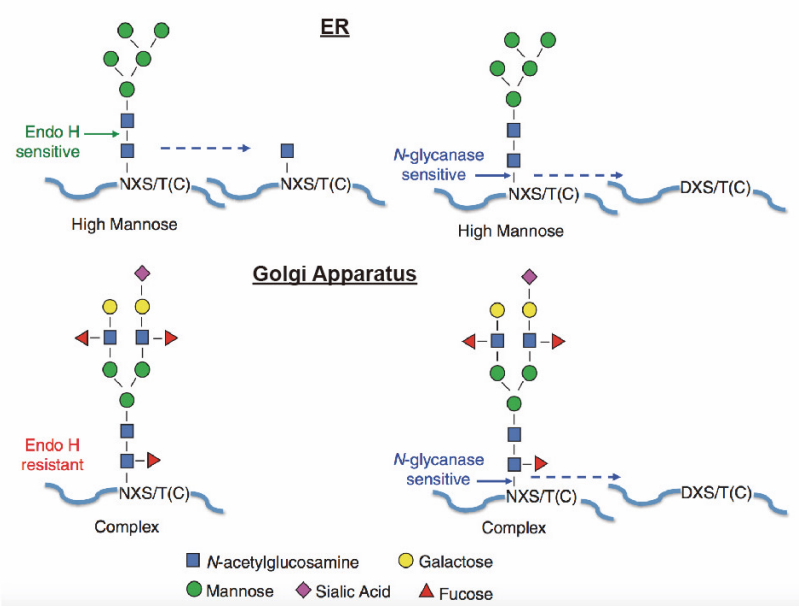

Figure 10. Application of Endo H and PNGase F treatment. Glycosylated proteins with high mannose N-glycans in ER, ERGIC, and cis-Golgi are susceptible to Endo H activity. The modification of sugar residues in the Golgi apparatus generates more complex glycans, which become resistant to Endo H treatment. In contrast, glycoproteins with high mannose or complex N-glycans are both sensitive to PNGase F activity. (Adapted from Stanley, 2011).

2.2.2 Models of intra-Golgi transport

Three major types of intra-Golgi transport mechanisms have been proposed: 1) vesicle transport, 2) cisternal maturation and 3) rapid partitioning (Figure 11). In the vesicle transport, the Golgi apparatus is typically viewed as a stable organelle, within which cargo proteins travel from one cisterna to another through anterograde COPI-coated vesicles. This model originates from the studies of protein secretion by Jim Jamieson and George Palade in 1967. However, the weakness of the vesicle transport model lies in the fact that rapid intra-Golgi traffic requires more than hundreds of vesicles per second (Glick and Luini, 2011). This gives rise to the model of cisternal maturation, proposed by Pierre-Paul Grassé in 1957 (Grasse, 1957). Cisternal maturation model dictates that Golgi cisternae serve as transient cargo carriers and COPI vesicles continuously recycle the Golgi-resident proteins, such as glycosylation enzymes, from older to younger cisternae (Glick and Luini, 2011). Alberto Luini in 1998 demonstrated that large secretory cargoes, such as procollagen type I, only exist in the Golgi tubule structures (around 300 nm in length) instead of within the vesicles, which are normally less than 100 nm in diameter (Bonfanti et al., 1998).

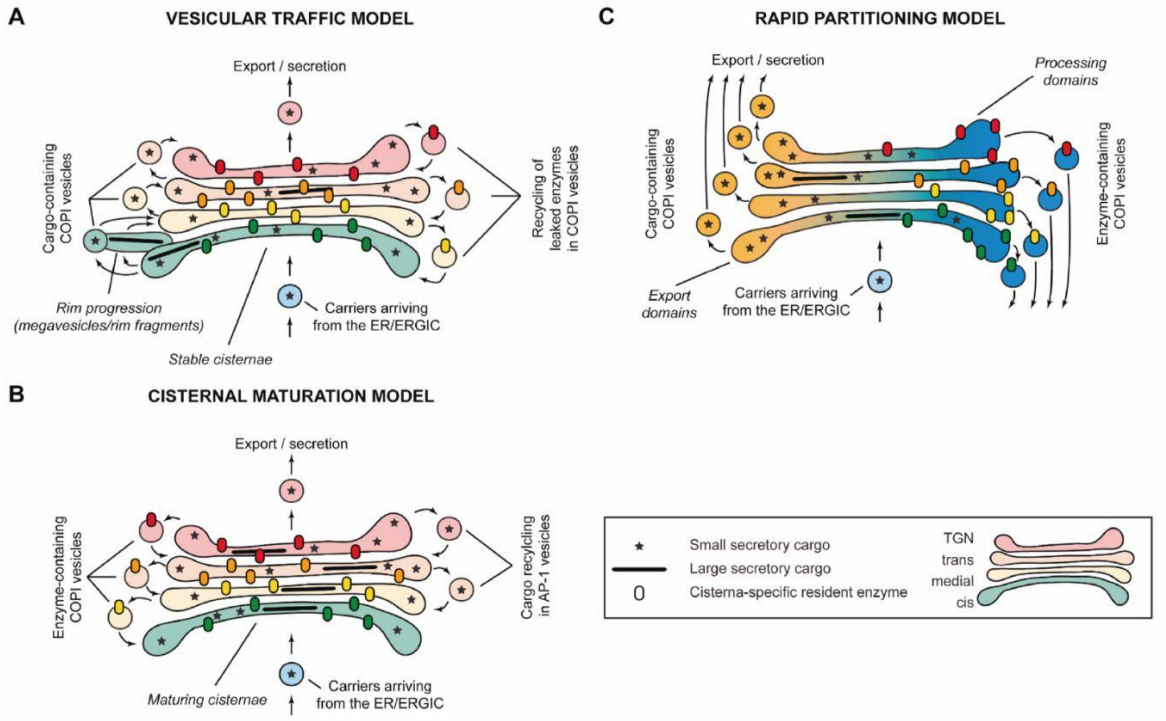

Figure 11. Three models of intra-Golgi transport. (A) Vesicular transport model (B) Cisternal maturation model and (C) Rapid partitioning model. ERGIC: ER-Golgi intermediate Compartment, TGN: Trans-Golgi-Network. (Lujan and Campelo, 2021)

Inspired by the finding of cargos exiting from Golgi apparatus at an exponential rate, the model of rapid partitioning was proposed by measuring the kinetics of temperature-sensitive VSVG-GFP and GFP-procollagen with inverse FRAP (iFRAP) (Patterson et al., 2008). Secretory cargos arrive and partition at different cisterna of Golgi apparatus, which operate as processing and export domains. In consequence, the rapid partitioning model implies that the cargos exit the Golgi apparatus from all cisternae and not only at the trans-side as suggested in the other models. Although the data of rapid partitioning model readily explain the transport of both small and large molecules and intra-Golgi trafficking through vesicles or tubules, it cannot easily explain how Golgi cisternae forms as discrete subcompartments and the polarized distribution of Golgi-resident enzymes (Glick and Luini, 2011). In the field, the cisternal maturation is the most accepted model but including some variations to cope with the requirement of different transport speed depending on the cargo and the different size of cargos to be transported (Boncompain and Perez, 2013).

2.2.3 Proteins localized at Golgi

As mentioned above, the secretory cargoes bud from the ERES in COPII-coated vesicles and deliver to the Golgi apparatus for further modification and sorting. This process involves the docking of vesicles and the fusion of membranes, requiring a set of matching Golgi-localized golgins, SNARE proteins, Rab GTPases and multisubunit tethering complexes of conserved oligomeric Golgi (COG) and Golgi-associated retrograde protein (GARP) (Witkos and Lowe, 2017).

2.2.3.1 Golgin Family

Electron microscopy studies showed that proteinaceous components play an important role in maintaining the Golgi cisternae together as a stacked unit (Franke et al., 1972; Cluett and Brown, 1992). Most progress in understanding the systematic and quantitative proteomics data of Golgi membrane fractions has been made in the past 20 years (Bell et al., 2001; Shin et al., 2020; Yates et al., 2005). Golgins are a family of long coiled-coil proteins of Golgi apparatus with similar topologies. Each Golgi cisterna is decorated with a distinct set of golgins via their C-terminus, with GM130 and GMAP-210 at *cis*-Golgi and golgin-97 and golgin-245 at *trans*-Golgi in mammals (Gillingham and Munro, 2016) (Figure 12).

GM130 (a.k.a. golgin-95) was the first component of the Golgi matrix purified and identified (Fritzler et al., 1993). GM130 is localized to the *cis*-Golgi due to its interaction with Golgi reassembly stacking protein 65 (GRASP65) (Barr et al., 1997). Knockdown of GM130 via siRNA treatment induces the fragmentation of the Golgi complex and aberrant sialylation of glycans, detected by GS-II lectin (Puthenveedu et al., 2006). GM130 can also bind to the C-terminal of the vesicle docking protein p115 and Rab1 (Nakamura et al., 1997). The activation of Rab1 is required for the recruitment of p115 onto the COPII-coated budding vesicles (Moyer et al., 2001). Depletion of GM130 or GMAP-210 also reduced the trafficking of temperature sensitive VSVG to the plasma membrane (Roboti et al., 2015).

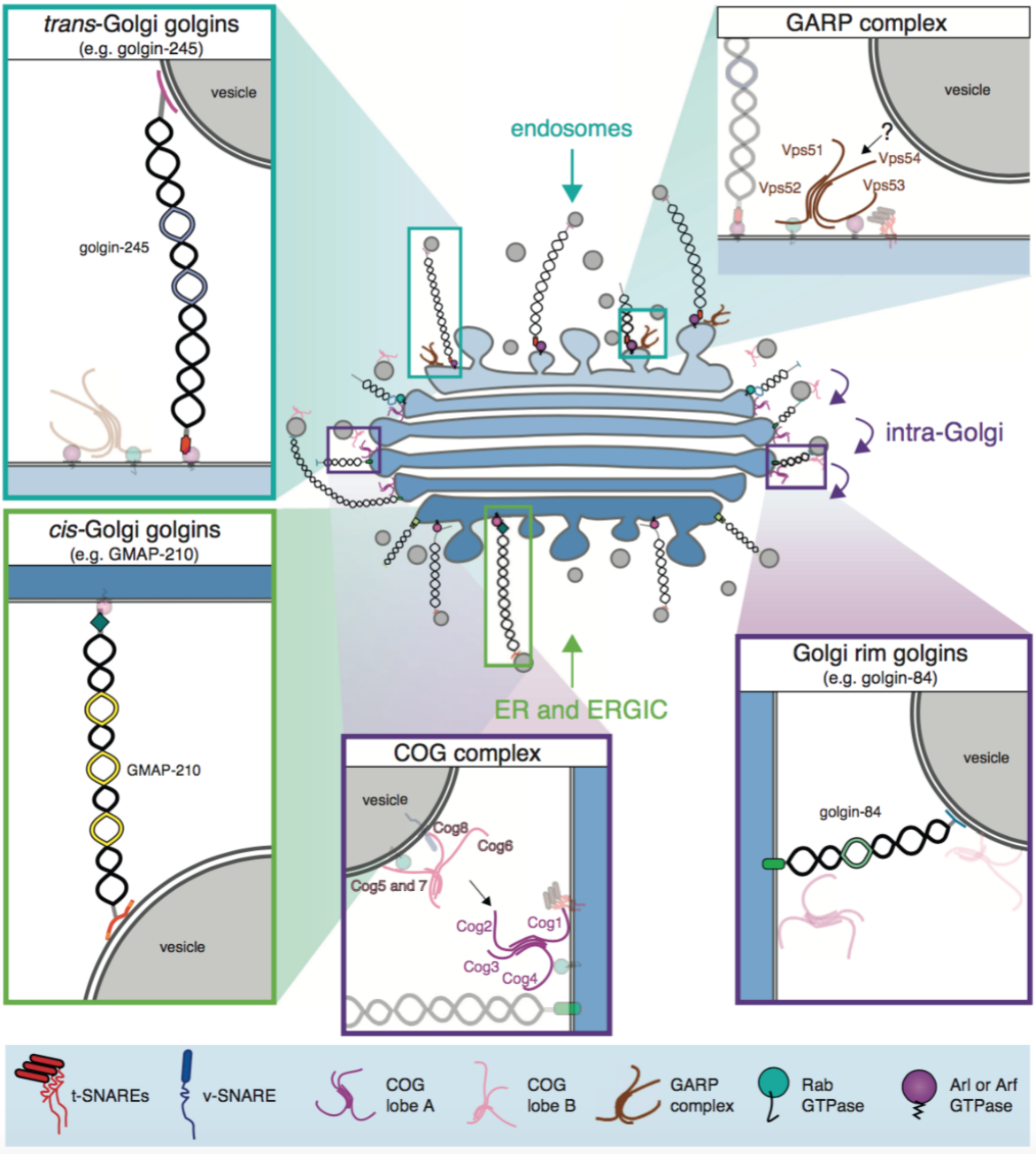

Figure 12. Different golgins and tethering complexes in the distinct regions of Golgi apparatus. The golgins are long, coiled-coil proteins, extending from the Golgi surface. They differ in localization and tethering specificity, with golgins at the cis-Golgi capturing ER- and ERGIC- derived vesicles, whereas golgins localized to cisternal rims capturing intra-Golgi transport vesicles, and trans-Golgi golgins capturing endosome-derived carriers. The COG complex consists of two lobes: lobe A (Cog1–4) predominantly associated with Golgi membranes, and lobe B (Cog5–8), which is found on vesicles. The GARP complex is composed of four subunits (Vps51–54) and contributes to tethering of vesicles at the trans-Golgi, but the mechanisms remain poorly defined.

The largest golgin in mammalian cells, Giantin (Golgin B1; 370 kDa), is localized to Golgi rims via its short transmembrane domain, with no N-terminal extension in the Golgi lumen. Giantin plays a role in the maintenance of Golgi structures and regulates intra-Golgi and retrograde transport, through the binding of p115 on COPI-coated vesicles (Koreishi et al., 2013; Linstedt et al., 2000; Sönnichsen et al., 1998). Another vesicle population with golgin-84 and CASP, can also mediate the docking of COPI-coated vesicles to the Golgi membrane, enriched with Golgi-resident enzymes, whereas p115-golgin tethered vesicles shows the presence of p24 family and putative cargo receptors (Malsam et al., 2005). Taken together, the data indicated the golgin tethers define the subpopulations of intra-Golgi transport and further facilitate the cargo sorting in a selective manner. Studies in rats and in zebrafish have demonstrated the role of Giantin in the development of bones and cartilage (Katayama et al., 2011; Stevenson et al., 2021; Wong and Munro, 2014).

2.2.3.2 COG Family

Conserved oligomeric Golgi (COG) complex is evolutionarily conserved in vertebrates, important for proper Golgi structure and protein sorting and glycosylation enzyme recycling (Blackburn et al., 2019; Quental et al., 2010; Ungar et al., 2002). COG complex is made up of 8-subunit peripheral membrane proteins, which can be subdivided into 2 lobes, lobe A (COG1–4) and lobe B (COG5–8). Putative model of lobe A and B assembly is proposed through electron microscopy, revealing the preferential attachment of lobe A to the Golgi membrane, and lobe B to the vesicles (Willett et al., 2016) (Figure 13). Firstly illustrated in 2004, malfunctions in the COG complex result in COG-specific type II congenital disorders of glycosylation (CDG), including mis-glycosylated N-linked or O-linked glycoproteins and glycolipids (Climer et al., 2015; Wu et al., 2004). It is of note that the functional interaction of the COG complex with SNAREs and Rabs plays an important role in vesicle tethering and docking. The interactome of COG-SNAREs and COG-Rabs have been screened through yeast two-hybrid or pull-down assays, and reviews have shown that COG subunits interact with 14 of Golgi-localized SNAREs (e.g. STX5, STX6, STX16, GS27, SNAP29, etc) and with 12 of Rab proteins (e.g. Rab1, Rab2a, Rab4a, Rab6, Rab10, Rab14, Rab30, Rab36, Rab39, Rab 41, etc) (Willett et al., 2013). Recent development from the lab of V. Lupashin aims at depleting one subunit of the COG complex (namely COG4) in an acute way to investigate primary effects on COG-dependent vesicles both at the level of the cargo and of the molecular machineries associated with these vesicles (Sumya et al., 2022). Their

results demonstrate that the depletion of COG significantly causes the relocalization of Golgi SNAREs, and redistribution of Golgi-resident enzymes into COG-dependent vesicles.

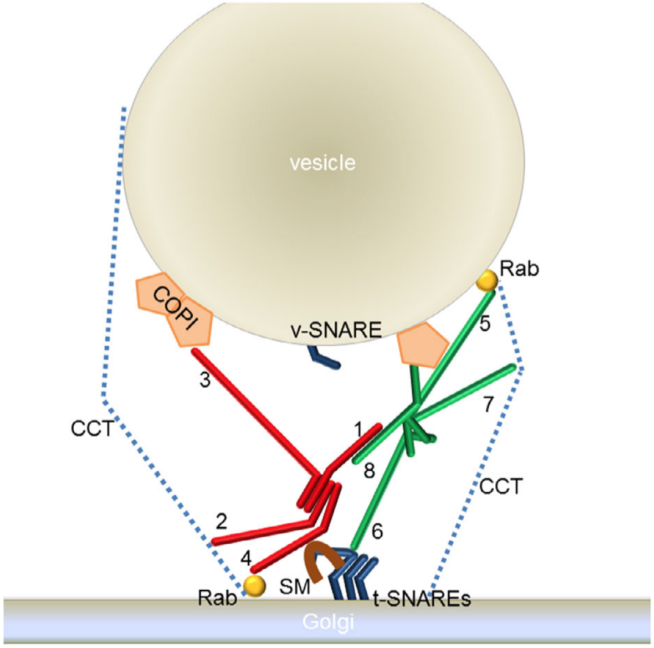

Figure 13. Putative model of lobe A (COG1-4) and lobe B (COG5-8) interaction with other components (such as SNAREs and Rabs) of vesicle fusion machinery during vesicle tethering. (Blackburn et al., 2019)

2.2.3.3 Rab proteins

The Rab proteins belong to the largest family of small GTPases, with more than 60 members identified in mammals (Klöpper et al., 2012). Rab proteins possess a GTPase fold with 6-stranded β-sheet flanked by 5 α-helices, which is commonly seen in all the members of Ras superfamily (Pfeffer, 2005). Rab proteins cycle between membrane GTP-bound (active) and cytosolic GDP-bound (inactive) forms, which allows them to recruit the effector proteins (e.g. motor proteins, SNAREs, cytoskeleton regulators, etc.) to specific membrane compartments, and in turn to facilitate the vesicle fusion, formation and transport (Homma et al., 2021; Hutagalung and Novick, 2011) (Figure 14). Among the Rab protein members, Rab1, Rab2, Rab6, Rab18, Rab33, Rab41 and Rab43 are involved in the maintenance of Golgi complex and pre-Golgi protein transport, as well as Rab3, Rab7, Rab8, Rab9, Rab10, Rab11, Rab13, Rab14, Rab21, Rab22, Rab31, Rab29, Rab39 in the morphology of TGN and post-Golgi trafficking (Goud et al., 2018).

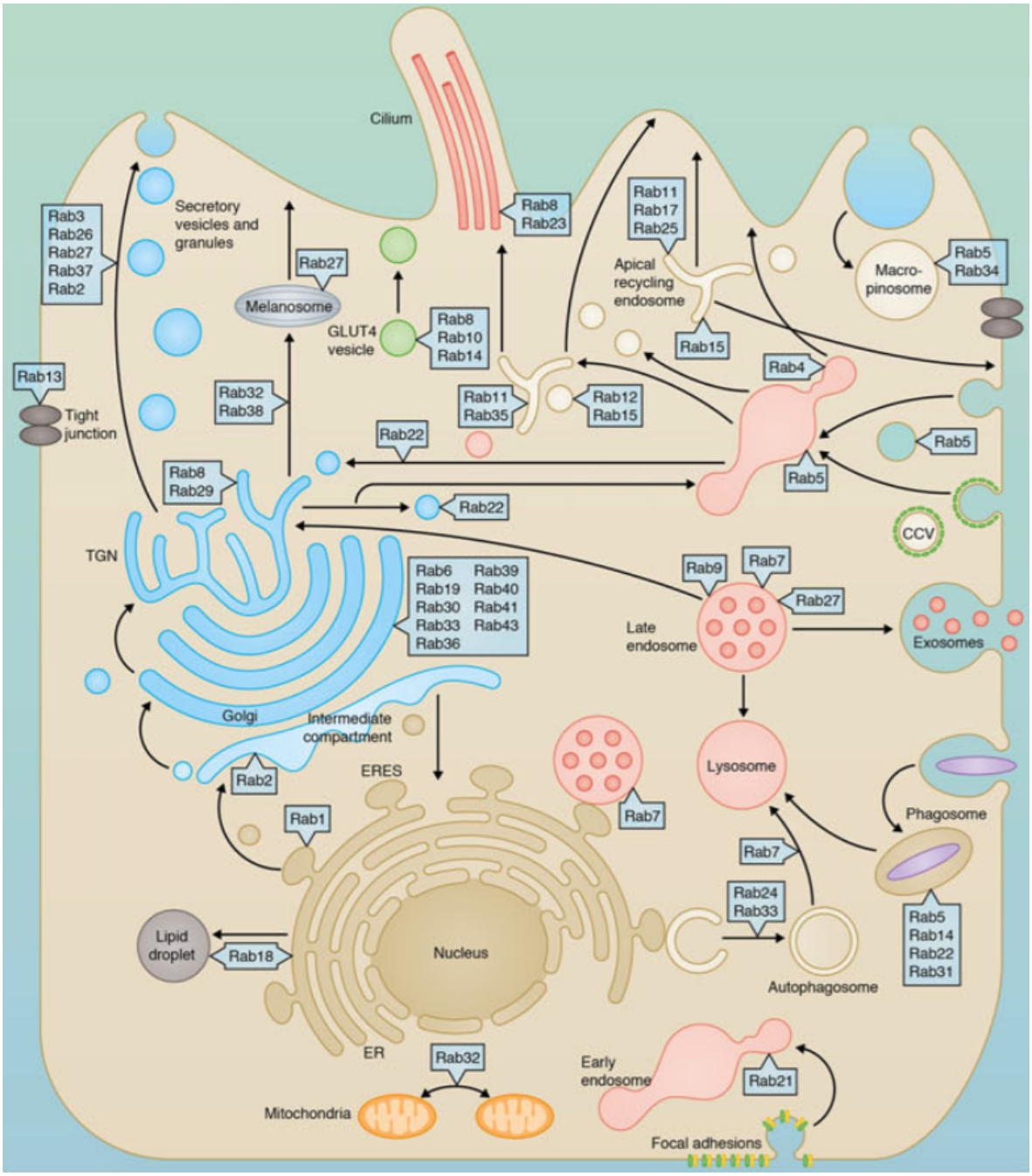

Figure 14. Overview of Rab functions and distribution in the cell. Distinct rab GTPases are localized in different membrane compartments to regulate specific membrane trafficking pathways (Zhen and Stenmark, 2015).

Rab1 and Rab2 both serve as key regulators of vesicular transport between ER and Golgi apparatus. Rab1 has been extensively studied for its association with ERGIC-53/p58 positive membranes of ER–Golgi intermediate compartment (Saraste et al., 1995). The recruitment of Rab1, together with its GEF – TRAPP I, facilitates the interaction of Rab1, GM130, cytoplasmic protein p115 and GRASP65, which leads to the fusion of COPII-coated

vesicles in the *cis*-Golgi face (Moyer et al., 2001). It is of note that Rab1 is involved in the intra-Golgi trafficking and COPI-dependent retrograde transport, through its association with GBF1, the GEF of ArfI (Plutner et al., 1991; Monetta et al., 2007). In addition, Rab2 shares many of the same effector complexes as Rab1, such as GM130, p115 and GMAP-210, as well as GRASP55, in the ER–Golgi intermediate compartment and *cis*-Golgi membrane (Saraste, 2016; Short et al., 2001). Evidence has also shown that Rab2 stimulates the recruitment of COPI in a PKC-dependent manner (Tisdale, 2003). Taken together, these data reveal the pivotal role of Rab1 and Rab2 in the bi-directional transport between ER and Golgi.

2.2.3.4 Glycosylation enzymes

Based on the similarities of amino acid sequences or catalytic activity, the Carbohydrate-Active Enzyme (CAZy) database describes 173 glycoside hydrolases (GHs) families, 115 glycosyltransferases (GTs) families, 42 polysaccharide lyases (PLs) families, 20 carbohydrate esterases (CEs) families and 17 auxiliary activities (AAs) families (http://www.cazy.org/). In mammals, the Golgi apparatus is home to hundreds of GTs, glycosidases and nucleotide sugar transporters. Most of the GTs are type II integral proteins, and share a common architecture, consisting of a short cytoplasmic N-terminal domain, a single-pass transmembrane domain (TMD) and a C-terminal catalytic region in the lumen. These glycosylation enzymes have a non-uniform distribution in the Golgi cisternae. The relative position of the enzymes at steady state often reflects a series of sequential reactions in glycan synthesis (Figure 15).

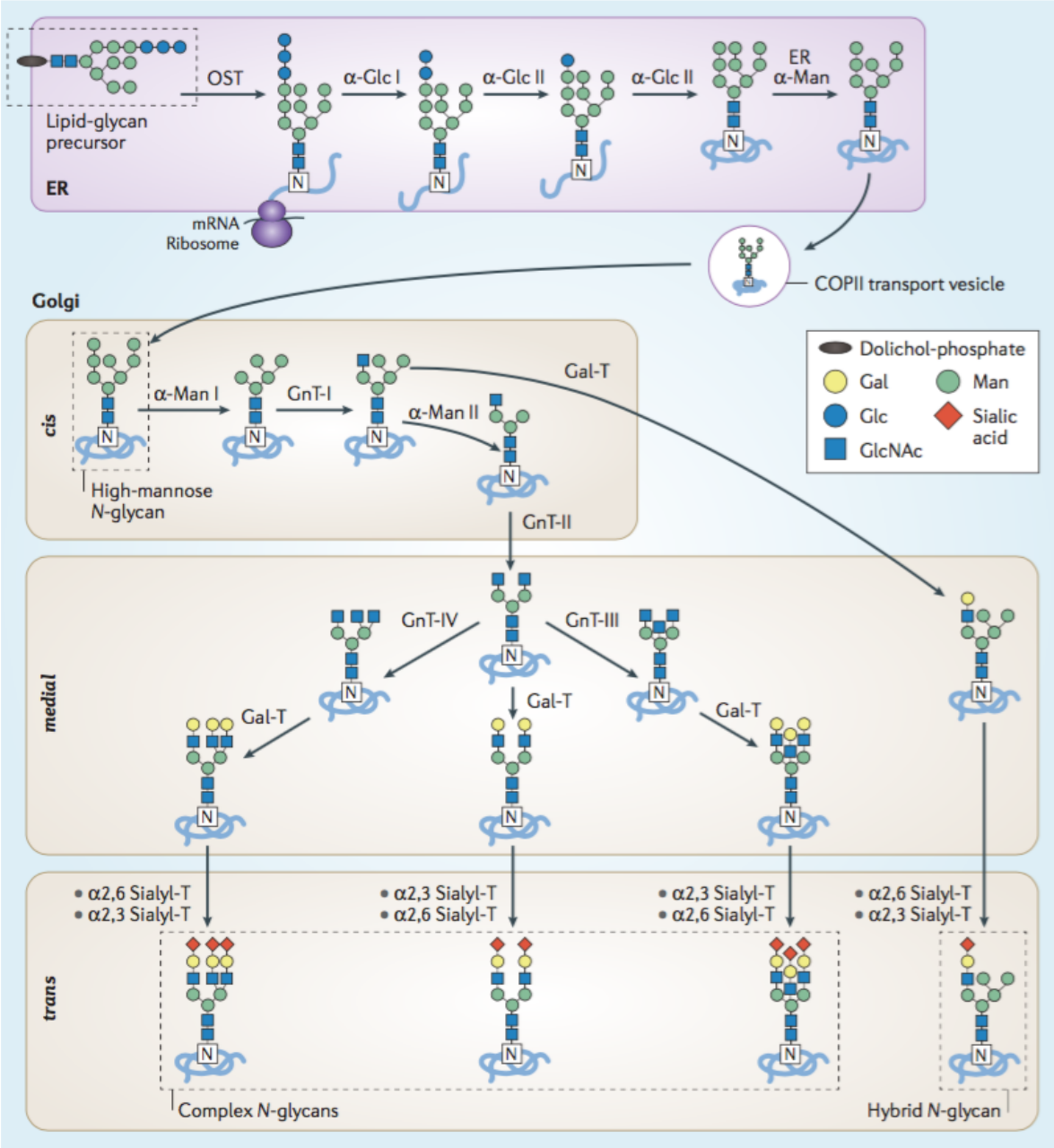

Figure 15. Schematic representation of N-glycan biosynthesis reaction in the secretory pathway. The initiation of N-linked glycosylation occurs in the ER with the transfer of a lipid-glycan precursor by oligosaccharyltransferase (OST). The following modification, including addition or trimming, of the sugars is later moved in the Golgi apparatus by α-mannosidase I and II (α-Man I and II), GalNAc-transferase I–IV (GalNT-I–IV), β1,4 galactosyltransferases (B4GalT1), α2,3-sialyltransferase (α2,3-ST) and α2,6 sialyltransferase (α2,6 ST) in a cis-to-trans distribution (Reily et al., 2019).

2.2.3.4.1 Functions of glycosylation enzymes

N-linked glycosylation is initiated by the transfer of a lipid-glycan precursor en bloc by oligosaccharyltransferase (OST), and is then processed for further modifications of glycans in the Golgi apparatus. In the 1970s, α-mannosidase II (ManII) was firstly identified in the fractions of Golgi membranes from the rat liver (Dewald et al., 1973; Tulsiani and Touster, 1985). Mannosidases are glycosyl hydrolases and can catalyze the removal of both 1,3-linked and 1,6-linked mannoses, which acts as the first committed step for the formation of complex N-glycans (Shah et al., 2008). Regulation of complex glycan structures by ManII contributes to protein folding, maturation and promotes the protein degradation through the proteasome pathway (Demaretz et al., 2021).

Among the seven members of β-1, 4-galactosyltransferase gene (B4GALT) family, B4GalT1 is the first enzyme to be identified and characterized, residing in the *trans*-Golgi cisternae and TGN (Roth and Berger, 1982; Nilsson et al. 1993). In some cell types, B4GalT1 is localized to the plasma membrane, where it acts as a receptor for oligosaccharide ligands in the extracellular matrix and plays an essential role in sperm-egg recognition (Hathaway et al., 2003; Shur and Hall, 1982; Youakim et al., 1994). Numerous other Golgi-resident proteins are also identified on the cell surface or secreted into extracellular spaces, with many of which remain incompletely understood (Uhlén et al., 2019). A recent paper reveals that the intramembrane protease SPPL3 predominantly contributes to the proteolysis and secretion of distinct Golgi-resident enzymes, including B4GALT1, GalNT2 and Man1A1, which are also present in human plasma (Hobohm et al., 2022).

2.2.3.4.2 Localization of glycosylation enzymes

Golgi-resident GTs are type II transmembrane proteins, sharing a common topology with a short cytosolic N-tail, a TMD, a luminal stem region and C-terminus. Despite these common structural domains, GTs show very little sequence homology at the level of the amino acid sequence. The TMD length (16-22 hydrophobic aa) is crucial for the localization of Golgi-resident enzymes (Munro, 1991). The plasma membrane is thought to be thicker than ER and Golgi in fungi and vertebrates, supported by the electron microscopy data, and consequently the TMD length of membrane proteins is longer for later compartments of secretory pathway than for the ER (Mitra et al., 2004; Sharpe et al., 2010; Welch and Munro, 2019). Increasing the TMD length of ST6Gal1 from 17 aa to 23 aa leucines alters the

localization from Golgi to plasma membrane, supporting the so-called “bilayer thickness model” (Munro, 1995) (Figure 16A).

A second model for GT retention is based on the observation of homo-/hetero-/oligomerization of Golgi-resident enzymes, which prevented their entry into vesicle trafficking and could be in turn retained in the certain Golgi cisternae, due to their large complex sizes (Banfield, 2011; Machamer, 1991) (Figure 16F). In this kin-recognition model, the best example is the association of ManII and GalNT1 through their stem region in the lumen (Nilsson et al., 1994). Another example is observed in the trimeric complex of B4GalT1-Sialyltransferase1(ST1)-ST2, involved in the early biosynthetic pathway of ganglioside precursors. Interestingly, ST1 is required for the association of B4GalT1-ST2, suggesting that the maturation of glycolipid is dependent on particular glycosyltransferases in distinct regions (Giraudo and Maccioni, 2003).

Interestingly, 13 aa extension at the N-terminal cytoplasmic tail of B4GalT1 long isoform (398 aa) contributes to its expression on the plasma membrane, resulting from differential transcription initiation (Lopez et al., 1991). Chimeric constructs with the long cytoplasmic tail of B4GalT1 with transmembrane target a reporter to the plasma membrane, whereas the short form is restricted to the *trans*-Golgi (Russo et al., 1992; Hathaway et al., 2003). Another study also showed that the 6 amino acid cytoplasmic tail of B3GalT1 alone was localized at Golgi (Milland et al., 2002). However, with the chimeric form of B4GalT1 cytoplasmic tail with ER-resident human invariant chain (Ii), the cytoplasmic tail of B4GalT1 alone was not sufficient to retain the hybrid protein in the Golgi (Nilsson et al., 1991). A more recent study demonstrated that the length of the N-terminal cytosolic tail and the transmembrane domain of ST negatively affects Golgi retention, and that the C-terminus of ST is sufficient to contribute to the Golgi retention (Sun et al., 2021).

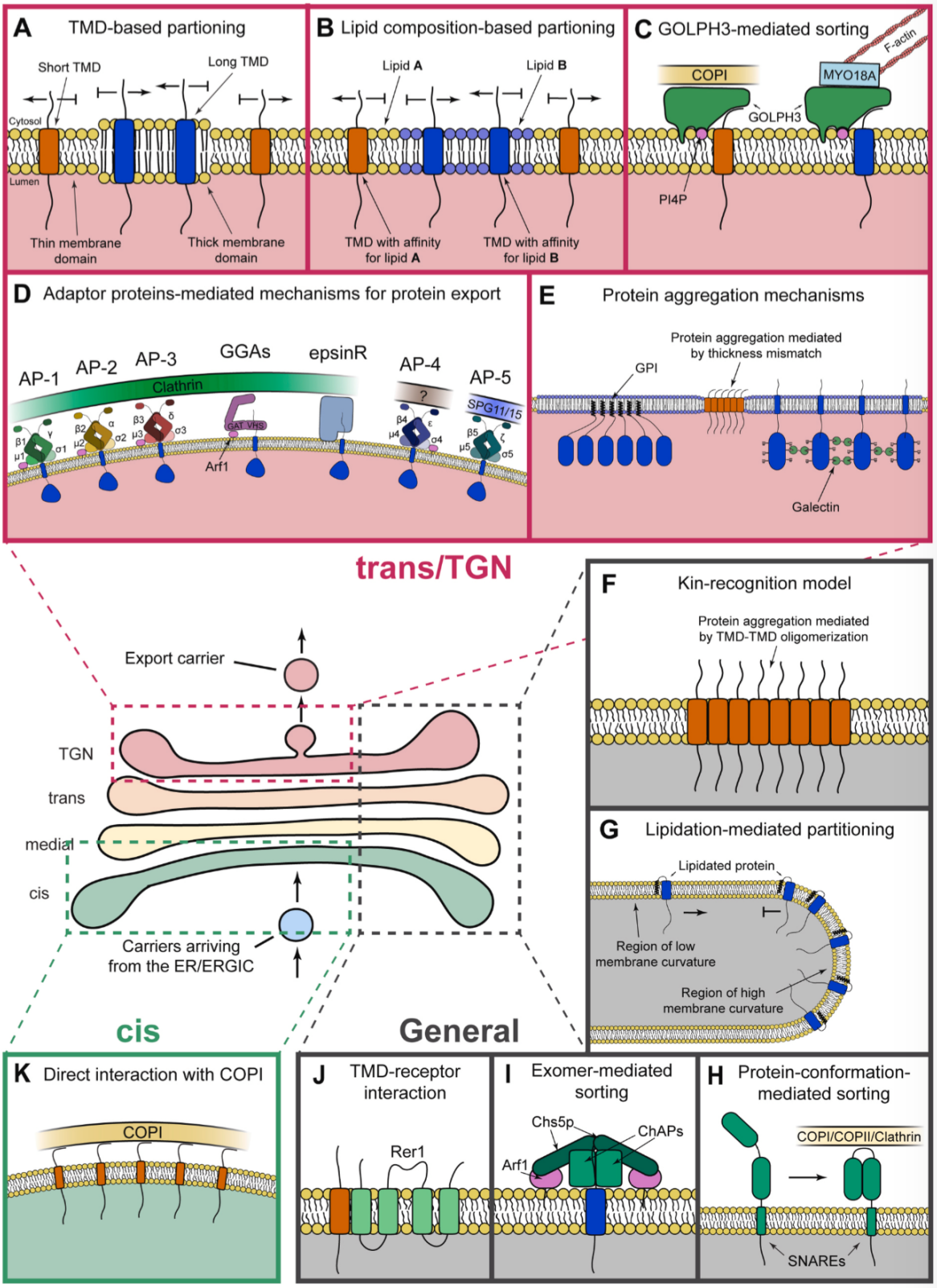

Figure 16. The molecular mechanisms of protein sorting and retention at the Golgi complex. Schematic representation of the reviewed mechanisms of protein sorting and retention at the trans-Golgi in (A-E), general in (F-J), or cis-Golgi in (K). (A) TMD-based partitioning. Secretory cargoes with longer TMDs (with >17 aa; in blue) segregate from Golgi-resident enzymes with shorter TMDs (≤17 aa; in orange). (B) Lipid-composition-

based partitioning. The cartoon shows how the amino acid composition of a protein's TMD drives the segregation into the matching membrane regions. (C) GOLPH3/Vps74-mediated sorting. GOLPH3 (in green) binds PI4P (in pink) at the trans-Golgi membranes, interacting with the cytosolic tail of TM proteins (in red and blue), with the COPI coat (in beige), and/or with the actin (in red laments) through MYO18A (in light blue). (D) Adaptor-mediated secretory protein (in blue) sorting with clathrin coat (in green), SPG11 and SPG15 coat (in blue) and with Arf1 (in pink). (E) Protein aggregation mechanisms. The aggregation of GPI (in black)-APs (in blue) induces partitioning into lipid rafts (blue membrane). Galectins (in green) cause protein aggregation by bridging the protein's luminal domains (in blue) by their N- and O-glycosylation motifs (in black). (F) The kin-recognition model. The oligomerization of Golgi-resident proteins (in orange) acts as a steric impediment that prevents their loading into transport carriers. (G) S-palmitoylated TM proteins (TMD in blue, palmitoylation in black) preferentially partition into the highly curved rims of the Golgi cisternae for sorting and export. (H) The cytoplasmic domain of SNAREs (in green) switches between an open (left) and a closed (right) conformation to interact with coat complexes (COPI, COPII, or clathrin). (I) The exomer (in green) is an adaptor protein complex that selects cargoes (in blue) for their trafficking to the PM. Each exomer binds two Arf1 (in pink) through Chs5p monomers. (J) Protein receptors Rer1 (in green) interact with TM clients (in orange) by their TMDs for protein sorting. (K) Direct interaction of some cis-Golgi-resident enzymes (in orange) with the COPI coatomer (in beige). The interaction is mediated by the cytosolic tail of the enzyme. (Lujan and Campelo, 2021)

3. Retrograde transport from the Golgi apparatus to the Endoplasmic Reticulum

In the protein secretory pathway, the biogenesis of proteins starts at the ER and requires delivery of these proteins to their final destinations within or outside of the cell by antegrade trafficking processes. During this process, the Golgi apparatus serves as a central hub to accommodate not only the cargoes but also the glycosylation enzymes. Golgi-to-ER retrograde transport is of importance to ensure the stable localization of the ER- or Golgi-resident proteins, to control the quality and function of Golgi-localized enzymes, and maintain lipid composition and components, which may be reused for further rounds of transport.

3.1 Treatment of nocodazole and brefeldin A (BFA)

How the Golgi complex maintains its structure and homeostasis through retrograde transport has been under debate since the 1980s. Nocodazole is a synthetic tubulin-binding agent, which can lead to the microtubule disassembly as well as the formation of Golgi ministacks (Iida and Shibata, 1991). In support of glycosylation enzyme recycling, one of the first evidence indicated that GalT redistributed at a slow but continuous flux to the same peripheral sites as ERGIC-53, upon nocodazole treatment. Cycloheximide, a protein

synthesis inhibitor, was present together with the nocodazole treatment, suggesting this observation was not due to the newly synthesized proteins (Cole et al., 1996).

Another common approach is antiviral antibiotic brefeldin A (BFA), which can block the ER-Golgi transport and the disassembly of the Golgi apparatus (Fujiwara et al., 1988). Studies have indicated that GBF1 acts as a key target of BFA, inducing the binding of Arf1 in the cis-Golgi as well as Arf4/5 and BIG1/2 in the TGN, facilitating the the recruitment of COP1 in the early Golgi comparements as well as clathrin-dependent coats at TGN (Lowery et al., 2013; Niu et al., 2005). The effects of BFA leads to a rapid re-localization of ManII from Golgi to ER through immunofluorescence staining and accumulates the chimeric proteins of VSVGtsO45-TGN38 in the ER upon temperature shift (Cole et al., 1998; Lippincott-Schwartz et al., 1989).

3.2 Microinjection of a dominant-negative mutant of Sar1

Studies from the Warren's laboratory did not support the recycling of Golgi-resident proteins, acetylglucosaminyltransferase I, or giantin in a nocodazole-treated model for Golgi mini-stacks (Shima et al., 1998). In contrast, microinjection of a dominant-negative mutant of Sar1 (H79G), which inhibits the recruitment of COPII complex onto ER membranes, triggers the gradual redistribution of GalNT2 from the Golgi complex to the ER over 3 hours (Storrie et al., 1998). Using photobleaching and FRAP measurements, the mean rate for Golgi-to-ER retrograde movement of B4GalT1 was estimated at 3.6% per minute, supporting the underlying recycling pathway of Golgi-resident enzymes (Sengupta and Lippincott-Schwartz, 2013).

3.3 Manipulation of ER trapping assay

To eliminate the non-specific effect of drug treatment, a modified chemically induced dimerization (CID) system was applied to test if Golgi-resident enzymes recycled through the ER. This rapamycin-induced system used the ER-retained protein Ii attached to FRB (e.g. Ii-FRB) and FKBP12-tagged Golgi enzymes or the ER-Golgi recycling protein ERGIC-53 (Pecot and Malhotra, 2006). Despite rapid recycling of FKBP12-ERGIC-53 through the ER, FKBP12 fused to the Golgi-resident enzymes remain stably located in the Golgi upon the treatment of rapamycin. This result may be due to the competition between the endogenous FKBP13 and FKBP12-tagged with Golgi enzyme, and thus inhibits the binding of FRB in the ER (Sengupta et al., 2015).

The ER-trap assay was then modified to utilize 2 plasmids of Ii-FKBP12 (e.g. Ii-FKBP12) and FRB-tagged Golgi enzymes (e.g. ManII-FRB), which reside in the ER and Golgi respectively. In presence of rapamycin, the robust trapping of Golgi-resident protein in the ER could be observed without changing the Golgi structural integrity, confirmed by the steady-state distribution of endogenous βCOP, ManII and B4GalT1 (Sengupta et al., 2015). These results implied that using Ii-FRB in the previous work may have underestimated the extent of Golgi-to-ER retrograde transport. With this modified method, it is now possible to detect the continuous recycling of Golgi enzymes back to the ER in real-time, paving the way for further exploration of mechanistic insights in retrograde transport.

3.4 Mechanisms of Golgi-to-ER transport

3.4.1 COPI-dependent retrograde transport

3.4.1.1 Retrograde transport for type I proteins

Resident soluble and transmembrane proteins undergo the processes of retention and retrieval to secure their stable distribution in the ER or Golgi, which requires the capture of the escaped ER proteins and the Golgi-to-ER retrograde transport. The cisternal maturation model of cargo transport through the Golgi apparatus implies that the Golgi-resident enzymes are continuously retrieved back from the trans- to cis- cisternae to ensure identity of the Golgi cisternae. Single-pass transmembrane proteins can be categorized into two main subtypes: Type I protein with luminal N-terminus and cytosolic C-terminus; Type II protein with cytosolic N-terminus and luminal C-terminus. Studies have demonstrated that Golgi-to-ER retrieval of type I transmembrane proteins bind to COPI-coated vesicles through direct interaction with their cytosolic C-terminal di-lysine motifs (KKXX or KXKXX), a canonical signal for ER retention (Jackson et al., 1990; Nilsson et al., 1989) (Figure 17A). The crystal structures of α-COP and β-COP demonstrate the dilysine-motif recognition (Ma and Goldberg, 2013). Another class of ER-retrieval signal, bi-arginine internal motif (ϕRXR) or FFXXBB-based motifs, has been shown on the cytosolic domains of distinct ion channels and receptors (Gassmann et al., 2005; Zerangue et al., 1999) (Figure 17A). These ER-retention/retrieval motifs serve a key role in COPI-dependent cargo recognition, which in turn regulates the targeted protein functions and their expression levels on the cell surface (Arakel and Schwappach, 2018) (Figure 17B).

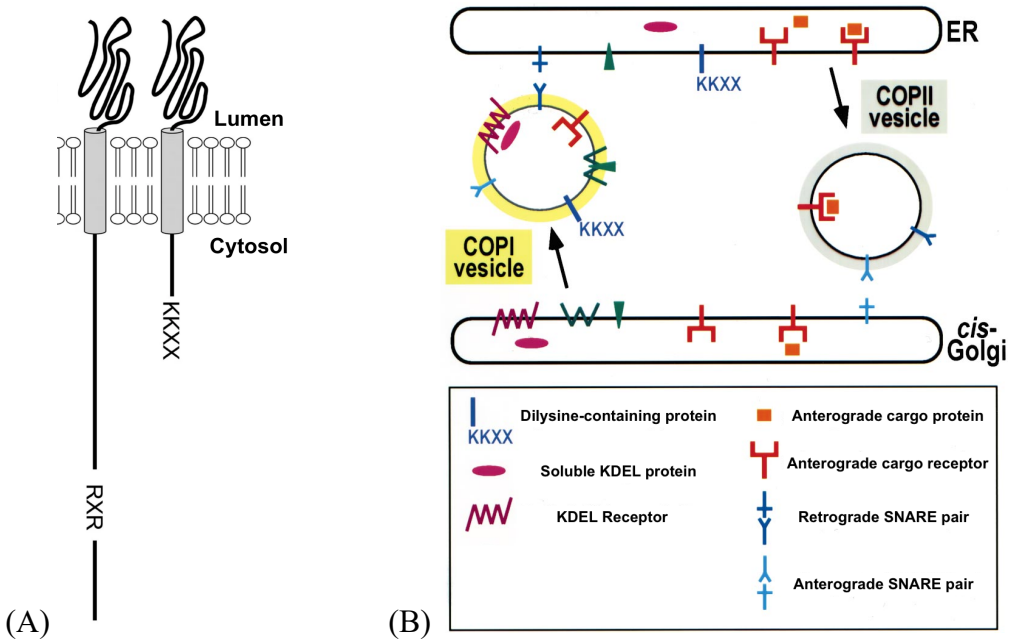

Figure 17. Schematic representation of typeI protein and model of COPI-mediated pathway. (A) Type I transmembrane proteins share common cytosolic motifs for ER retention. Left: bi-arginine internal motif (such as ϕRXR or FFXXBB-based motifs). Right: di-lysine motifs (such as KKXX or KXKXX). (B) Model of COPI-mediated retrograde transport. COPII-coated vesicles carry the anterograde cargoes and COPI-coated vesicles carry the retrograde cargoes. Some retrograde cargoes with dilysine-based motifs (e.g. KKXX) will be integrated into the COPI-coated vesicle through direct interaction with COPI. Other soluble cargoes containing KDEL will be captured by the KDEL receptor, and then recycled back to the ER. (Gaynor et al., 1998; Shikano and Li, 2003)

3.4.1.2 Retrograde transport for soluble cargoes containing H/KDEL sequences

In the 1990s, 2 genes encoded ER retention-defective 1 (ERD1) and ERD2 were firstly discovered in yeast, mediating the retention of soluble proteins in the ER (Hardwick et al., 1990; Semenza et al., 1990). Later in humans, 3 human KDEL receptors, ERD21, ERD22 and ERD23 were identified experimentally, whereas little is known about the functional role of ERD23 involved in the secretory pathway (Lewis and Pelham, 1990; Lewis and Pelham, 1992). The amino acid sequences among the 3 KDELR showed nearly identical (>90%), whereas the mRNA expression levels of ERD22 (~200%) is significantly higher than that of ERD21, and ERD23 (~5%), quantified relative to ERD21 (100%) in Hela cells (Raykhel et al., 2007). Systematic examinations also revealed that ERD21 favors KDEL-motif over HDEL-motif, and ERD23 prefers HDEL-motif over KDEL-motif, for which KDEL-motif and HDEL-motif are the most common ER-retrieval signal in all human soluble proteins.

Soluble proteins, such as ER-resident chaperones (e.g. GRP78, GRP94, PDI, etc.), bear the C-terminal luminal KDEL motif in mammals. The crystal structure of chicken KDELRs reveals the 7 transmembrane domains of KDELRs undergo a pH-dependent conformational switches upon the binding of KDEL sequences (Bräuer et al., 2019; Wu et al., 2020). The change of conformation of KDELR induced by the binding of KDEL exposes a di-lysine motif which enables direct binding to COPI. The stable complex of KDELR with its ligand favors the acidic environment in the Golgi (pH=6.2), and the dissociation of the complex can be achieved in the ER (pH=7.2-7.4), promoting the protein retrieval from Golgi apparatus back to ER (Wilson et al., 1993).

Upon binding of KDEL motif to KDELR, KDELR can be phosphorylated by protein kinase A (PKA), which recruits the COPI complex, and ultimately promotes the Golgi-to-ER retrograde transport along with the cargos (Cancino et al., 2014). Moreover, a study also indicated that the binding of KDELR with its ligand, in a GPCR-like fashion, activated a pool of Golgi Gαq/11 proteins and Src kinases, which consequently modulates the intra-Golgi transport and maintains the Golgi homeostasis (Giannotta et al., 2012; Pulvirenti et al., 2008). Interestingly, a report has indicated that the complex of myc-TGN38 and anti-myc antibody conjugated with terminal KDEL-motif can together be internalized and recycled from the cell surface to ER, and further processed to N-linked glycosylation (Miesenböck and Rothman, 1995). This experiment also implied the localization of KDELR in the post-Golgi or TGN. Additionally, recent studies have shown a small fraction of KDELR1 also localizes on the cell surface as a membrane receptor for mesencephalic astrocyte-derived neurotrophic factor, and the KDELRs cycle between plasma membrane and Golgi via clathrin-dependent pathway (Becker et al., 2016; Jia et al., 2021).

3.4.1.3 Retrograde transport for glycosylation enzymes

Glycosylation enzymes are type II transmembrane proteins, lacking canonical signal for interaction with COPI subunits. However, more evidence has indicated that Golgi glycosylation enzymes are continuously recycled from Golgi back to ER, with the involvement of COPI-coated vesicles (Cole et al., 1998; Lippincott-Schwartz et al., 1989). A recent study demonstrated direct binding of the cytoplasmic tail of some *cis*-Golgi resident glycosylation enzymes, including GalNAc-1-phosphotransferase, C2GNT1, GALNT3 and GALNT8, with the δ and ζ subunits of COPI (Liu et al., 2018). Studies performed in yeast have demonstrated the role of Vps74 in the retention of glycosyltransferases in the Golgi

apparatus (Tu et al., 2008). It has been reported that Golgi phosphoprotein 3 (Golph3), the mammalian homolog of Vps74, supports the incorporation of some Golgi enzymes into COPI vesicles (Eckert et al., 2014) (Figure 16C). Knockdown of Golph3 suppressed the expression of ST6GAL1 and B4GalT5, lowered the levels of N-glycosylation and in turn blocked the cell migration and cell growth (Isaji et al, 2014; Rizzo et al., 2021). However, Golph3 is not required for incorporation of GalNAc-1-phosphotransferase and C2GNT1 into β-COP vesicles (Liu et al., 2018). A recent report revealed that both Golph3 and Golph3L, a paralogue of Golph3, are broad-spectrum cargo adaptors for numerous Golgi-resident proteins docking to the COPI-coated vesicles, with 102 out of 249 proteins (41%) of COPI proteome identified (Welch et al., 2021).

To achieve membrane trafficking, vesicle docking and membrane fusion also require the physical and functional interaction of COG complex with a set of Golgi-localized golgins, SNARE proteins, and so on. Multiple approaches, such as knockout (KO), knockdown (KD) and knock-sideways, have been performed to elucidate the detailed functions of COGs (Bailey Blackburn et al., 2016; Blackburn and Lupashin, 2016; Zolov and Lupashin, 2005; Willett et al., 2014). The depletion of COG subunits causes a massive accumulation of COG complex-dependent vesicles, malglycosylation of N- and O-linked glycans and mislocalization or degradation of Golgi-resident glycosylation enzymes, such as ManII, B4GalT1, B3GalT2, ST3Gal1 and GalNT1 (Foulquier, 2009; Shestakova et al., 2007). By means of auxin-inducible degron (AID) system, a recent report shows the acute depletion of COG4 significantly displaces the COG1, COG3 and COG8 complex, decreases the localization of β- and γ-COP, and in turn affects the expression and localization of MGAT1 and B4GalT1 (Sumya et al., 2022).

3.4.2 Rab6-dependent retrograde transport

Rab6-dependent retrograde transport has also been observed, a pathway which can be hijacked by ricin or Shiga toxin (Fuchs et al., 2007; Utskarpen et al., 2006). Rab6 is enriched on post-Golgi compartments, facilitating the intra-Golgi as well as recycling endosomes-to-TGN transport (Martinez et al., 1994; Mallard et al., 2002). It has been documented the existence of two Rab6 isoforms, Rab6A and Rab6A′, which only differ in 3 amino acid residues in the GTP-binding domains (Echard et al., 2000). 2 isoforms also show the functional differences, with Rab6A involved in the Golgi-to-ER transport and Rab6A’ in the endosome-to-trans-Golgi pathway. Pioneering work revealed that Golgi enzymes rely on

Rab6 GTPase to return back to the ER, using tubules rather than vesicles (Girod et al., 1999; White et al., 1999). In spite of this COPI-independent pathway in the late 1990s, it remains relatively uncharacterized with only a handful of coordinated molecules. The Rab6-mediated tubulation is initiated through membrane curvature, to which the lipid composition may contribute. The presence of lysophospholipid in the Golgi yields a positive curvature in the membranes, depending on the activities of opposing lipid-modifying enzymes, phospholipase A (PLA) and lysophospholipid acyltransferase (LPAT) (Yang et al., 2011). It is hypothesized that the balance of these two enzyme activities at the Golgi membranes determine whether to undergo the COPI-dependent vesicular transport or COPI-independant tubular transport. If LPAT shows lower activities than PLA, which generates lysophospholipid through the hydrolysis of phospholipids, the loss of phospholipid would then decrease the tubule lengths and the retraction of Golgi membrane (Heffernan and Simpson, 2014).

Rab6-dependent tubulation also depends on the dynein-dynactin motor complex, linked with the cargo and the associated membrane with cytoskeleton. Both Rab6A and Rab6A' isoforms can specifically interact with dynein light chain roadblock type 1 (DYNLRB1), colocalized at the Golgi complex with Rab6 (Wanschers et al., 2008). Dynactin can also bind to both Rab6A isoforms and be recruited to the Golgi membranes, together with the dynactin subunit p150-glued and p50-dynamitin (Short et al., 2002). These studies have also implicated the α-helical coiled-coil homodimer protein, Bicaudal-D (BICD), as another effector of the dynein–dynactin motor complex. BICD is highly conserved across species, such as *Drosophila melanogaster* and *Caenorhabditis elegans*, and serves as an important role during oogenesis (Mach and Lehmann, 1997). Two homologues in mammals, BICD1 and BICD2 colocalized with Rab6A as well as the dynein–dynactin complex on the trans-Golgi network and on the vesicles in the cytoplasm (Matanis et al., 2002; Short et al., 2002). The N-terminus of BICD can interact with cytoplasmic dynein, and the C-terminus of BICD binds to Rab6, together bridging the Golgi membranes and the motor complex and controlling the COPI-independent Golgi-to-ER transport (Hoogenraad, 2001; Matsuto et al., 2015).

Aside from the effects of Rab6 on the microtubule formation, it is worth considering how myosin motor proteins may participate in the retrograde transport. A conventional myosin, myosin II, can associate with the TGN membrane during the vesicle budding process (Stow et al., 1998). Treatment of myosin light chain kinase inhibitor, ML7, impairs BFA-

induced Golgi assembly, and the inhibition of actin ADP ribosylation through C2 toxin interrupts the arrival of Shiga toxin B subunit to the ER (Durán et al., 2003; Valderrama et al., 2001). However, since myosin II is not seen as a Golgi-resident protein, the precise mechanism and the functional role of myosin II in the retrograde transport remains unclear. A previous study showed that the formation of Rab6-myosinII complex contributes to their Golgi localization and the fission of Rab6-positive vesicles. It is of note that Rab6-myosinII complex is required for the anterograde transport of VSVGtsO45 to the plasma membrane and the Golgi-to-ER retrograde transport of Shiga toxin B (Miserey-Lenkei et al., 2010).

One of the first published studies showed that the Golgi-to-ER retrieval of ERGIC-53 and KDEL receptor, but not that of Shiga toxin B, is impaired with the micro-injection of anti-COPI antibodies (Girod et al., 1999). Overexpression of GTP-Rab6A and Rab6A' isoforms can both enhance the microtubule-dependent Golgi-to-ER recycling of ManII and B4GalT1 enzymes, whereas the GDP-Rab6A isoforms inhibit the ER redistribution of Golgi-resident enzymes in response to hypotonic stress (Jiang and Storrie, 2005; Young et al., 2005). To shed light on the Golgi-to-ER retrograde transport in real-time, the ER-trapping assay has been performed as mentioned previously. During the investigation of rapamycin-induced Golgi enzyme recycling back to the ER, long Golgi tubules, enriched with ST-FRB-EGFP, could be observed extending off the perinuclear Golgi and then breaking off from the tips (Sengupta et al., 2015). However, in presence of GDP-Rab6A, Man II-FRB-Venus remained concentrated in the compact Golgi complex upon the rapamycin treatment. Taken together, these results suggest that the activity of Rab6a is required for the ER redistribution of Golgi enzymes.

3.4.3 GALNTs activation (GALA) pathway

As discussed previously, KDELR can serve as not only a cargo receptor to capture the escaped ER-resident proteins in the Golgi complex, but also a signaling receptor in a GPCR-like fashion to activate a pool of Golgi Gαq/11 proteins and Src kinases (Giannotta et al., 2012; Pulvirenti et al., 2008). Src have major effects on Golgi structure, the activation of downstream dynamin 2, and the relocation of KDELR (Bard et al., 2003; Weller et al., 2010). In the GALA pathway, Src activation induces the Golgi-to-ER redistribution of GalNAc transferases (e.g. GALNT1) in tubular transport carriers, then significantly enhances the O-glycosylation, and in turn increases the levels of the Thomsen–Friedenreich antigen (Tn), which can be measured via HPL and VVL lectin staining (Gill et al., 2010). It was proposed

that the Golgi-to-ER transport of GalNTs is driven by the Src kinase and can be negatively regulated by ERK8 (Chia et al., 2019). The relocation of GALNTs can be induced by the growth factors, EGF and PDGF, or by the treatment of imidazole, consistent with the previous findings (Thomas and Brugge, 1997; Qiao et al., 2006)

The GALA pathway is highly involved in tumor development and metastasis, including breast, lung and liver cancers (Nguyen et al., 2017; Ros et al., 2020). However, the detailed mechanistic model of the GALA pathway remains unclear. A recent paper reveals that Src activation results in the increased levels of Arf1-GTP onto Golgi membranes, which is driven by GBF1 recruitment (Chia et al., 2021) (Figure 18). Interestingly, the activation of Src kinase does not drive the recruitment of β-COP onto the Golgi membranes in the early stage of GALA pathway (around 20 mins treatment of imidazole) (Chia et al., 2021). It has been demonstrated that ArfI is also involved in the formation of tubular carriers, with around 3 μm in length and 110 nm in diameter, on which are largely free of COPI complex and clathrin (Bottanelli et al., 2017). This may explain that COPI may not participate in the GalNT relocation upon Src activation. However, Src activation mediates the redistribution β-COP and γ-COP from the Golgi apparatus into the punctate structure containing GalNT1, after 4 hours of EGF treatment (Gill et al., 2010). Further investigation is still required to confirm the key regulator in the formation of transport carriers.

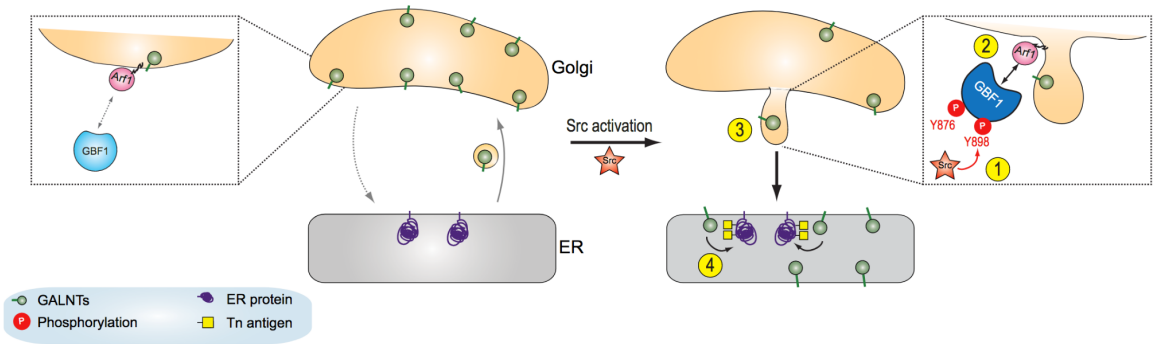

Figure 18. A model of Src-induced Golgi-to-ER retrograde trafficking of GalNT enzymes (GALA pathway). Under normal conditions, the interaction of GBF1-Arf is limited and retrograde transport is moderate with GalNTs predominantly localized to the Golgi apparatus (shown on the left). Upon Src activation, GBF1 is phosphorylated (Step 1), leading to increased affinity of Arf-GDP on Golgi membranes (Step 2). GalNTs are selectively relocated to the ER through the formation of Golgi tubules (Step 3). This increases the efficiency of O-glycosylation onto the ER-resident substrates (Step 4). (Chia et al., 2021)

3.4.4 Glycosylation malfunction in health and disease

3.4.4.1 N-glycans in cancer progression

Dysregulation of glycosylation has been implicated in multiple human diseases, such as congenital disorders of glycosylation (CDG) as well as auto-immune, infectious diseases and cancer. Studies demonstrated that the glycosylation pattern is widely used as a biomarker in various malignant cancers (Pinho and Reis, 2015). Colon and pancreatic cancer display elevated levels of sialyl-Lewis antigens (SLn) due to the up-regulation of several sialyltransferases (ST), including ST6GAL1, ST3GAL3 and ST3GAL4 and in turn led to poor prognosis and low survival rates in cancer patients (Nakayama et al., 1995; Chakraborty et al., 2018; Perez-Garay et al., 2013) (Figure 19). Enhanced expression of ST6GalI is also associated with pro-survival signaling pathways through the inhibition of FAS ligand-induced apoptosis (Britain et al., 2018) (Figure 19, B). The increased levels of sialylation on EGFR promote its activation and protect the anticancer drug gefitinib-mediated cell death (Swindall and Bellis, 2011) (Figure 19, C). Another type of glycan signature, Thomsen–Friedenreich antigen (Tn), can also be detected at high expression in most carcinomas, such as bladder, ovarian and breast cancer. Studies demonstrated that elevated surface level of Tn antigen is due to relocalization of some Golgi enzymes in the ER promoting cancer invasiveness through the GalNAc-T Activation (GALA) pathway, in which GalNAc-T family of enzymes serve as the initial enzymes of O-glycosylation (Gill et al., 2010). In addition, the abnormal synthesis of Tn is also associated with the dysregulation of C1GALT1, together with its specific chaperone COSMC, and in turn modulates cell adhesion and metastasis in various cancer types (Ju and Cummings, 2002; Sun et al., 2021). These studies highlight the importance of a detailed understanding and of a correct regulation of the intracellular trafficking of Golgi-resident glycosylation enzymes.

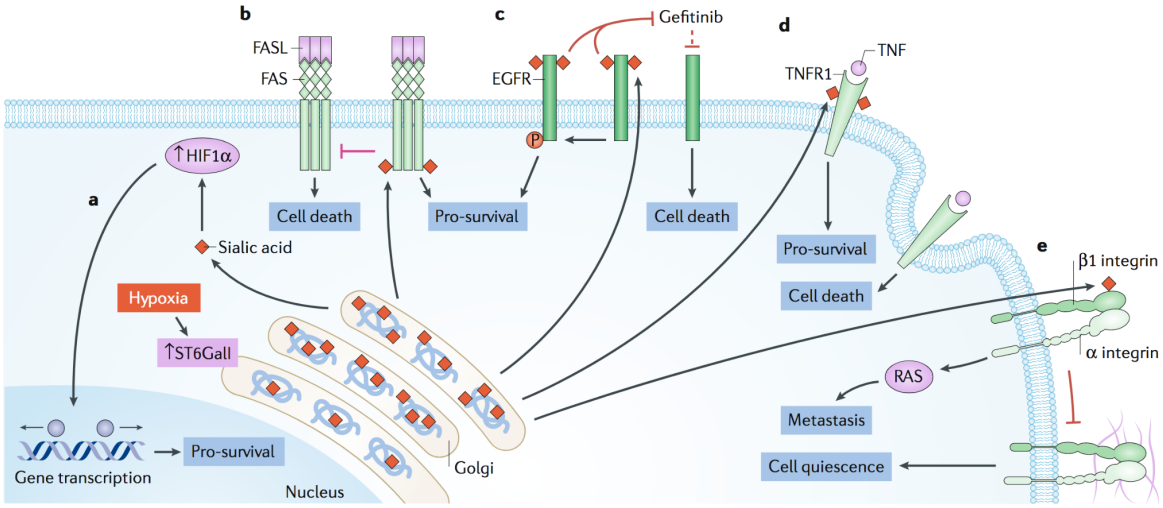

Figure 19. The dysregulation of ST6Gal1 results in abnormal sialylation, observed in many types of cancers. (A) Due to hypoxia, the increased expression and activity of ST6GalI leads to enhanced α2,6-sialylation, upregulating HIF1α and the expression of pro-survival HIF1α target genes, including growth factors and glucose transporters. (B) The sialylation of cell surface death receptor FAS by ST6Gal1 inhibits the apoptotic signaling and receptor internalization. (C) Increased expression of sialylated epidermal growth factor receptor (EGFR) enhanced its tyrosine kinase activity, the phosphorylation of its downstream targets, and the activation of pro-growth and survival genes. (D) Reduced α-2,6 sialylation prolonged the activation of tumor necrosis factor (TNF), and the internalization of TNF results in caspase activation and cell death. (E) Hypersialylation of β1 integrin in the Golgi apparatus inhibits its binding affinity to matrix proteins, such as type I collagen and fibronectin, and prevents downstream signaling. (Reily et al., 2019)

3.4.4.2 Chaperone dysfunction in disease

Likewise, dysregulation of KDEL-mediated retrograde transport is also associated with numerous diseases. One example is the chaperone named Calreticulin (CALR), which has been demonstrated to escape from the ER and be secreted at the cell surface with oncogenic consequences. Surface exposed CALR is caused by mutations in the exon 9, yielding CALR protein lacking the C-terminal KDEL sequences and has been reported in around 30% of patients with myeloproliferative neoplasms (MPNs) (Grinfeld et al., 2018; Nangalia et al., 2013). In addition, the expression of surface CALR has been identified in multiple human cancers, including many leukemias, lymphomas, bladder cancer and ovarian cancer (Chao et al., 2010). The surface exposed CALR acts as an “eat-me” signal and allows the dendritic cells to recognize the dying cancer cells, favoring the anti-tumor immune responses (Liu et al., 2020). On the other hand, the secretion of soluble CALR was also observed upon anticancer chemotherapy, which in turn stimulates wound healing and angiogenesis (Pike et al., 1998). These studies demonstrate why advancing our understanding

of the Golgi-to-ER retrograde transport pathways is important in the context of diseases, such as cancers. Our project aims at describing the kinetics and identifying mechanistic regulators of two Golgi-to-ER retrograde routes, the ER recycling of Golgi glycosylation enzymes and the KDEL-mediated ER retrieval pathway.

Results

1. Introduction

1.1 Retention Using Selective Hooks (RUSH) assay

Many approaches have been developed in the past years to study the secretory pathways of a fraction of targeted proteins, such as photoconversion or photobleaching. Another classical method is to synchronize and monitor the transport of the tsO45 mutant protein of VSVG tagged with GFP, upon the temperature shift from 40°C to 32°C. However, there is still a need for a versatile trafficking assay to analyze the transport of diverse cargos, especially under physiological conditions. The Retention Using Selective Hooks (RUSH) assay developed in our lab provides new insights into protein transport and a quantitative analysis to track the secretory cargoes in real-time. The RUSH assay, based on Streptavidin-SBP (Streptavidin binding peptide) interaction, allows to synchronize the transport of cargos from the ER to downstream compartments, such as plasma membrane and endosomal system, and to get rid off the steady-state equilibrium between anterograde, retrograde, neo-synthesis and degradation pathways (Boncompain et al., 2012). This synchronization system does not rely on the protein aggregation mechanisms, such as methods based on mutant of FKBP domains (Rivera et al. Science 2000, Casler et al. Mol Biol Cell 2020), and therefore does not induce ER deformation or ER stress. In addition, RUSH assay also provides the possibility to synchronize the traffic of several cargoes simultaneously in one cell, and to analyze the protein secretion kinetics in multiple transport pathways.

The bicistronic RUSH plasmids with diverse hooks and cargoes have been generated in the lab, which can be thus used to examine the trafficking of various protein types. On one hand, the use of mutated form of stromal interaction molecule 1 (STIM1-NN; type I protein) and human invariant chain of the major histocompatibility complex (Ii; type II protein), fused to streptavidin, allows the stable localization of the hooks in the ER. In addition, the fusion of the KDEL-motif to the C-terminus of streptavidin enables its retention in the lumen of ER. Streptavidin fused to the N-terminus of Golgin-84 could be used as a cytoplasmic hook in the Golgi apparatus (Boncompain et al., 2012). On the other hand, the RUSH assay could be applied to monitor the protein traffic of diverse cargoes, fused to SBP-EGFP as a reporter, such as calreticulin (CALR; soluble protein), β-secretase 1 (BACE1; type I protein), targeting domain of Golgi enzymes (ManII* and ST*; type II protein), tumor necrosis factor (TNF; type II protein), CC chemokine receptor 5 (CCR5; transmembrane protein), etc (Boncompain

et al., 2012; Fourriere et al., 2016; Jin et al., 2018; Liu et al., 2020; Tan et al., 2020). Owing to the interaction of streptavidin and SBP, the reporter protein can be retained in the ER, and then released with the addition of biotin. The authors have demonstrated the simultaneous imaging of ER-to-Golgi, intra-Golgi, and post-Golgi transport in living cells, consistent with the previous study (Boncompain et al., 2012). The RUSH-synchronized secretory protein transport allows us to acquire real-time protein transport at physiological temperature as well as quantitative measurements of traffic kinetics in the secretory pathway.

To better understand the mechanisms of intracellular trafficking, the RUSH assay is amenable to high-content screening, enabling the identification of key regulatory factors and further the exploration of novel therapeutic strategies during disease development. Through the study of RUSH-synchronized soluble secretory GFP, fused to SBP (ss-SBP-EGFP), the authors identified and validated a series of protein secretion-inhibitory drugs from the Prestwick chemical library. 12 out of 1200 approved drugs were selected in the large-scale screens, inhibiting the extracellular accumulation of ss-SBP-EGFP (Zhao et al., 2018). These secretion inhibitors vary in their effects on protein synthesis, morphology of ER network and integrity of Golgi apparatus in the conventional protein secretion pathway (Zhao et al., 2018). For another example of RUSH-synchronized SBP-EGFP-CCR5, which is a main co-receptor for the entry of HIV-1, the authors also identified 15 strongest hits from 2 libraries, including Prestwick Chemicals (1200 drugs) and U.S. National Cancer Institute (NCI; 2824 drugs). 3 out of the 15 selected drugs demonstrated with specificity to the transport of CCR5, but not that of CCR1 and CXCR4. The treatment of 3 of the molecules also inhibited the HIV-1 infection and viral production in human macrophages, paving a way to a new therapeutic avenue (Boncompain et al., 2019).

1.2 Reversible RUSH assay

Synchronous release of the reporter from the hook occurs upon the addition of biotin, thanks to the high affinity of biotin towards streptavidin. However, biotin has a small dissociation rate to streptavidin, impairing its detachment from streptavidin and reversibility of the RUSH assay. The discovery of Artificial Ligand of Streptavidin (ALiS) overcame this drawback (Terai et al., 2015). With the collaboration with Takuya Terai from University of Tokyo, the association and dissociation of streptavidin-ALiS system through high-throughput screening of a chemical library was described. Their results demonstrate that the direct binding constants between streptavidin and ALiS-1 is 5.8×10^{-6} M, compared to that between

streptavidin and biotin is around 10^{-14} M (Terai et al., 2015). Their later findings also show improved solubility of ALiS-3 in PBS by 5-fold in contrast to ALiS-1, while with similar binding constants of 5.6×10^{-6} M (Tachibana et al., 2017). Using ALiS-1 and ALiS-3 in RUSH assay, it could be clearly seen that ALiS entered the cells and induced the ER-to-Golgi transport of the truncated form of a Golgi enzyme α-mannosidase 2 (ManII-SBP-EGFP) upon the treatment of ALiS derivatives, similar to the effects of biotin-induced anterograde transport (Tachibana et al., 2017; Terai et al., 2015).

In contrast to biotin, the treatment of ALiS brought the reversibility to RUSH assay and enabled the quantitative analysis of Golgi-to-ER retrograde transport. The authors showed that the anterograde transport of ManII-SBP-EGFP can be observed from ER to Golgi apparatus in 1 hour with the treatment of ALiS-3, and the reporters can be detected back to the ER after ALiS-3 washout for 1.5 hour, as confirmed by the quantification of kinetics (Tachibana et al., 2017). The process of ALiS-3-mediated anterograde and retrograde transport can be achieved for several cycles. This not due to newly synthesized protein in the ER, since transport occurs in the presence of cycloheximide, a protein synthesis inhibitor.

2. Objectives

How the Golgi apparatus regulates the protein or lipid synthesis and transport through retrograde transport has been extensively discussed since the 1980s. With the microinjection of dominant-negative form of Sar1 or the treatment of nocodazole or BFA, the recycling of some Golgi-resident proteins back to the ER could be observed in the previous literature (Cole et al., 1996; Lippincott-Schwartz et al., 1989; Storrie et al., 1998). The method of ER-trap assay also provides a way to detect the continuous Golgi-to-ER recycling of glycosylation enzymes in real-time. However, the tools are missing to monitor and analyze the mechanisms between ER and Golgi, especially for Golgi-to-ER retrograde transport. Therefore, we took advantage of the reversible RUSH assay in this project, focusing on the retrograde transport from Golgi apparatus back to ER.

2.1 Explore the Golgi-to ER retrograde transport pathways and identify the regulatory factors through reversible RUSH assay

We started our study by analyzing the KDEL-mediated retrieval pathway of Golgi cargoes. Streptavidin fused to a KDEL motif was stably co-expressed in HeLa cells with truncated form of Golgi enzymes α-mannosidase 2 (ManII*) or sialyltransferase (ST*), fused to SBP-EGFP, as reporter proteins (See the manuscript in Figure 1). Through reversible RUSH assay, we aim to achieve the synchronization of both anterograde and retrograde transport of Golgi reporters in a population of cells, and the transport kinetics of *cis*- and *trans*-Golgi cargos is to be quantified and analyzed. It is important to note that the Golgi-to-ER retrograde transport we examine here occurs through the KDEL-mediated pathway.

To further explore the Golgi-to-ER recycling of Golgi-resident glycosylation enzymes, we also use an “immobile” ER-resident protein fused with Streptavidin. Our experiments aim to demonstrate the anterograde and retrograde transport in real-time through the use of Ii-Str as a ER stable hook and ManII*- or ST-SBP-EGFP as reporters (See the manuscript in Figure 2). These two sets of data allow quantitative measurements of the KDEL-mediated transport and glycosylation enzymes recycling pathways through the ER and enable us to test regulatory factors for these two transport pathways.

Studies have revealed that different glycosylation enzymes were recycled through COPI-dependent or Rab6-dependent pathways. To identify some regulatory factors in Golgi-ER retrograde transport, siRNA knockdown experiments, targeting to some known regulators,

such as Golgi phosphoprotein 3 (GOLPH3), Conserved Oligomeric Golgi (COG) complex, and Rab6, are to be performed in the above-mentioned cell lines. Depletion of different subunits of the COG complex led to the dysfunction and mislocalization of diverse glycosylation enzymes, which consequently result in severe diseases known as Congenital Disorders of Glycosylation (CDG) (D'Souza et al., 2020; Ondruskova et al., 2021; Zolov and Lupashin, 2005). We expect to highlight differential regulators, some involved in the KDEL-mediated pathway and others in the ER recycling of glycosylation enzymes. A kinetics analysis of two retrograde pathways in the siRNA depleted cells is to be conducted.

2.2 Examine the Golgi-to ER retrograde transport of Golgi-resident enzymes

Evidence has shown that Golgi glycosylation enzymes are continuously revisiting the ER. We then apply the reversible RUSH assay to study the recycling of the full length Golgi-resident enzymes, including fucosyltransferase 8 (FUT8) and polypeptide N-acetylgalactosaminyltransferase 1 and 4 (GalNac-T1 and -T4), fused to SBP-mCherry and SBP-EGFP, respectively. The ER-retention of full length enzymes and reversible RUSH assay is to be examined and analyzed through quantitative measurement. The depletion of some selected regulatory factors is also tested through RNA interference.

Evaluating the transport of Golgi enzymes in the context of their overexpression might disturb their trafficking mechanisms, we thus try to analyze the transport of Golgi enzymes at their endogenous level. Using CRISPR/Cas9 or CRISPaint, we edited the gene encoding for MAN2A1, GALNT1 and B4GALT1 to insert SBP-EGFP or SBP-mNeonGreen (Mali et al., 2013; Schmid-Burgk et al., 2016). In order to create less artifacts, both hooks of streptavidin fused with KDEL and ER stable hook were expressed in the selected heterozygous clones. With the clonal cell lines, we performed reversible RUSH assay, and examined the bidirectional transport of endogenous Golgi glycosylation enzymes through the KDEL-mediated and glycosylation enzyme recycling pathways.

The synchronization techniques combining the RUSH assay and the use of ALiS enabled us to monitor the anterograde and retrograde transport between ER and Golgi apparatus in real-time and in a quantitative way. Our current results confirmed the existence of two distinct Golgi-to-ER retrograde transport routes, including KDEL-mediated and glycosylation enzymes recycling pathways.

3. Manuscript in preparation

"Synchronization of transport of Golgi glycosylation enzymes enabled a quantitative analysis of Golgi-to-ER retrograde transport"

Yen-Ling Lian, Séverine Divoux, Gaelle Boncompain and Franck Perez
Dynamics of Intracellular Organization Laboratory, Institut Curie, PSL Research University, Centre National de la Recherche Scientifique, UMR 144, Paris, France.

Abstract

Bidirectional transport of proteins between the endoplasmic reticulum (ER) and the Golgi apparatus is essential to ensure proper localization of enzymes in these intracellular compartments enabling them to achieve their function. However, tools are missing to quantitatively analyze transport mechanisms between ER and Golgi, especially for retrograde Golgi-to-ER transport. Here we show that synchronization of Golgi-to-ER retrograde transport is enabled by combining the Retention Using Selective Hooks (RUSH) assay and artificial ligands of Streptavidin (ALiS). Using "dynamic" or "immobile" ER hooks, KDEL-mediated ER retrieval and ER recycling of Golgi glycosylation enzymes was quantitatively analyzed and showed differences in their kinetics. In addition, we tested the role of the known regulators of retrograde transport, COG3 and Rab6, in these Golgi-to-ER transport routes. Finally, we demonstrated that we can get rid of working with overexpressed Golgi glycosylation enzymes and generated genome-edited cells leading to synchronization of the bidirectional transport of endogenous Golgi glycosylation enzymes.

Introduction

In mammalian cells, protein transport across cellular compartments is essential for many functions, such as nutrient uptake, adhesion or signaling. Multiple trafficking pathways co-exist in cells conveying proteins in the anterograde and retrograde directions. At the center of the trafficking routes, the Golgi apparatus processes and sorts cargos. In the anterograde direction, from endoplasmic reticulum (ER) to post-Golgi compartments such as the plasma membrane or the endosomal system, newly synthesized proteins are post-translationally modified by Golgi-resident enzymes and sorted to their final destination. In the opposite direction, the Golgi-to-ER and the intra-Golgi retrograde transport pathways ensure stable localization of ER resident proteins and correct localization of Golgi glycosylation enzymes, respectively. Proper localization of proteins in intracellular compartments is essential to ensure function. For instance, ER chaperones are needed to help folding of proteins in the lumen of ER and Golgi glycosylation enzymes are required to present in the appropriate sub-Golgi compartments, as they act to decorate proteins with glycans in a sequential manner.

Soluble proteins, such as ER-resident chaperones, bear the C-terminal luminal KDEL motif (Munro and Pelham, 1987). Upon the binding of the KDEL motif to KDEL receptor (KDEL-R), the di-lysine retrieval motif is exposed and COPI is recruited, promoting Golgi-to-ER retrograde transport of the complex (Lewis et al. 1990, Bräuer et al., 2019). Golgi glycosylation enzymes are type II transmembrane proteins, lacking canonical signal for interaction with COPI subunits. However, evidence has indicated that Golgi glycosylation enzymes are continuously recycled from Golgi back to ER, with the involvement of COPI-coated vesicles (Lippincott-Schwartz et al., 1989; Cole et al., 1998). At steady-state about 10% of glycosylation enzymes are localized in the ER (Rhee et al. 2005). A study demonstrated that some cis-Golgi resident glycosylation enzymes bind directly with the δ and ζ subunits of COPI thorugh their cytoplasmic tail (Liu et al., 2018). Some regulators of retrograde transport have been identified such as components of Conserved Oligomeric Golgi (COG complex) or the small GTPase Rab6 (Girod et al., 1999; Sengupta et al., 2015; Smith et al., 2009; White et al., 1999; Zolov and Lupashin, 2005).

In some pathological conditions, improper localization of ER-resident or Golgi-resident proteins have been demonstrated. One example for ER-retrieval mediated by the KDEL motif is the chaperone named Calreticulin (CALR), which has been revealed to escape from the ER and be secreted at the cell surface leading to oncogenic properties. The expression of surface CALR has been identified in multiple human cancers, including many

leukemias, lymphomas, bladder cancer and ovarian cancer (Chao et al., 2010). In tumor development and metastasis, including breast, lung and liver cancers, ER localization of Golgi glycosylation enzymes through the GalNAc-T activation (GALA) pathway have been described (Nguyen et al., 2017; Ros et al., 2020). Relocation of GalNAc-Ts enzymes is induced by growth factor stimulation or Src activation, and leads to aberrant glycosylation associated with elevated levels of the Thomsen–Friedenreich antigen (Tn) (Gill et al., 2010). These studies demonstrate why advancing our understanding of the Golgi-to-ER retrograde transport pathways is important in the context of diseases, such as cancers.

Very few prior studies attempted to set out a dynamic analysis of the Golgi-to-ER retrograde transport of Golgi reporter proteins (Pecot and Malhotra, 2006; Sengupta et al., 2015). However, as the Golgi apparatus is a dynamic organelle, maintaining its organization thanks to bidirectional trafficking flows, the steady state analysis of protein localization is not sufficient to understand modifications in the Golgi-to-ER transport pathways and/or to identify regulators of these pathways.

In this study, we used synchronization of both anterograde and retrograde transport of Golgi reporter proteins, taking advantage of the Retention Using Selective Hooks (RUSH) assay (Boncompain et al. 2012), combined with Artificial Ligand of Streptavidin (ALiS) to empower reversibility of the RUSH assay (Terai et al., 2015). Using either a dynamic ER or an immobile hook, we quantified kinetics of both KDEL-mediated ER retrieval and the ER recycling of Golgi glycosylation enzymes, respectively. Our set-up enabled us to show the role of COG3 in both pathways, while Rab6 depletion led to impairment of KDEL-mediated retrograde transport of a sialyltransferase reporter selectively. In addition, to overcome troubles generated by overexpressing Golgi glycosylation enzymes, we engineered endogenously tagged Golgi glycosylation enzymes using CRISPR-Cas9 approaches. Synchronization of the transport of endogenous Golgi glycosylation enzymes indicated differences in their kinetics of anterograde transport to the Golgi, whereas their induced KDEL-mediated retrograde transport showed similar kinetics.

Results

The reversible RUSH assay enables a dynamic and quantitative analysis of KDEL-mediated Golgi-to-ER transport

The steady-state localization of proteins not only is a consequence between anterograde and retrograde transport, but also involves protein synthesis and degradation rates. To dissect protein transport, synchronization is thus necessary to get rid of this equilibrium and to give access to the quantitative analysis of a wave of transport of a given cargo. The Retention Using Selective Hooks (RUSH) assay in its initial development allows synchronization of the anterograde transport of any protein by interaction between a Streptavidin-fused hook and a SBP (Streptavidin-binding peptide)-fused reporter (Boncompain et al., 2012). The interaction is released by addition of biotin. However, the affinity of biotin for streptavidin is high (Kd = 10^{-13} M) impairing detachment of biotin from Streptavidin and thus reversibility of the RUSH assay. Artificial Ligands of Streptavidin (ALiS) have lower affinity for Streptavidin (Kd = 10^{-6} M) than biotin. This allows synchronization of anterograde transport of Golgi proteins from the ER and of retrograde transport from Golgi to ER, upon incubation of ALiS and its washout, respectively (Tachibana et al., 2017; Terai et al., 2015). In the present study, ALiS-3 was used as it is the most water-soluble ALiS developed, and consequently the easiest ALiS to wash out using buffer and medium (Tachibana et al. 2017). In all experiments, cells were pre-incubated and kept with cycloheximide to prevent new protein synthesis, which would interfere with our analysis. Clonal cell populations stably expressing the constructs of interest were used to ensure homogenous levels of expression and consequently homogeneous kinetic behavior to the applied treatments.

Using this set-up, we conducted a quantitative analysis in real-time of the KDEL-mediated Golgi-to-ER pathway. The N-terminal part comprising the cytosolic and transmembrane domains of the Golgi glycosylation enzyme Mannosidase II (ManII*) or sialyltransferase (ST*) was used as a *cis*- and *trans*-Golgi reporter protein respectively. The SBP and EGFP were fused to C-terminus of the Golgi reporters, exposing SBP to the lumen of the intracellular compartments as previously described (Fig. 1A) (Boncompain et al., 2012). ManII*-SBP-EGFP was co-expressed using a bi-cistronic plasmid with Streptavidin fused to the KDEL motif (Str-KDEL). Without treatment, ManII*-SBP-EGFP is continuously retrieved in the ER thanks to the Streptavidin-SBP interaction and the presence of the KDEL motif on the protein complex (Fig. 1A and time 00:00 Fig. 1B). Upon incubation with ALiS-3,

ManII*-SBP-EGFP is transported to the Golgi apparatus. Stable localization in the Golgi apparatus was observed after 1 h of incubation with ALiS-3 (Fig. 1B). Then, ALiS-3 was washed out. In the absence of ALiS-3, ManII*-SBP-EGFP is retrieved to the ER (thanks to interaction with Str-KDEL) in less than 1 h (Fig. 1B). Consecutive addition and washout of ALiS-3 were performed a second time demonstrating that ManII*-SBP-EGFP reached the Golgi apparatus upon detachment of Str-KDEL and then re-association. Multiple cycles of transport could be performed even though the limitation we encountered is the presence of cycloheximide, which becomes toxic for longer term.

We then extended our analysis by using another Golgi targeted cargo composed of the N-terminal cytosolic tail and the transmembrane domain of sialyltransferase (ST*). Cells stably expressing Str-KDEL_ST*-SBP-EGFP and Str-KDEL_ManII*-SBP-mCherry were co-cultured to compare the transport kinetics of these reporters under the same conditions (Fig. 1C). Quantification showed that anterograde transport of ST*-SBP-EGFP and ManII*-SBP-mCherry to the Golgi apparatus is occurring at a similar speed, whereas the retrograde transport speed of ST*-SBP-EGFP (26.3 min) is slight longer than that of ManII*-SBP-EGFP (14.4 min) (Figure 2D). This observation may due to the localization of cargos in different Golgi sub-compartments. In addition, the volume of the Golgi apparatus was quantified during the transport of ManII*-SBP-EGFP and ST*-SBP-EGFP between ER and Golgi. HeLa cells engineered to knock-in EGFP at the N-terminus of Giantin (GFP-Giantin^{EN}) were transiently transfected with Str-KDEL and ManII*-SBP-mCherry or ST*-SBP-mCherry (Fourriere et al., 2016). The volume of the Golgi apparatus increased during the anterograde transport of Golgi cargos and then decreased upon their induced retrograde transport (Supplementary Fig.1).

Our data show that we get access to efficient synchronization in a population of cells of both anterograde and retrograde transport of Golgi reporters. Our quantitative analysis of Golgi-to-ER transport dynamics indicated that KDEL-mediated retrograde transport of Golgi reporters occurs in a time window of 1h.

Reversible RUSH using an ER stable hook allows analysis of ER recycling of Golgi glycosylation enzymes

The identity of Golgi cisternae is maintained by the retrieval of the Golgi-resident glycosylation enzymes from later cisternae. Thus, in addition to their steady-state localization in the Golgi apparatus, about 10% of glycosidases are present in the ER thanks to their Golgi-to-ER retrograde transport (Cole et al., 1998; Rhee et al., 2005). Very little is known about

the kinetics of transport of the Golgi glycosylation enzymes in physiological conditions (Sengupta et al., 2015).

With the same Golgi reporters previously described, we used an ER stable hook composed of an isoform of the Invariant chain (Ii) of the major histocompatibility complex fused to Streptavidin (Ii-Str) in its luminal domain (Fig. 2A) (Boncompain et al., 2012; Schutze et al., 1994). The stable localization of Ii-Str in the ER was confirmed with the high mannose patterns through the treatment of endoglycosidase H, indicating Ii-Str does not reach early Golgi compartments (Supplementary Fig. 2). Anterograde and retrograde transport could be observed in real-time by co-expressing Ii-Str and ManII*-SBP-EGFP (Fig. 2B) or ST*-SBP-EGFP (Fig. 2C). We co-cultured cells expressing Ii-Str_ManII*/ST*-SBP-EGFP with cells expressing Str-KDEL_ManII*SBP-mCherry to compare kinetics of retrograde transport of Golgi glycosylation enzymes and of retrograde transport mediated by the KDEL motif (Fig. 2B, C). The time necessary for 50 % of the reporters to reach either the Golgi apparatus or the ER (half-time) were quantified to assess kinetics of anterograde and retrograde transport, respectively (Fig. 2D). No significant difference was observed both for anterograde and retrograde transport of ManII* and ST* reporters when used in combination with Str-KDEL. No significant difference was observed for bidirectional transport of ManII* and ST* reporters when used in combination with Ii-Str. These data indicate that the speed to reach the Golgi (anterograde) or the ER (retrograde) is not dependent on the reporter. The KDEL-mediated retrograde transport has a shorter half-time (14.4 min for ManII* and 26.3 min for ST*) than the half-time of the glycosylation enzymes recycling pathway (36.9 min for ManII*-SBP-GFP and 37.6 min for ST*) (Fig. 2D). The retrograde transport mediated by the KDEL motif is faster than the recycling of Golgi glycosylation enzymes through the ER.

Knockdown of COG3 delays the retrograde transport mediated by the KDEL motif and impairs the recycling of glycosylation enzymes through the ER

Conserved Oligomeric Golgi (COG) complex is a tethering complex orchestrating intra-Golgi trafficking (Willett et al., 2013). Using RNA interference, we assessed the role of COG3 in both Golgi-to-ER retrograde transport pathways: KDEL-mediated and ER recycling of glycosylation enzymes. Knockdown of COG3 (80% efficiency, Supplementary. Fig. 3) did not show any effect on the anterograde transport of ManII*-SBP-EGFP hooked by Str-KDEL (Fig.3A, 3E), or on the anterograde transport of ST*-SBP-EGFP hooked either by Str-KDEL or Ii-Str (Fig3B, 3C, 3F). However, depletion of COG3 led to delayed kinetics of KDEL-mediated ER retrieval of ST*-SBP-EGFP compared to cells transfected with control siRNA

(Fig3A-B). This effect was rescued when cells expressed siRNA-resistant COG3 (Fig. 3D-F). We also tested the effects of COG3 depletion on the transport kinetics of full-length fucosyltransferase (FUT8). The KDEL-mediated retrograde transport of FUT8(fl)-SBP-EGFP is also delayed in cells depleted for COG3, compared to cells treated with siRNA control (Supplementary Fig 4). There was no effect on the retention of reporters (ManII*, ST* or FUT8(fl)) in the ER (using Str-KDEL hooks and no treatment) was observed. This might be explained by the slight delay of KDEL-mediated retrograde transport occurring after COG3 depletion, which is not affecting steady-state localization of Str-KDEL. ER recycling of ST*-SBP-EGFP (using Ii-Str hook) was not observed upon depletion of COG3 (Fig. 3C), while occurring in cells transfected with control siRNA with a similar kinetics as measured previously (Fig. 2C).

Our data indicate that COG3 is involved in intra-Golgi transport of KDEL-R though not completely required, and is necessary for intra-Golgi retrograde transport of Golgi glycosylation enzymes.

Knockdown of Rab6 delays the retrograde transport of ST* but not of ManII*

Previous studies have shown the involvement of Rab6 in retrograde transport pathways (Girod et al., 1999; Miserey-Lenkei et al., 2010; Sengupta et al., 2015, White et al., 1999). We therefore tested the role of Rab6 on synchronized retrograde transport pathways using our set-up. Using siRNA against Rab6A, between 60% to 80% of depletion of Rab6 was achieved (Supplementary Fig. 3). In cells depleted for Rab6, no major effect on the transport of ManII* was observed (Fig. 4A). A slight acceleration of anterograde transport of ManII* towards the Golgi was detected. This seems to be specific to Rab6 depletion as anterograde transport of ManII* kinetics is similar to control cells when a siRNA-resistant Rab6 construct is expressed (Fig. 4D-E). However, a strong delay in the KDEL-mediated retrograde transport of ST* was observed (Fig. 4B) whereas the effect on the ER recycling of ST* (Ii-Str hook) is moderate (Fig. 4C). Kinetics of KDEL-mediated ER retrieval of ST* is restored in cells depleted for Rab6 when a siRNA-resistant Rab6 is expressed, being then similar to cells treated with siRNA control (Fig. 4D, 4F). These data are difficult to interpret. One could suggest that Rab6 is involved in the intra-Golgi trafficking of ST*, which dictates its capability to interact with Str-KDEL.

Bidirectional synchronized transport of endogenous Golgi glycosylation enzymes

Evaluating the transport of Golgi glycosylation enzymes in the context of their overexpression might disturb their intra-Golgi localization and trafficking mechanisms, we thus set out to synchronize the bidirectional transport of endogenous Golgi glycosylation enzymes using genome-editing approaches, namely CRISPR-Cas9 with homologous recombination (HR) or CRISPaint (Fig. 5A) (Schmid-Burgk et al., 2016). Three human Golgi glycosylation enzymes, namely ManII, GalNAc-T1 and GalT, encoded by the genes MAN2A1, GALNT1 and B4GALT1 respectively, were targeted with gRNA close to the stop codon in order to create C-terminal fusion with SBP-EGFP or SBP-mNeonGreen (Fig. 5A). Positive cells (either EGFP positive or mNeonGreen positive) were enriched by sorting. Fluorescent signal was detected in the Golgi apparatus as confirmed by staining with anti-GM130 antibody (Supplementary Fig. 5A). Str-KDEL was then introduced in enriched cells by lentiviral transduction (Fig. 5A) and enabled the efficient retention of ManII^{EN}-SBP-mNeonGreen, GalNAc-T1^{EN}-SBP-mNeonGreen and GalT^{EN}-SBP-EGFP in the ER in the absence of treatment (Fig. 5B-C, Supplementary Fig. 5A). We generated clonal cell lines to achieve homogeneous response to transport regulation using the RUSH and reversible RUSH assays. After genomic characterization (data not shown), we intentionally worked with heterozygous clones to keep non-tagged copies of the enzymes in the event that the labeling would affect their function. The analysis in real-time of the anterograde transport upon addition of ALiS-3 showed that we were able to quantitatively monitor the transport from ER to Golgi of the endogenous enzymes with varying kinetics depending on the enzymes. Stable localization in the Golgi apparatus of GalNAc-T1^{EN}-SBP-mNeonGreen was obtained faster than the one of ManII^{EN}-SBP-mNeonGreen (Fig. 5B-C). Upon washout of ALiS-3, Golgi-to-ER retrograde transport was induced. The KDEL-mediated ER retrieval of ManII^{EN}-SBP-mNeonGreen and GalNAc-T1^{EN}-SBP-mNeonGreen showed similar kinetics as expected (Fig. 5B-C). Interestingly, the KDEL-mediated retrograde transport of GalT^{EN}-SBP-EGFP was not observed upon washout of ALiS-3 in contrast to the co-cultured control cells expressing ManII*-SBP-mCherry (Supplementary Fig. 5B). One could suggest this is due to a lack of interaction between GalT^{EN}-SBP-EGFP and Str-KDEL in the sub-Golgi compartments where GalT^{EN}-SBP-EGFP is located, but this would require further investigation.

Combining genome-editing methods with the RUSH and reversible RUSH assays, we could get access to the kinetics of anterograde and retrograde transport of endogenous Golgi glycosylation enzymes used as Golgi reporters in the population of cells.

Discussion

In this study, we have developed a quantitative assay to monitor the anterograde and retrograde transport between the ER and the Golgi apparatus in real-time, utilizing the RUSH assay together with ALiS (instead of the non-displaceable biotin). We focused our analysis on the retrograde transport routes based on KDEL-mediated ER retrieval thanks to the "dynamic" hook Str-KDEL and on the ER recycling of Golgi glycosylation enzymes using the "immobile" hook Ii-Str. Prior studies dissected the KDEL-based transport using diverse reporter proteins, such as Shiga toxin B-KDEL , ssHRP-KDEL or KDEL-BODIPY633 (Cancino et al., 2014; Johannes et al., 1997). However, these tools were not suitable for a real-time analysis of KDEL-mediated retrograde transport and quantification of the transport kinetics. ER trapping methods based on FKBP-FRAP/FRB interaction domains fused to the ER retained invariant chain (Ii) and to Golgi glycosylation enzymes in combination with rapamycin were developed to monitor the ER recycling of Golgi glycosylation enzymes (Sengupta et al., 2015; Pecot and Malhotra, 2006). These two studies led to discrepancy in the interpretation. The first study concluded that ER recycling of Golgi glycosylation enzymes does not occur (Pecot and Malhotra, 2006), while the second study demonstrated that ER recycling of Golgi glycosylation enzymes could be detected after modifying the assay to prevent loss of binding capacity of the trap due to the presence of an endogenous binder (Sengupta et al., 2015). Our assay also used an Ii fusion protein as an ER trap (Ii-Str) for SBP-tagged Golgi reporter. The interaction is based on Streptavidin-SBP interaction getting rid of the troubles previously encountered with FKBP-FRAP/FRB domains. We demonstrated here that combination of the RUSH assay with ALiS allows synchronization of the ER-to-Golgi transport upon washout of ALiS giving access to dynamic analysis of the ER retrieval KDEL-mediated or the ER recycling of Golgi glycosylation enzymes using Str-KDEL and Ii-Str hooks, respectively.

We show that these two Golgi-to-ER transport pathways have different kinetics. KDEL-mediated ER retrieval occurs faster than the ER recycling of Golgi glycosylation enzymes. Sengupta et al. did not provide quantification of real-time imaging experiments of the ER recycling of ManII* but still pictures show that stable ER relocation of ManII* occurs between 2h and 4h of incubation with rapamycin (Sengupta et al., 2015). Our quantification indicated that ManII* or ST* are fully trapped in the ER 1.5h after the washout of ALiS-3. This difference might be explained by differences in the expression levels of the constructs, the fusion domains used (FRB vs. SBP) and/or the presence of rapamycin.

Based on the synchronization method that we developed, we tested the effects of the depletion of proteins previously shown to regulate retrograde transport, namely COG3 and Rab6. Our data show that COG3 affects both KDEL-mediated and Golgi enzymes retrograde pathway, in accordance with existing data that have demonstrated the role of COG3 in intra-Golgi transport (Smith et al., 2009; Zolov and Lupashin, 2005). COG3 might be involved not only in the intra-Golgi transport of the Golgi reporters themselves (here ManII*, ST* and FUT8(fl)), but also of the KDEL-R. Depletion of Rab6 led to delayed KDEL-mediated transport of ST* whereas did not affect the one of ManII*. One could suggest that Rab6 is directly or indirectly involved in the intra-Golgi transport of ST* determining its binding capacities of ST*-SBP-FP with Str-KDEL in Golgi sub-compartments. We did not detect any effects of depletion of Rab6 on the retrograde transport (Ii-based) of ManII*, whereas the expression of Rab6-T27N strongly reduced ER recycling of ManII* as well as the Golgi-to-ER retrograde transport of Shiga toxin B-fragments (Sengupta et al., 2015; White et al., 1999). Experimental conditions, mostly the use of a dominant-negative mutant versus siRNA depletion, might explain this discrepancy.

The overexpression of Golgi glycosylation enzymes either truncated or full-length probably led to a less accurate localization in the Golgi cisternae. In addition, glycosyltransferases assemble as hetero-oligomers, which are required for proper Golgi targeting, according to the kin recognition model (Banfield, 2011; Nilsson et al., 1993). Partners of glycosylation enzymes might be missing overexpressing cells leading to altered trafficking. To overcome these limitations, we engineered endogenous Golgi glycosylation enzymes by genome editing and generated cells with knocked-in SBP-FP domains close to their C-terminus. We demonstrated that synchronized transport both in the anterograde and retrograde directions were achieved. However, retrograde transport of GalT (encoded by B4GALT1) did not occur after washout of ALiS-3 (even after a long time). Studies have proposed the existence of hetero-oligomers B4GalT1-ST6Gal1 in the Golgi apparatus (de Graffenried and Bertozzi, 2004). This may explain why our attempts to observe the Golgi-to-ER retrograde transport of endogenous B4GalT1 did not reach to our expectation. It is possible that the endogenous B4GalT1 forms hetero-oligomers with ST6Gal1, which prevent the Streptavidin from accessing SBP, and thus avoids the retrograde transport from Golgi-to-ER.

In summary, we established a quantitative assay to monitor the retrograde transport between the Golgi apparatus and the ER in real-time, combining the RUSH assay and ALiS. Dissecting Golgi-to-ER transport routes both KDEL-mediated and of Golgi glycosylation

enzymes is relevant to characterize and understand trafficking defects occurring in pathological processes, such as cancer. Our assay now gives access to a descriptive analysis of mechanisms of retrograde transport in various cellular contexts but also paves the way to the identification of regulators of retrograde transport pathways.

Materials and Methods

Reagent

Dulbecco's modified Eagle medium (DMEM), penicillin–streptomycin (P/S), sodium pyruvate, puromycin, lipofectamine 3000, lipofectamine RNAiMAX, Leibovitz L15 phenol red free medium (#21083027), Opti-MEM, goat anti-Mouse IgG (H+L) poly-HRP (#32230) and goat anti-Rabbit IgG (H+L) poly-HRP (#32260), Phusion DNA polymerase (F530S) were purchased from Thermo Fisher (Carlsbad, CA). Fetal bovine serum (FBS) was purchased from Biosera (Nuaille, France). Geneticin (EU0601) was purchased from Euromedex (Souffelweyersheim, France). Cycloheximide (C4859) was purchased from Sigma-Aldrich (St Louis, MO) and TransIT-Lenti was purchased from Mirus (Madison, WI). ALiS-3 was synthesized by Mcule (Palo Alto, CA) as previously described (Terai et al., 2015). The following antibodies were used: anti-GM130 (BD Transduction Laboratories, #610823, 1:1000 for IF); anti-Streptavidin (Santa Cruz Biotechnology, S10D4, 1:500 for IF); anti-HA tag (clone 12CA5) (Proteins and Antibodies Laboratory, Institut Curie, 1:2000 for WB); anti-COG3 (Sigma-Aldrich, HPA040353, 1:2000 for WB); anti-Rab6 (Santa Cruz Biotechnology, sc-310, 1:1000 for WB); anti-Actin (Sigma-Aldrich, A3853, 1:5000 for WB). Fluorochrome conjugated secondary antibodies were purchased from Jackson ImmunoResearch (Cambridge, UK).

Cell Culture, transfection and viral infection

HeLa cells were grown in culture medium (DMEM supplemented with 10% FBS, 1% penicillin and streptomycin, and 1mM sodium pyruvate at 37°C and 5% CO2. HeLa cells were transiently transfected with RUSH constructs, using calcium phosphate as previously described (Jordan et al., 1996). After 1 day, cells were processed for immunofluorescence staining or time-lapse imaging. To synchronize the transport of RUSH cargos, ALiS-3 was treated to the culture medium at a final concentration of 20 uM or 40 uM.

To generate the stable cell line, RUSH constructs were introduced into the lentiviral vector pCDH1 with a CMV promoter. 1.3 ug of lentiviral donor, 0.15 ug pMD2.G and 0.367

ug psPAX2 plasmids were transfected with 6 ul of TransIT-Lenti reagent into HEK293 LTV cells, which were plated on a 6 well plate at a density of 800000 cells per well, 24h before transfection. 48 hours after transfection, viral media was collected, mixed with protamine (Sigma) at a final concentration of 8 ug/ml, and introduced to HeLa cells. 48 hours after infection, the virus medium was replaced with culture medium containing puromycin (final concentration 5 ug/ml) or geneticin (final concentration 400 ug/ml).

Plasmids

All RUSH plasmids were constructed using bicistronic vectors, encoding both of hook and reporter proteins, as previously described (Boncompain et al., 2012). GFP-Rab6 was a gift from Stephanie Miserey-Lenkei (Institut Curie). pmCherry-C1 vector was subjected to PCR to provide cleavage sites at 5′ and 3′ ends of mCherry (forward: 5'-TTAATTACCGGTATGGTGAGCAAGGGCGAG -3' and reverse: 5' - TTAATTGCGGCCGCCTTGTACAGCTCGTCCAT - 3'). The PCR product was inserted into GFP-Rab6 plasmid to generate mCherry-Rab6. GFP-hCOG3 was a gift from Lupashin Vladimir (University of Arkansas for Medical Sciences, United States). pmCherry-C1 vector was subcloned to generate mCherry-hCOG3.

Genome editing through CRISPR-Cas9 and CRISPaint

To produce the endogenously tagged glycosylation enzymes in HeLa cells, we inserted SBP-GFP in the C-terminus of GalT using CRISPR-Cas9, and SBP-mNeonGreen in the C-terminus of ManII and GalNAc-T1. The design of gRNAs were firstly predicted in a web tool, CHOPCHOP version 3 (https://chopchop.cbu.uib.no/), and the gRNAs closed to the stop codon of the coding region were selected (ManII: 5' - AAGTCAGGTTCACCTCAAC - 3'; GalNAc-T1: 5' - TCTCAGAATATTTCTGGCA - 3'; GalT: 5'-GGACACCGAGCTAGCGTTT - 3'). HeLa cells were plated in a 10cm dish and transfected next day with 15 ug donor plasmid, consisting of 1kb homologous arms of GalT genome sequences, upstream and downstream of gRNA cutting site, 3.75 ug gRNA with U6 promoter, 3.75 ug pcDNA3.3-TOPO_hCas9 (a gift from Nicolas Manel, Institut Curie), and 2.5 ug pIRES-puro3 as a selection marker, using calcium phosphate. 24 hours after transfection, cells were treated with 5 ug/ml puromycin for 1 day, and then incubated with antibiotic-free medium.

To construct an universal donor for CRISPaint approach, a kind gift, pCRISPaint_SBP-mNeonGreen, from Kasper Mygind (Copenhagen University), was

subjected to PCR to remove the start codon of SBP (forward: 5' - CGCTGGATCCGACGAGAAGACCACTGGTTG - 3'; reverse: 5' - GACCTTAATTAACTTGTACAGCTCGTCCATGC - 3'). HeLa cells were seeded in a 6 well plate for transfection next day, and 1ug universal donor of pCRISPaint_SBP-mNeonGreen, 1ug gRNA targeting to MAN2A1 or GALNT1, 1 ug frame selector with pSpCas9(BB)-2A-Puro, using lipofectamine 3000 according to manufacturer's instructions. 48 hours after transfection, cells were treated with 1 ug/ml puromycin for 1 day, and then replaced with antibiotic-free medium.

For the validation of the genome-edited allele in the knock-in cell lines, the genomic DNA was extracted with the NucleoSpin Tissue kit (Macherey-Nagel, #740952.50) according to the manufacturer's protocol. The PCR amplification of the targeting regions was performed using Phusion High-Fidelity PCR Kit (New England Biolabs, E0553S), for 30 cycles of 98°C for 10 sec, 60-68°C for 30 sec and 72°C for 1 min 30 sec, with indicated sets of primers in Table 1.

RNA interference experiment

HeLa cells were plated in a 6 well plate, and next day siRNA duplexes were transfected per well with 1ul of 10 uM siRNA (Table 2) and 7.5 ul lipofectamine RNAiMAX in 200 ul OptiMEM, as indicated in the manufacturer's instructions. siRNA against luciferase was used as depletion control. 72 hours after transfection, cells were processed to live-cell imaging or western blotting. For the rescue experiments of depleted cells, after 48 hours, the medium was replaced and cells were treated with 3.5ug rescue plasmids, using calcium phosphate.

Fluorescence microscopy and time-lapse imaging

HeLa cells were fixed in 4% paraformaldehyde (Electron Microscopy Sciences) for 10 min, and then permeabilized by 0.5% saponin, containing 2% BSA in PBS, for 10 min at room temperature. Cells were incubated with primary antibodies of interest, followed by conjugated secondary antibodies. Cells were then mounted using Mowiol (Calbiochem). Immunofluorescence staining samples were detected by Leica DM6000 widefield microscope, equipped with a CoolSnap HQ2 (Photometrics) CCD camera. Time-lapse microscopy was performed by a Nikon Eclipse Ti-E mic microscope, equipped with an Evolve EMCCD camera (Photometrics), with an incubator at 37°C. Images acquired by the MetaMorph software (Molecular Devices) and were analyzed in Fiji software. Fluorescent signals in the

Golgi were quantified thanks to Mathieu Maurin (Institut Curie, U932) for creating the macro in Fiji. Images and composite figures were prepared using Adobe Illustrator software (Adobe Systems Inc., San Jose, CA). To measure the volume of Golgi apparatus, confocal time-lapse images were analyzed in Imaris software and then normalized to the maximum value of time-lapse series.

Statistical analysis

Histological analysis and parametric data were presented as means ± S.E.M. If not specifically mentioned, differences between groups were tested by using the paired Student's t-test. Multiple comparisons were analyzed by one-way ANOVA with repeated measurement. The level of significance was uniformly defined at $P< 0.05$.

Figures

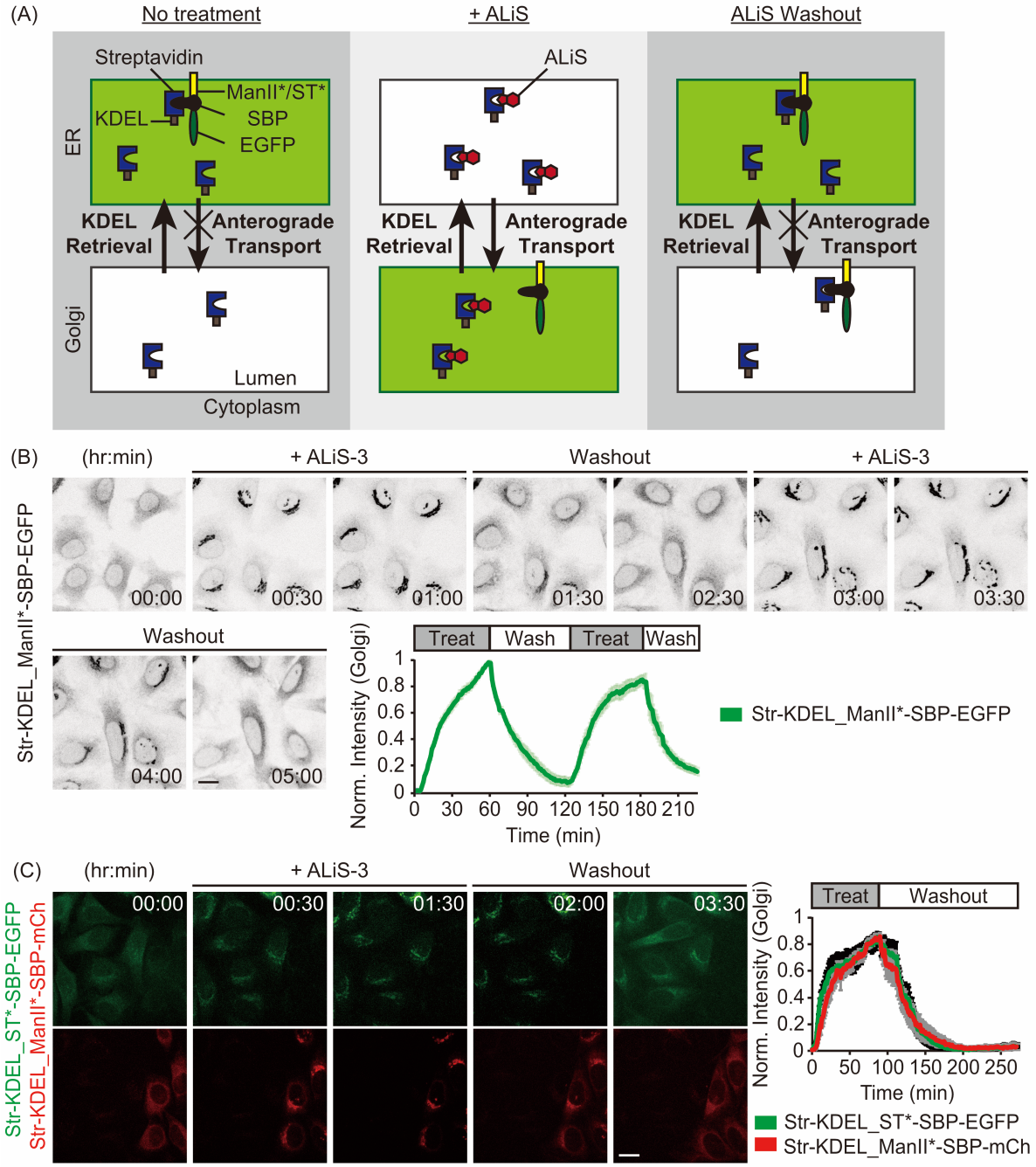

Fig. 1 Reversible RUSH assay using ALiS to quantify kinetics of Golgi-to-ER KDEL-mediated retrograde pathway. (A) Str-KDEL served as an ER hook, and ManII*- or ST*-SBP-EGFP was used as a Golgi reporter. The dissociation and re-association of the hook and reporter between ER and Golgi were induced by the treatment with ALiS (Artificial Ligand of Streptavidin) and its washout respectively. (B-C) Time-lapse images of HeLa cells stably expressing Str-KDEL and ManII*-SBP-EGFP (B), ST*-SBP-EGFP and ManII*-SBP-mCherry (C). Cells were pre-incubated with cycloheximide (25 ug/ml) for 20 min, then ALiS-3 was added (20 µM) from 0 to 1 hour (B) or 1.5 hours (C) respectively. Then ALiS-3 was washed out. The graphs showed fluorescence intensity of ManII*-SBP-GFP (B) and ST*-SBP-EGFP (C) in the Golgi apparatus at each time point, and normalized to the maximum value of the time-lapse series. Values are means ± S.E.M from three independent experiments with analysis of at least 10 fields. Scale bar: 20 µm.

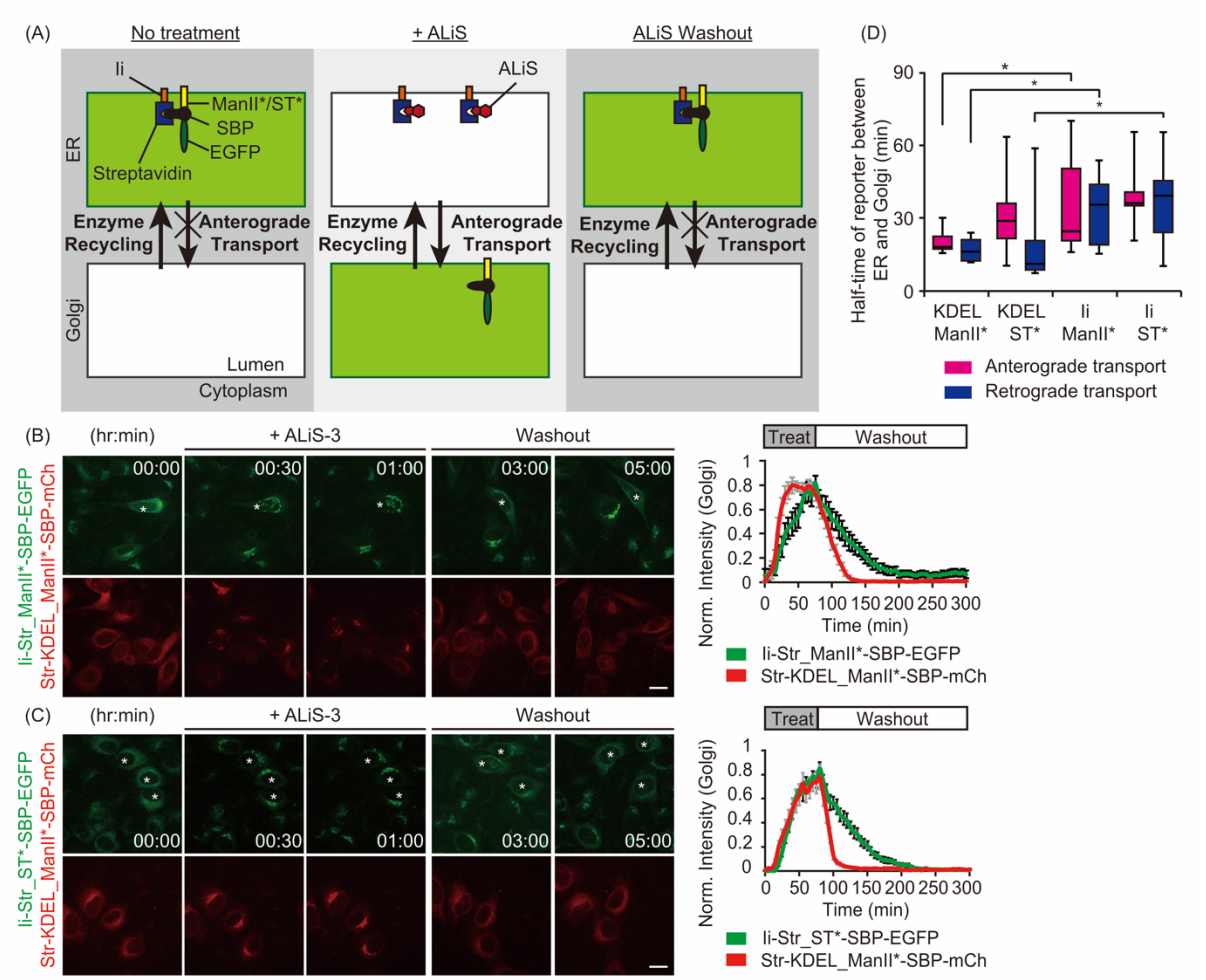

Fig. 2 Reversible RUSH assay to monitor Golgi glycosylation. (A) Ii-Str as an "immobile" ER-resident hook, and ManII*- or ST*-SBP-EGFP was used as a Golgi reporter. The dissociation and re-association of the hook and reporter between ER and Golgi were induced by the treatment and washout of ALiS respectively. (B-C) Time-lapse images of HeLa cells stably expressing Ii-Str and ManII*-SBP-EGFP (B), ST*-SBP-EGFP (C), co-cultured with cells expressing Str-KDEL and ManII*-SBP-mCherry as an internal control in (C). Cells were pre-incubated in cycloheximide (25 ug/ml) for 20 min, then treated with ALiS-3 (40 µM) from 0 to 1 h, and ALiS-3 was subsequently washed out. The graphs showed fluorescence intensity of ManII*-SBP-EGFP in (B) and ST*-SBP-EGFP in (C) in the Golgi apparatus at each time point, and normalized to the maximum value of the time-lapse series. (D) Quantification of half-time of transport of the reporters (ManII*-SBP-EGFP or ST*-SBP-EGFP) between ER and Golgi for the indicated constructs (Str-KDEL or Ii-Str hooks). Values are means ± S.E.M from three independent experiments with analysis of at least 10 fields. Scale bar: 20 µm.

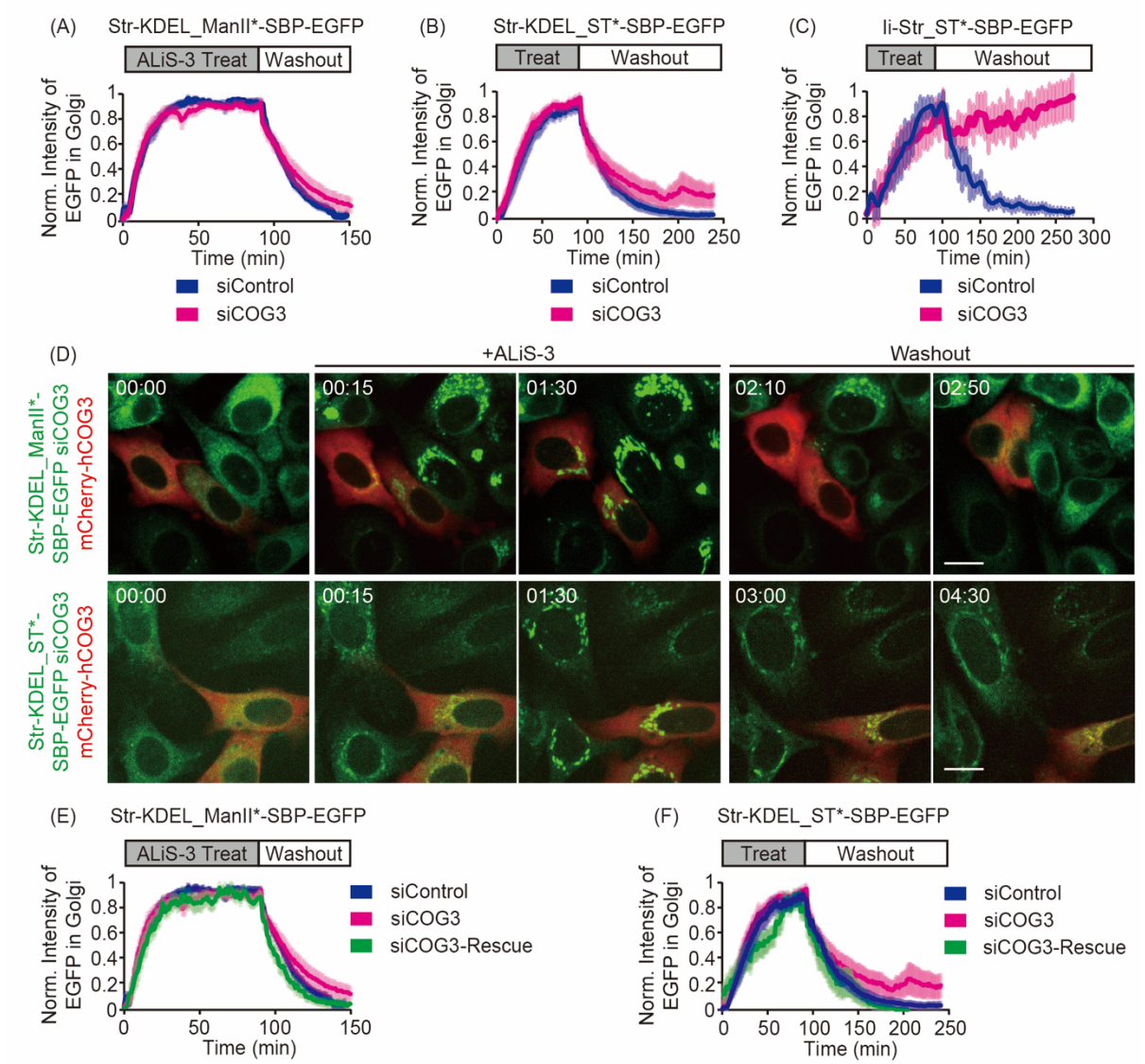

Fig. 3 COG3 depletion affects the KDEL-mediated retrograde transport and glycosylation enzyme recycling through the ER. (A-C) Kinetic analysis of time-lapse images in HeLa cells, stably expressing ManII*-SBP-EGFP (A) and ST*-SBP-EGFP (B-C), with the hooks of Str-KDEL or Ii-Str. 72 h after siRNA transfection against COG3, cells were pre-incubated in cycloheximide (25 ug/ml) for 20 min, then treated with ALiS-3 (20 µM) from 0 to 1.5 h, and ALiS-3 was subsequently washed out. (D-F) 48 h after siRNA transfection against COG3, cells were transfected with mCherry-hCOG3 for another 24 h. The graphs showed fluorescence intensity of ManII*-SBP-EGFP (E) or ST*-SBP-EGFP (F) in the Golgi apparatus at each time point, and normalized to the maximum value of the time-lapse series. Values are means ± S.E.M from three independent experiments with analysis of at least 10 fields. Scale bar: 20 µm.

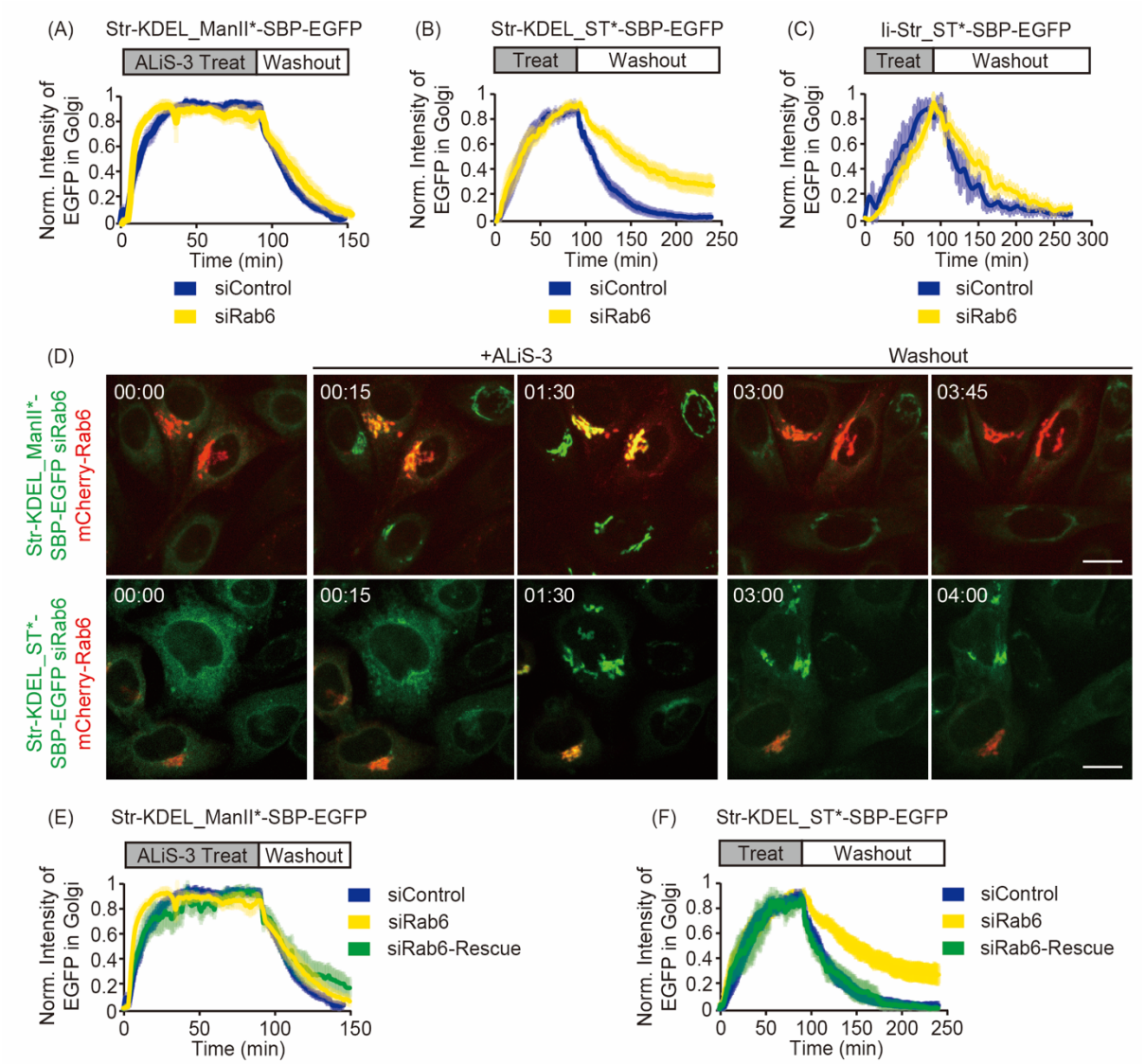

Fig. 4 Knockdown of Rab6 delays the retrograde transport of ST*, but not of ManII*. (A-C) Kinetic analysis of time-lapse images in HeLa cells, stably expressing ManII*-SBP-EGFP (A) or ST*-SBP-EGFP (B-C), with the hooks of Str-KDEL (A, B) or Ii-Str (C). 72 h after siRNA transfection against Rab6, cells were pre-incubated in cycloheximide (25 ug/ml) for 20 min, then treated with ALiS-3 (20 μM) from 0 to 1.5 h, and ALiS-3 was subsequently washed out. (D-F) 48 h after siRNA transfection against Rab6, stable cell lines indicated were transfected with mCherry-Rab6 for another 24 h. The plots showed fluorescence intensity of ManII*-SBP-EGFP (E) or ST*-SBP-EGFP (F) in the Golgi apparatus at each time point, and normalized to the maximum value of the time-lapse series. Values are means ± S.E.M from three independent experiments with analysis of at least 10 fields. Scale bar: 20 μm.

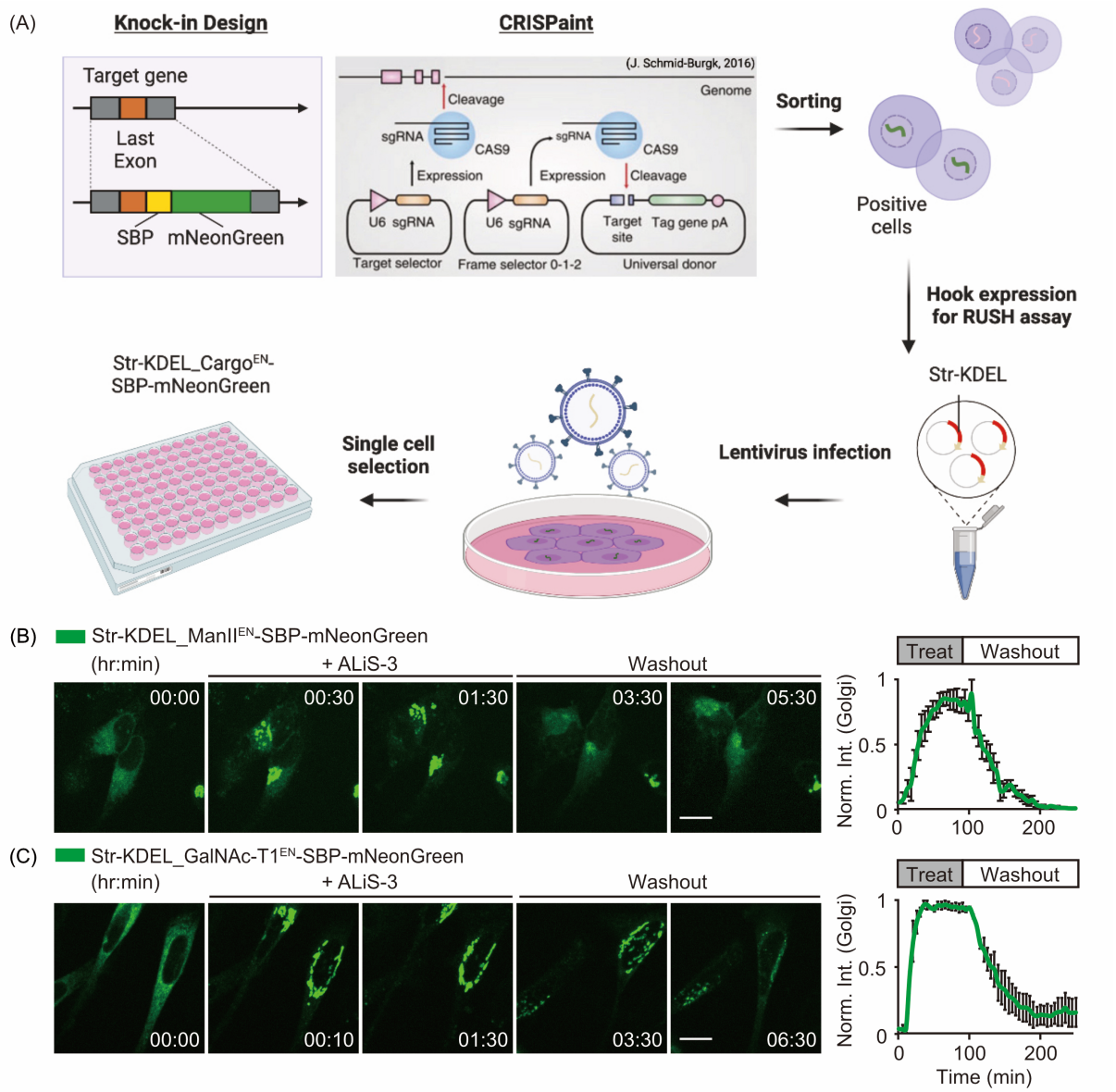

Fig. 5 Set-up "RUSH-synchronizable" endogenous Golgi enzymes. (A) Procedure to generate knock-in cell lines for RUSH assay targeting Golgi glycosylation enzymes. Through CRISPR-Cas9 or CRISPaint, HeLa cells were inserted with SBP-EGFP or SBP-mNeonGreen in the C-terminal of ManII and GalNAc-T1 before stop codon. Positive cells were enriched by sorting and transduced with lentiviruses to stably express Str-KDEL or Ii-Str hooks. Lastly, limiting dilutions were performed to select clones. (B-C) Time-lapse images of HeLa cells, stably expressing Str-KDEL and ManII^{EN}-SBP-mNeonGreen (B) or GalNAc-T1^{EN}-SBP-mNeonGreen (C), were pre-incubated in cycloheximide (25 ug/ml) for 20 min, then treated with ALiS-3 (20 µM) for 1.5 h, and then washout of ALiS-3 was performed as indicated. The plots showed fluorescence intensity of Golgi apparatus at each time point, and normalized to the maximum value of time-lapse series. Values are means ± S.E.M from two independent experiments with analysis of at least 10 fields.

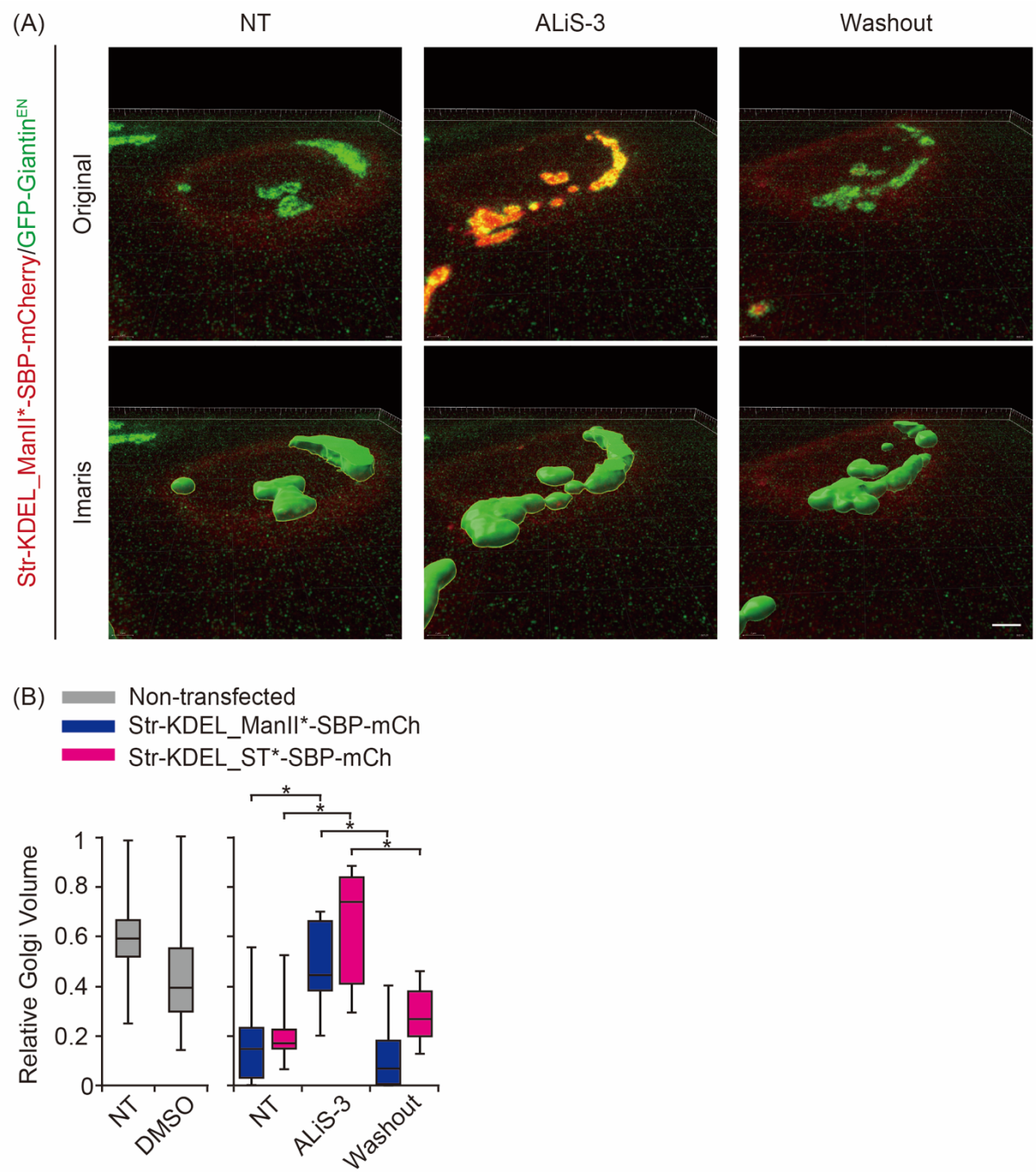

Supplementary Fig. 1 Changes of Golgi volume during the anterograde and retrograde transport of Golgi cargoes. (A) Knock-in GFP-Giantin^{EN} HeLa cells were transfected with Str-KDEL and ManII*-SBP-mCherry or ST*-SBP-mCherry. Quantification of Golgi volume changes in the indicated conditions using GFP-Giantin^{EN} as a Golgi mask. Scale bar: 2 μm. Confocal time-lapse images of HeLa cells were obtained with treatment of ALiS-3 for 1.5 h and then subsequent washout for 1 to 2 h.

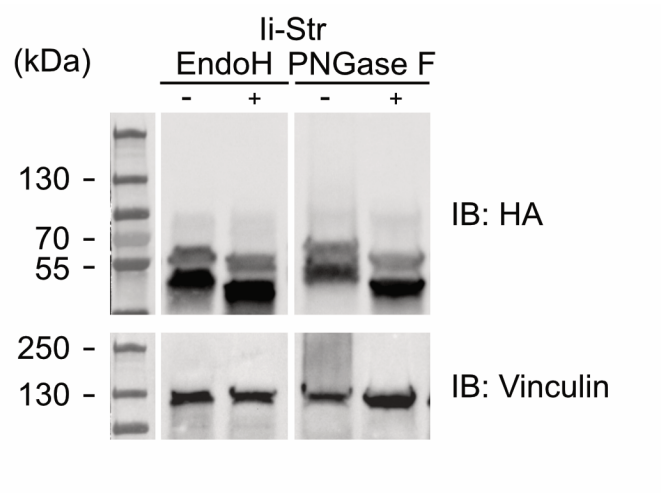

Supplementary Fig. 2 Ii-Str is stably resided in the ER.
Lysates of cells stably expressing the hook Ii-Str (containing an HA tag) were analyzed by immunoblot (IB) with or without treatment with endoglycosidase H (endoH) or peptide N-glycosidase F (PNGase F). Ii-Str was detected with an anti-HA antibody. Anti-vinculin IB served as a loading control.

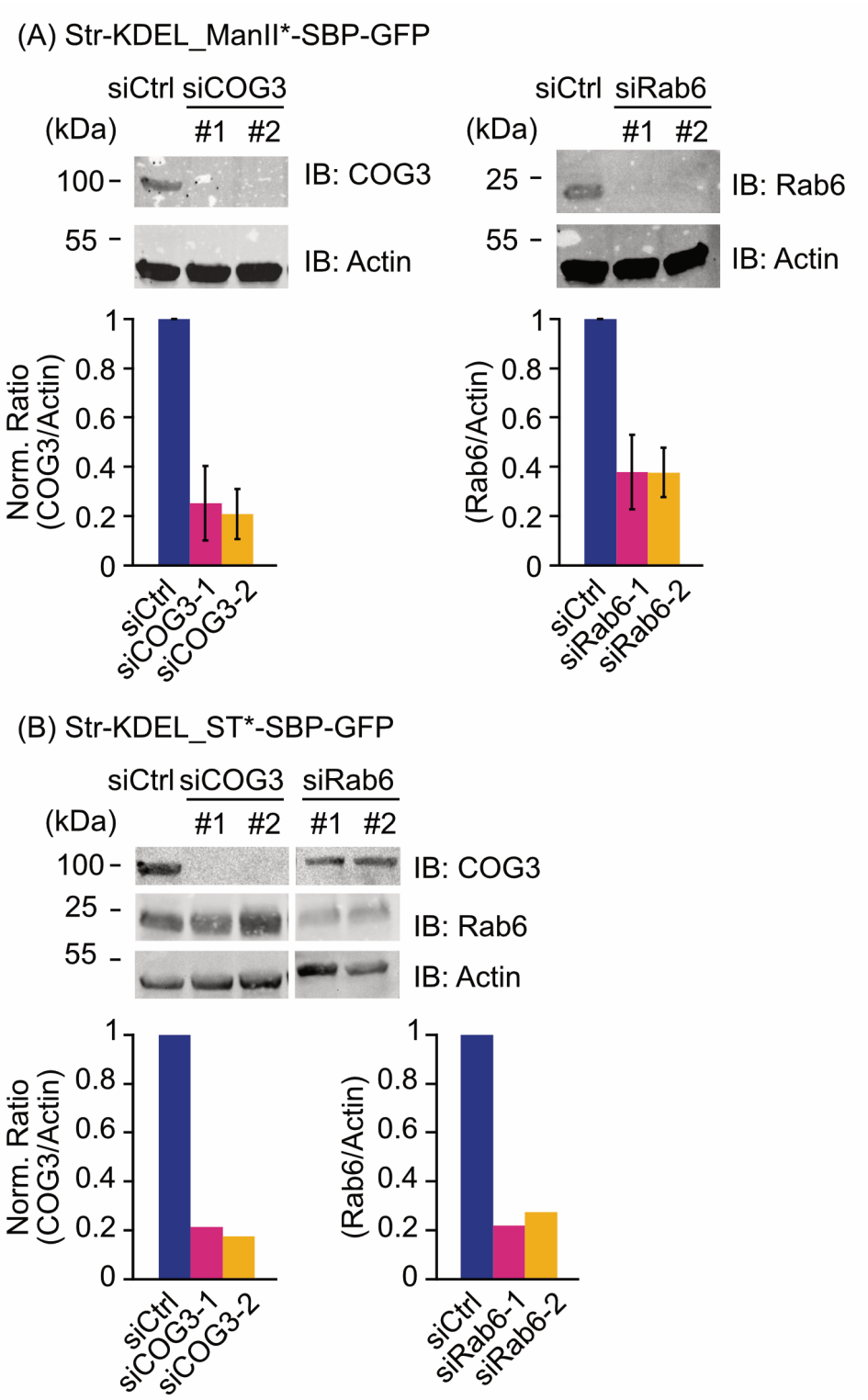

Supplementary Fig. 3 siRNA knockdown efficiency of COG3 and Rab6 in the stable lines. siRNA-induced knockdown against COG3 and Rab6 in the stable cell lines expressing ManII*-SBP-EGFP (A) and ST*-SBP-EGFP (B), together with the Str-KDEL. Cell lysates were collected after 72 h of siRNA treatment, analyzed by IB and normalized to control cell treated with siRNA against luciferase (siCtrl). Values are means ± S.E.M from two (A) or one (B) independent experiments.

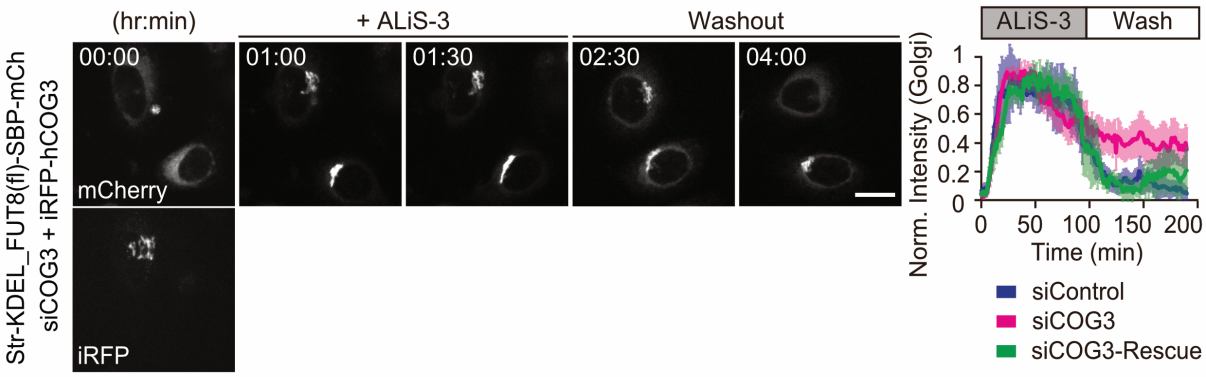

Supplementary Fig. 4 siRNA-induced COG3 depletion impairs the KDEL-mediated retrograde transport of full-length fucosyltransferase (FUT8). Str-KDEL served as an ER hook, and FUT8(fl)-SBP-mCherry was used as a Golgi reporter. Stable HeLa cells were treated with siRNA against COG3 for 48 h, and then transfected with iRFP-hCOG3 for another 24h before imaging. Cells were pre-incubated in cycloheximide (25 ug/ml) for 20 min, then treated with ALiS-3 (20 μM) from 0 to 1.5 h, and ALiS-3 was subsequently washed out. The plots showed kinetic analysis of time-lapse images, quantifying the fluorescence intensity of FUT8(fl)-SBP-mCherry in the Golgi apparatus at each time point, and normalized to the maximum value of time-lapse series. Values are means ± S.E.M from two independent experiments with analysis of at least 10 fields. Scale bar: 20 μm.

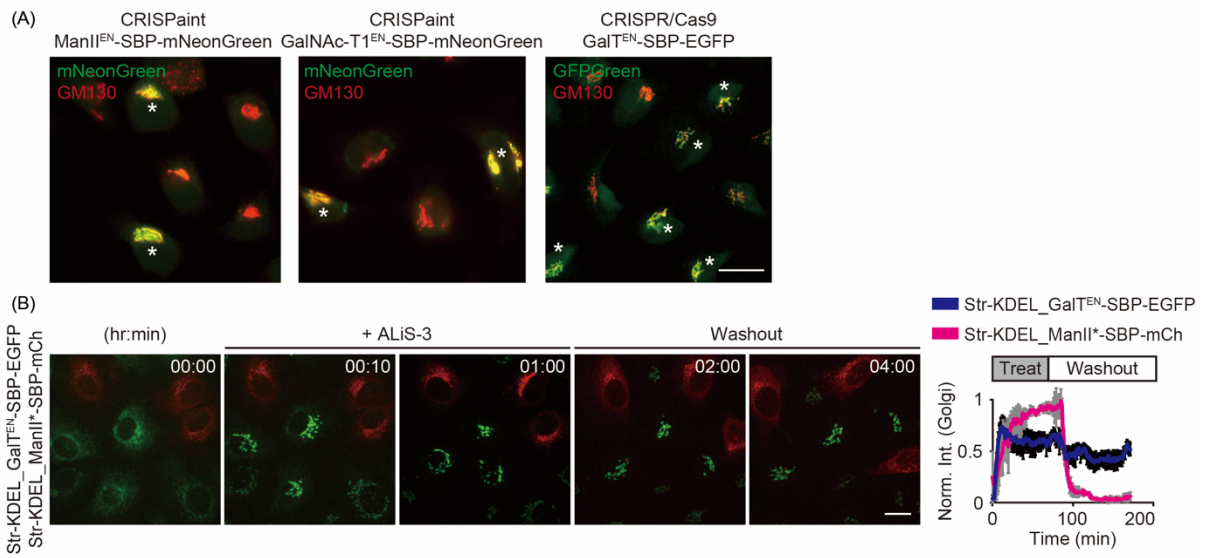

Supplementary Fig. 5 Endogenously tagged Golgi glycosylation enzymes and the synchronized transport of GalT^{EN}-SBP-EGFP. (A) Positive cells, expressing ManII^{EN}-SBP-mNeonGreen, GalNAc-T1^{EN}-SBP-mNeonGreen, and GalT^{EN}-SBP-EGFP were processed for immunofluorescence staining. Green corresponds to the fluorescence of EGFP or mNeonGreen and red shows the staining with anti-GM130 antibody, as a Golgi marker. (B) Hela cells expressing Str-KDEL and GalT^{EN}-SBP-EGFP were pre-incubated in cycloheximide (25 ug/ml) for 20 min, then treated with ALiS-3 (20 µM) from 0 to 1.5 h, and ALiS-3 was washed out as indicated. HeLa cells stably expressing Str-KDEL and ManII*-SBP-mCherry were co-cultured as an internal control of treatments. The plots showed fluorescence intensity in the Golgi apparatus at each time point, and normalized to the maximum value of time-lapse series. Values are means ± S.E.M from two independent experiments with analysis of at least 10 fields. Scale bar: 20 µm.

Tables

Table 1: Primers for genomic PCR

Primer	Sequence (5’ – 3’)	Note
8	CATGGTCCTGCTGGAGTTCGTG	Forward, 3’- EGFP
83	GTAGGTCAGGGTGGTCACGAG	Reverse, 5’- EGFP
142	CGGAATTCAAGCTCGGTGTCCCGATGTCCAC	Forward, 5’- GalT exon 6
556	CGGAATTCCGTGAGCAAGGGCGAGGAGCTG	Forward, 3’ - EGFP
867	CATGTTCTGAAGCCCTCC	Forward, 1kb upstream of GalT
868	GGCTGAGGCTCCCTCC	Reverse, 1kb downstream of GalT
869	GGCATGTCTATATCTCGCC	Forward, sequencing GalT in the region of the stop codon
870	GCAGCACTCTCCGAATTTTC	Reverse, sequencing GalT in the region of the stop codon
1262	CATTCTGACATTAAGGCCTTGAGTCATAAG	Forward, sequencing ManII in the region of the stop codon
1263	GGTTTATGGTACCTATGGAATTGCTTC	Reverse, sequencing ManII in the region of the stop codon
1476	ACAGAGCTTATGCCAGAATTAGGAC	Forward, sequencing GalNAc-T1 in the region of the stop codon
1477	CTGCTGAACGTGCTGTCATAATG	Reverse, sequencing GalNAc-T1 in the region of the stop codon
1748	GTTTCAGGTTCAGGGGGAGGTGT	Reverse, sequencing CRISPaint donor insert
1749	CCGAGCTCAACTTCAAGGAG	Forward, 3’ - mNeonGreen

Table 2: siRNA target sequence

Target	Sequence (5’ – 3’)	Note
Luciferase	#207:CGUACGCGGAAUACUUCGATT	
COG3	#532: AGACTTGTGCAGTTTAACA #533: GGAGCAGUGUGAUGCUAUA #534: AGUGCUGAGUAGGUAAUAG	#533 was used for time-lapse imaging
Rab6a	GAACGTTTCCGTAGCCTCA	

Reference

Banfield, D. K. (2011). Mechanisms of protein retention in the Golgi. *Cold Spring Harb Perspect Biol* **3**, a005264.

Boncompain, G., Divoux, S., Gareil, N., de Forges, H., Lescure, A., Latreche, L., Mercanti, V., Jollivet, F., Raposo, G. and Perez, F. (2012). Synchronization of secretory protein traffic in populations of cells. *Nat Methods* **9**, 493–498.

Bräuer, P., Parker, J. L., Gerondopoulos, A., Zimmermann, I., Seeger, M. A., Barr, F. A. and Newstead, S. (2019). Structural basis for pH-dependent retrieval of ER proteins from the Golgi by the KDEL receptor. *Science* **363**, 1103–1107.

Cancino, J., Capalbo, A., Di Campli, A., Giannotta, M., Rizzo, R., Jung, J. E., Di Martino, R., Persico, M., Heinklein, P., Sallese, M., et al. (2014). Control Systems of Membrane Transport at the Interface between the Endoplasmic Reticulum and the Golgi. *Developmental Cell* **30**, 280–294.

Chao, M. P., Jaiswal, S., Weissman-Tsukamoto, R., Alizadeh, A. A., Gentles, A. J., Volkmer, J., Weiskopf, K., Willingham, S. B., Raveh, T., Park, C. Y., et al. (2010). Calreticulin Is the Dominant Pro-Phagocytic Signal on Multiple Human Cancers and Is Counterbalanced by CD47. *Sci. Transl. Med.* **2**,.

Cole, N. B., Ellenberg, J., Song, J., DiEuliis, D. and Lippincott-Schwartz, J. (1998). Retrograde transport of Golgi-localized proteins to the ER. *J Cell Biol* **140**, 1–15.

de Graffenried, C. L. and Bertozzi, C. R. (2004). The roles of enzyme localisation and complex formation in glycan assembly within the Golgi apparatus. *Current Opinion in Cell Biology* **16**, 356–363.

Fourriere, L., Divoux, S., Roceri, M., Perez, F. and Boncompain, G. (2016). Microtubule-independent secretion requires functional maturation of Golgi elements. *Journal of Cell Science* jcs.188870.

Gill, D. J., Chia, J., Senewiratne, J. and Bard, F. (2010). Regulation of O-glycosylation through Golgi-to-ER relocation of initiation enzymes. *Journal of Cell Biology* **189**, 843–858.

Girod, A., Storrie, B., Simpson, J. C., Johannes, L., Goud, B., Roberts, L. M., Lord, J. M., Nilsson, T. and Pepperkok, R. (1999). Evidence for a COP-I-independent transport route from the Golgi complex to the endoplasmic reticulum. *Nat Cell Biol* **1**, 423–430.

Johannes, L., Tenza, D., Antony, C. and Goud, B. (1997). Retrograde Transport of KDEL-bearing B-fragment of Shiga Toxin. *Journal of Biological Chemistry* **272**, 19554–19561.

Jordan, M., Schallhorn, A. and Wurm, F. M. (1996). Transfecting mammalian cells: optimization of critical parameters affecting calcium-phosphate precipitate formation. *Nucleic Acids Res* **24**, 596–601.

Lewis, M. J. and Pelham, H. R. (1990). A human homologue of the yeast HDEL receptor. *Nature* **348**, 162–163.

Lippincott-Schwartz, J., Yuan, L. C., Bonifacino, J. S. and Klausner, R. D. (1989). Rapid redistribution of Golgi proteins into the ER in cells treated with brefeldin A: evidence for membrane cycling from Golgi to ER. *Cell* **56**, 801–813.

Liu, L., Doray, B. and Kornfeld, S. (2018). Recycling of Golgi glycosyltransferases requires direct binding to coatomer. *Proc. Natl. Acad. Sci. U.S.A.* **115**, 8984–8989.

Miserey-Lenkei, S., Chalancon, G., Bardin, S., Formstecher, E., Goud, B. and Echard, A. (2010). Rab and actomyosin-dependent fission of transport vesicles at the Golgi complex. *Nat Cell Biol* **12**, 645–654.

Munro, S. and Pelham, H. R. (1987). A C-terminal signal prevents secretion of luminal ER proteins. *Cell* **48**, 899–907.

Nguyen, A. T., Chia, J., Ros, M., Hui, K. M., Saltel, F. and Bard, F. (2017). Organelle Specific O-Glycosylation Drives MMP14 Activation, Tumor Growth, and Metastasis. *Cancer Cell* **32**, 639-653.e6.

Pecot, M. Y. and Malhotra, V. (2006). The Golgi Apparatus Maintains Its Organization Independent of the Endoplasmic Reticulum. *MBoC* **17**, 5372–5380.

Rhee, S. W., Starr, T., Forsten-Williams, K. and Storrie, B. (2005). The Steady-State Distribution of Glycosyltransferases Between the Golgi Apparatus and the Endoplasmic Reticulum is Approximately 90:10: Golgi Glycosyltransferase Distribution. *Traffic* **6**, 978–990.

Ros, M., Nguyen, A. T., Chia, J., Le Tran, S., Le Guezennec, X., McDowall, R., Vakhrushev, S., Clausen, H., Humphries, M. J., Saltel, F., et al. (2020). ER-resident oxidoreductases are glycosylated and trafficked to the cell surface to promote matrix degradation by tumour cells. *Nat Cell Biol* **22**, 1371–1381.

Schmid-Burgk, J. L., Höning, K., Ebert, T. S. and Hornung, V. (2016). CRISPaint allows modular base-specific gene tagging using a ligase-4-dependent mechanism. *Nat Commun* **7**, 12338.

Schutze, M. P., Peterson, P. A. and Jackson, M. R. (1994). An N-terminal double-arginine motif maintains type II membrane proteins in the endoplasmic reticulum. *EMBO J* **13**, 1696–1705.

Sengupta, P., Satpute-Krishnan, P., Seo, A. Y., Burnette, D. T., Patterson, G. H. and Lippincott-Schwartz, J. (2015). ER trapping reveals Golgi enzymes continually revisit the ER through a recycling pathway that controls Golgi organization. *Proc. Natl. Acad. Sci. U.S.A.* **112**,.

Smith, R. D., Willett, R., Kudlyk, T., Pokrovskaya, I., Paton, A. W., Paton, J. C. and Lupashin, V. V. (2009). The COG complex, Rab6 and COPI define a novel Golgi retrograde trafficking pathway that is exploited by SubAB toxin. *Traffic* **10**, 1502–1517.

Tachibana, R., Terai, T., Boncompain, G., Sugiyama, S., Saito, N., Perez, F. and Urano, Y. (2017). Improving the Solubility of Artificial Ligands of Streptavidin to Enable More Practical Reversible Switching of Protein Localization in Cells. *ChemBioChem* **18**, 358–362.

Terai, T., Kohno, M., Boncompain, G., Sugiyama, S., Saito, N., Fujikake, R., Ueno, T., Komatsu, T., Hanaoka, K., Okabe, T., et al. (2015). Artificial Ligands of Streptavidin (ALiS): Discovery, Characterization, and Application for Reversible Control of Intracellular Protein Transport. *J. Am. Chem. Soc.* **137**, 10464–10467.

White, J., Johannes, L., Mallard, F., Girod, A., Grill, S., Reinsch, S., Keller, P., Tzschaschel, B., Echard, A., Goud, B., et al. (1999). Rab6 Coordinates a Novel Golgi to ER Retrograde Transport Pathway in Live Cells. *Journal of Cell Biology* **147**, 743–760.

Willett, R., Ungar, D. and Lupashin, V. (2013). The Golgi puppet master: COG complex at center stage of membrane trafficking interactions. *Histochem Cell Biol* **140**, 271–283.

Zolov, S. N. and Lupashin, V. V. (2005). Cog3p depletion blocks vesicle-mediated Golgi retrograde trafficking in HeLa cells. *Journal of Cell Biology* **168**, 747–759.

4. Supplementary information

4.1 KDEL-mediated transport tubular carriers

In the results sections, we have performed the reversible RUSH assay with the truncated form ManII* and ST*, and measured the volume changes of the Golgi apparatus during anterograde and retrograde transport. We also extended our observation with the detailed structures of Golgi apparatus in the retrograde transport. HeLa cells engineered to knock-in EGFP at the N-terminus of Giantin (GFP-GiantinEN) were transiently transfected with Str-KDEL and ManII*-SBP-mCherry, and then treated with ALiS-3 for 1.5 hours. Upon the washout of ALiS-3, ManII*-SBP-mCherry is retrieved to the ER and the detailed transport carriers could be observed. The tubules are extending from the Golgi apparatus and carrying the Golgi cargos ManII*, in absence of the Golgi membrane.

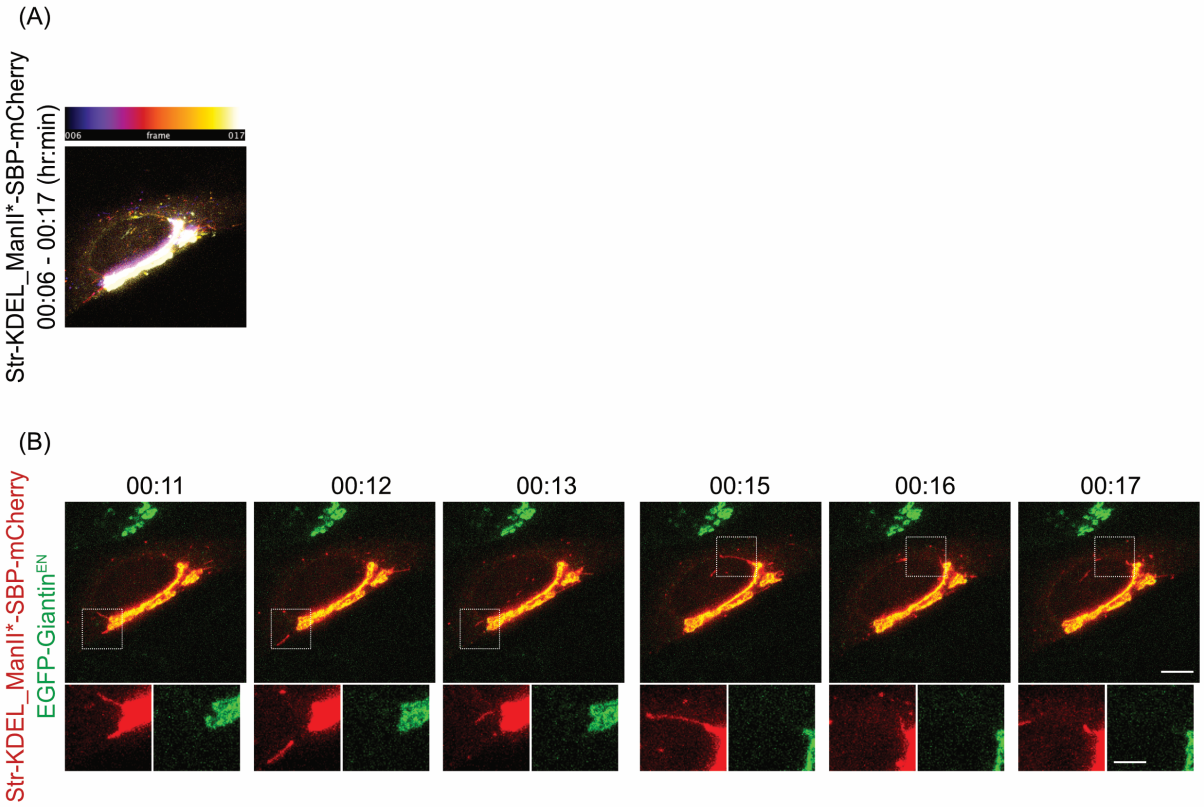

Fig 1. KDEL-mediated transport tubular carriers. Knock-in GFP-GiantinEN HeLa cells were transfected with Str-KDEL and ManII*-SBP-mCherry. Confocal time-lapse images of HeLa cells were obtained with treatment of ALiS-3 (20 μM) for 1.5 h and then subsequent washout for 1 to 2 h. Extending Golgi tubules visualized through the application of temporal-color code (Image J) (A), and the detailed Golgi tubules carriers (B). Scale bar: 20 μm and 2 μm for enlarged images.

4.2 Golgi-to ER retrograde transport of Golgi-resident full-length enzymes

4.2.1 Some difficulties in generating the stable cell lines for reversible RUSH assay

Several Golgi enzymes full length, including mannosidase α class 2A member 1 (MANII), polypeptide N-acetylgalactosaminyltransferase 1 and 4 (GalNac-T1 and T4), and β-galactoside α-2,6-sialyltransferase 1 (ST), were tested, and their retention (at ER), release (to Golgi apparatus) and retrieval (back to ER) status were verified in the reversible RUSH assays.The current difficulties we have confronted for the past years were that we didn't observe the ER recycling of several Golgi enzymes, no matter for KDEL-retrival or glycosylation enzyme recycling pathways, such as for GalNac-T1 and ST . Sometimes we could obtain the clonal cells with nice KDEL recycling, but not for glycosylation enzyme recycling, as for GalNac-T4 and ST.

Table 1: Stable cell lines generated for reversible RUSH assay

Stable cell lines	Retention (ER)	Release (Golgi)	Retrieval (ER)
Str-KDEL_ManII(fl)-SBP-EGFP (Transient)	✓	No trafficking	-
Ii-Str_ManII(fl)-SBP-EGFP (Transient)	✓	No trafficking	-
Str-KDEL_GalNac-T1(fl)-SBP-EGFP	✓	✓	✗
Ii-Str_GalNac-T1(fl)-SBP-EGFP	✓	✓	✗
Str-KDEL_FUT8(fl)-SBP-mCherry	✓	✓	✓
Ii-Str_FUT8(fl)-SBP-mCherry	✓	✓	✗
Str-KDEL_GalNac-T4(fl)-SBP-EGFP	✓	✓	✓
Ii-Str_GalNac-T4(fl)-SBP-EGFP	✓	✓	✗
Str-KDEL_ST(fl)-SBP-EGFP	✓	✓	✗
Ii-Str_ST(fl)-SBP-EGFP	✓	✓	✗

4.2.2 KDEL-mediated retrograde transport of GalNac-T4(fl)

In order to gain insights on the Golgi-resident enzyme trafficking, stable cell lines, expressing Str-KDEL and full-length enzymes GalNac-T4(fl)-SBP-EGFP, were generated to test on RUSH assays. We could observe GalNac-T4(fl)-SBP-GFP was transported from ER to Golgi apparatus upon the treatment of ALiS-3, and retrieved back to ER through KDEL-mediated pathway with the removal of ALiS-3 (Fig. 2A). To examine whether Rab6 could regulate the full-length Golgi-resident enzyme recycling, siRNA treatments against Rab6 were performed. Surprisingly, despite the natural localization of GalNac-T4 in medial-Golgi compartments, depletion of Rab6 disrupted the Golgi-to-ER recycling of GalNac-T4(fl) (Fig. 2B). Re-expression of iRFP670-Rab6 could rescue the delayed KDEL-mediated retrograde transport of GalNac-T4(fl), confirmed by the quantification of kinetics. Collectively, we demonstrate that ER retrieval of e full-length Golgi-resident enzymes recycling through KDEL-mediated pathway, whereas it remains to be further investigated for the differential effects of COG3 and Rab6 as retrograde transport regulators.

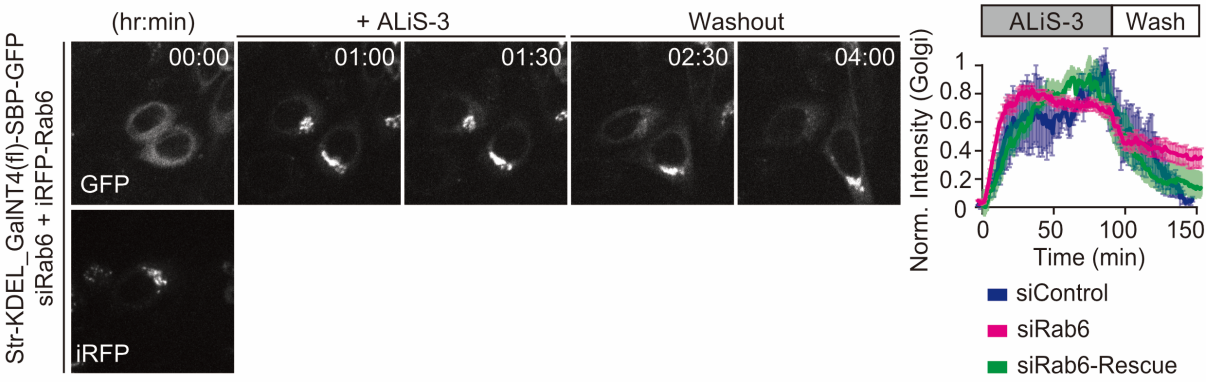

Fig. 2. siRNA-induced Rab6 impairs the KDEL-mediated retrograde transport of GalNac-T4(fl). Kinetic analysis of confocal time-lapse images in HeLa cells, stably expressing GalNac-T4(fl)-SBP-GFP, with the hooks of Str-KDEL. siRNA transfection against Rab6 was performed for 48 hours, and then iRFP670-Rab6 is transfected for another 24 hours before imaging acquisition. Cells were pre-incubated in cycloheximide (25 ug/ml) for 20 mins, then treated with ALiS-3 (20 μM) from 0 to 1.5 hours. Cells were then washed with PBS for 3 times and incubated with Leibovitz medium. The plots showed fluorescence intensity of GalNac-T4(fl)-SBP-GFP in the Golgi at each time point, and normalized to the maximum value of the time-lapse series. Values are means ± S.E.M from two independent experiments with analysis of at least 10 fields. Scale bar: 20 μm.

4.3 Some glycosylation enzymes do not recycle through Golgi-to-ER retrieval pathways

4.3.1 Difficulties in generating the stable cell lines for "RUSH-synchronizable" endogenous Golgi enzymes

The set-up of "RUSH-synchronizable" endogenous Golgi glycosylation enzymes allows us to get access to the bidirectional transport kinetics at an endogenous level. The ER-retention and ER-to-Golgi transport could be detected in most cell lines, with the knock-in of SBP-mNeonGreen or SBP-EGFP. However, ER-recycling could only be observed in the *cis*- and *medial*-Golgi enzymes (i.e. ManII^{EN} and GalNac-T1^{EN}) through KDEL-mediated pathway, but not *trans*-Golgi enzyme (i.e. GalT^{EN}), even with another retrieval signal of HDEL. In addition, we did not see the ER-retrieval through glycosylation enzyme recycling pathway, with the expression of invariant chain hook. Furthermore, in the homozygous clones, no ER-retrieval of GalT^{EN} was observed after the washout of ALiS. We also generated the endogenously tagged Golgi glycosylation enzymes in a breast cancer cell line, SUM159, whereas we did not observe the ER-retrieval of GalT^{EN}. This observation was probably not due to the cell line difference.

Table 2: Stable cell lines generated for "RUSH-synchronizable" endogenous Golgi enzymes

Stable cell lines (CRISPR/Cas9 knock-in)	Retention (ER)	Release (Golgi)	Retrieval (ER)
Str-KDEL_ManII^{EN}-SBP-mNeonGreen	✓	✓	✓
Ii-Str_ManII^{EN}-SBP-mNeonGreen	✓	✓	✗
Str-KDEL_GalNac-T1^{EN}-SBP-mNeonGreen	✓	✓	✓
Ii-Str_GalNac-T1^{EN}-SBP-mNeonGreen	✓	✓	✗
FUT8^{EN}-SBP-mNeonGreen (Low expression)	-	-	-
Str-KDEL_GalT^{EN}-SBP-EGFP	✓	✓	✗
Str-KDEL_GalT^{EN}-SBP-EGFP (SUM159 cell)	✓	✓	✗
Str-KDEL_GalT^{EN}-SBP-EGFP (Homozygote)	✓	✓	✗
Str-myc-HDEL_GalT^{EN}-SBP-EGFP	✓	✓	✗
Ii-Str_GalT^{EN}-SBP-EGFP	✓	✓	✗

4.3.2 "RUSH-synchronizable" endogenous Golgi enzymes using CRISPR-Cas9 and/or CRISPaint with ER stable hook

As previously mentioned, the KDEL-retrieval of GalNac-T1^{EN} could be achieved through the reversible RUSH assay. In order to compare the KDEL-mediated pathway to glycosylation enzyme recycling pathway, ER stable hook was expressed in the knock-in cell line. The retention of GalNac-T1^{EN} in the ER could be observed, thanks to the expression of invariant chain fused to streptavidin (Ii-Str). Although the signals of GalNac-T1^{EN}-SBP-mNeonGreen were localized in the Golgi apparatus with the treatment of ALiS-3, the ER recycling could not be observed with ALiS washout. According to the immunostaining images, the expression of invariant hook could still be detected with anti-streptavidin antibody, but no ER recycling of GalNac-T1^{EN} was observed even after overnight washout of ALiS.

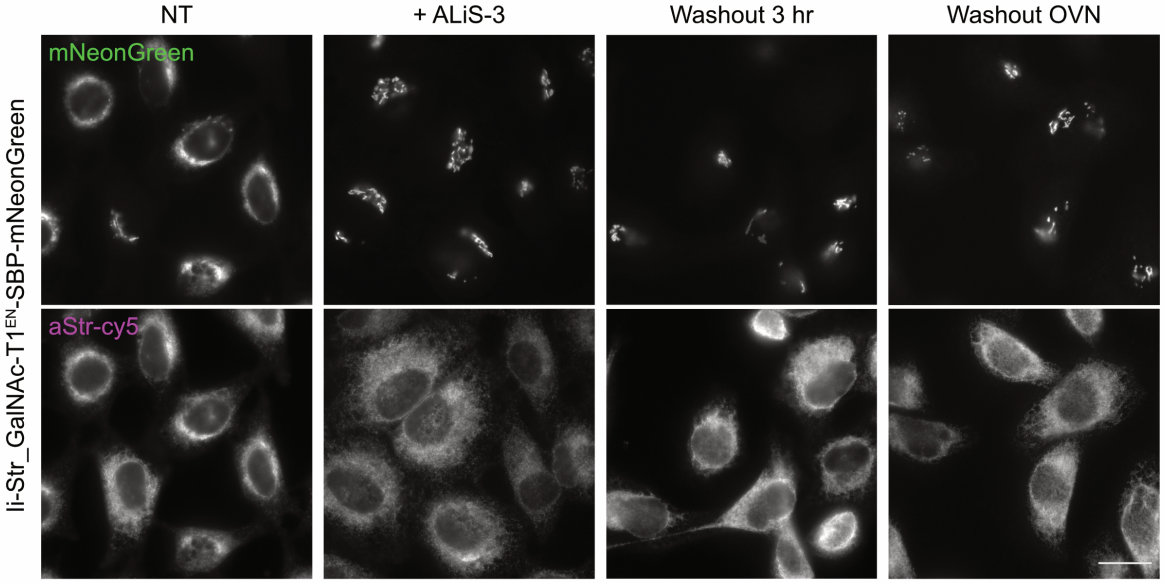

Fig. 3. "RUSH-synchronizable" endogenous GalNac-T1^{EN}-SBP-mNeonGreen does not retrieve through glycosylation enzyme recycling pathway. CRISPaint knock-in cells, expressing Str-KDEL and GalNac-T1^{EN}-SBP-mNeonGreen were pre-incubated in cycloheximide (25 ug/ml) for 20 mins, then treated with ALiS-3 (20 μM) for 1.5 hr. Cells were then washed with PBS for 3 times and incubated with culture medium for 3 hrs or overnight, in presence of cycloheximide. The upper panel of the immunofluorescence staining images corresponds to the fluorescence of mNeonGreen and the lower panel shows the immunostaining with anti-Streptavidin antibody. Scale bar: 20 μm.

4.4 Verification of the ER-retrieval in the genome-edited cell lines

4.4.1 Genomic DNA sequences of the CRISPR/Cas9 and CRISPaint-edited knock-in cells

The genomic DNA of the heterozygous clones were extracted from the engineered knock-in cell lines, and then PCR genotyping was performed to validate the genomic DNA sequences in the gRNA cutting regions. For Man2A1 and GALNT1, both non-edited and edited allele are edited as expected, the deletion of some amino acid was due to the gRNA cutting with CRISPaint strategy. No amino acid deletion in the genome of B4GALT1 is detected, whereas the ER-retrieval of 3 knock-in cell lines was observed, especially through the glycosylation enzyme recycling pathway.

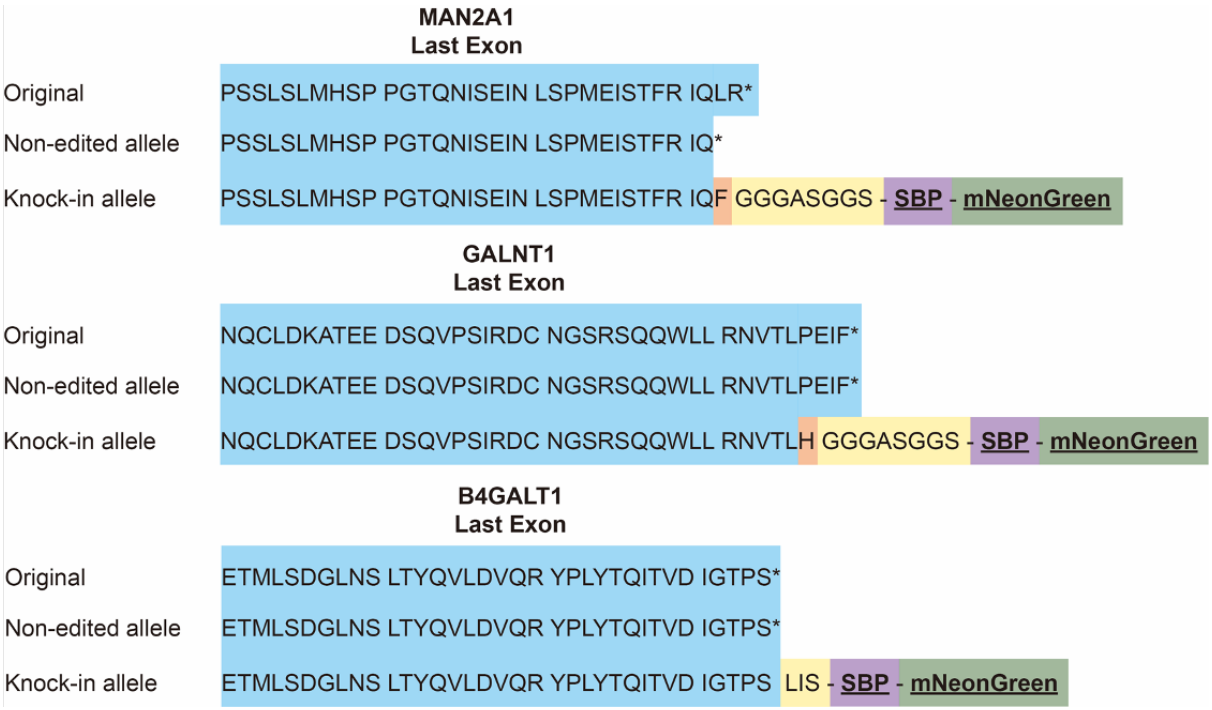

Fig. 4. Verification of the genomic DNA sequences in the knock-in cell lines through PCR genotyping. The genomic DNA of heterozygous clonal cells, expressing ManII^{EN}-, GalNac-T1^{EN}-SBP-mNeonGreen and GalT^{EN}-SBP-EGFP, were extracted and performed the PCR genotyping. Non-edited and knock-in edited alleles were distinguished through different sets of primers, indicated in the manuscript Table 1.

4.4.2 Examination of the Golgi-to-ER retrograde transport through the treatment of Nocodazole and BFA

The KDEL-mediated Golgi-to-ER pathway relies on the capture of KDEL-retrieval signal by the KDEL receptor, which may not reach distal Golgi regions and forbid the KDEL-retrieval of trans-Golgi enzymes. It has been shown that GalT redistributed at a slow but continuous flux to the same peripheral sites as ERGIC-53, upon nocodazole treatment (Cole et al., 1996). To this end, we thus tested the effects of nocodazole treatment in the knock-in cells, expressing GalT^{EN}-SBP-EGFP. In the beginning, Golgi enzyme GalT^{EN} is retained in the ER thanks to hook expression of Str-myc-HDEL. With the treatment of nocodazole for 1.5 hr and the ALiS-3 for 40 mins, we could observe the release of GalT^{EN}-SBP-EGFP, together with dispersed mini-Golgi stacks. After the washout of ALiS and in presence of nocodazole, we could notice the ER-retrieval of the internal control ManII*-SBP-mCherry, but not that of endougenous GalT. The results indicated that the non-retrieval effect of endogenous GalT was not due to the accessibility of the KDEL receptor to trans-Golgi.

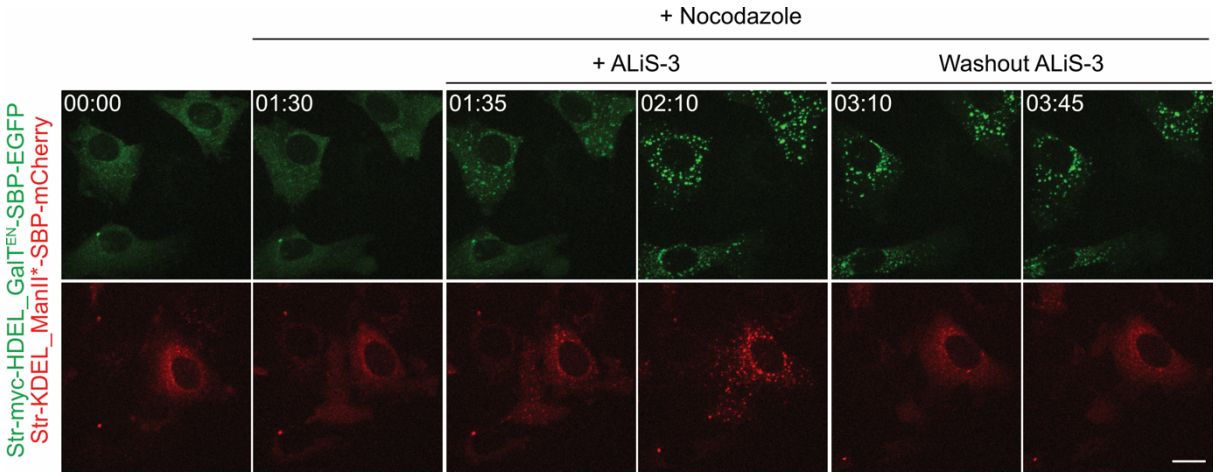

Fig. 5. Treatment of nocodazole does not enhance the KDEL-mediated recycling of endogenous GalT. Genome-edited knock-in cells, expressing GalT1^{EN}-SBP-EGFP and Str-myc-HDEL were pre-treated with cycloheximide (25 ug/ml) for 20 mins, then treated with nocodazole (10 μM) for 1.5 hr, and then ALiS-3 (20 μM) for 40 mins. Cells were then washed with PBS for 3 times and incubated with culture medium for 1.5 hrs, in presence of nocodazole and cycloheximide. Scale bar: 20 μm.

Aside from the treatment of nocodazole, another common approach to study ER-retrieval pathway is antiviral antibiotic brefeldin A (BFA), which can block the ER-Golgi anterograde transport and the in turn lead to the disassembly of the Golgi apparatus (Fujiwara et al., 1988). A study has also shown a rapid re-localization of ManII from Golgi apparatus back to the ER with the treatment of BFA (Lippincott-Schwartz et al., 1989). Therefore, we examined the induced ER-retrieval of GalNac-T1^{EN}-SBP-mNeonGreen with the addition of BFA, and tested whether the ER stable hook can still capture the reporter through the interaction of streptavidin-SBP. In the first panel, GalNac-T1^{EN}-SBP-mNeonGreen is retained in the ER owing to the invariant chain hook expression, as shown with anti-Streptavidin staining. With the treatment of ALiS-3, we can observe the localization of GalNac-T1^{EN}-SBP-mNeonGreen in the Golgi apparatus. Then, with the treatment of BFA, Golgi complex disassembles and the GalNac-T1^{EN}-SBP-mNeonGreen is redistributed back to the ER with or without the expression of Ii-Str hook. After the removal of BFA and ALiS-3, the hook and the reporter are able to interact with each other and are retained in the ER, along with Golgi reformation. These data indicate that the hook remains functional in the ER, and streptavidin can still capture the cargo after the travel.

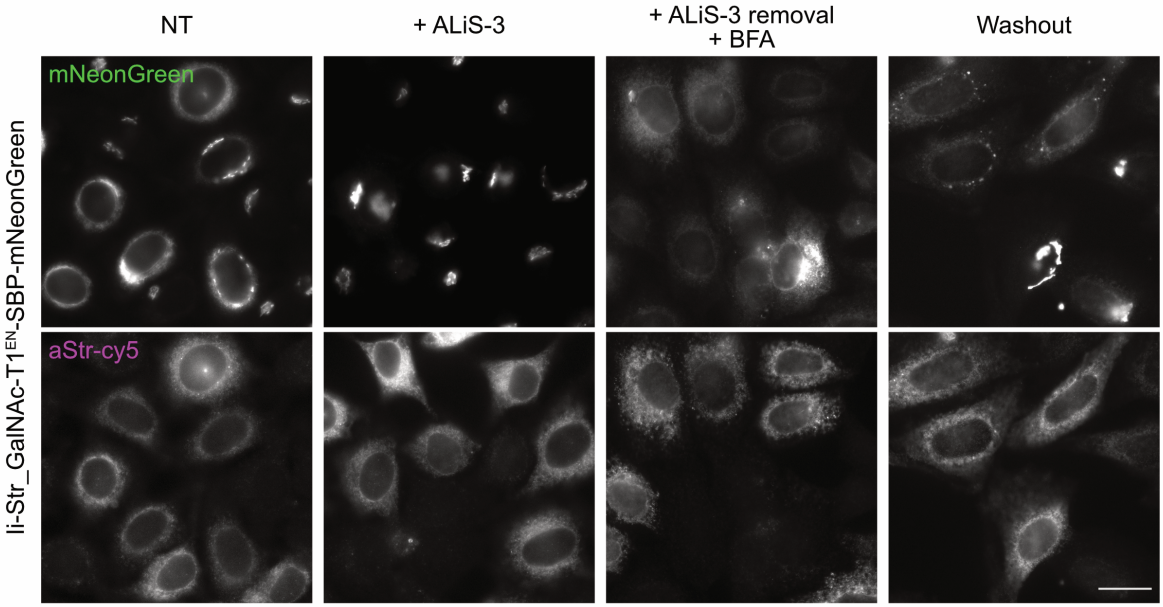

Fig. 6. ER-resident hook Ii-Str remains functional to capture the RUSH-synchronized GalNac-T1^{EN}-SBP-mNeonGreen in the ER upon the treatment of BFA. HeLa cells, stably expressing Ii-Str and GalNac-T1^{EN}-SBP-mNeonGreen, were pre-treated with cycloheximide (25 ug/ml) for 20 mins, followed by the treatment of ALiS-3 (20 μM) for 1.5 hr. Next, the genome-edited cells were washed with PBS for 3 times and then treated with BFA (1 uM) for 1.5 hr, in absence of ALiS-3. Lastly, cells were washed again with PBS for 3 times and changed to culture medium for 1.5 hrs, in presence of cycloheximide. Scale bar: 20 μm.

4.4.3 Protein topology and localization of SBP-EGFP insert in the genome-edited cells

Previously, we have observed the ER-retention in the "RUSH-synchronizable" endogenous Golgi-resident enzymes, but not the ER-retrieval especially through the glycosylation enzyme recycling pathway, using ER-stable hook. One possible reason for this outcome may be the incorrect topology and orientation of the targeted proteins. Golgi enzymes are type II proteins, containing a short N-terminus in the cytosol, a transmembrane domain and a giant enzymatic C-terminus in the lumen. We expect that our CRISPR/Cas9 knock-in strategy integrates and expresses the insertion of SBP-EGFP in the luminal domain of GalT in the C-terminus. To test this hypothesis, we treated the genome-edited cells with digitonin, a mild nonionic detergent for cell permeabilization, in a series of concentrations from 10 μM to 250 μM, together with saponin as a positive control. Solely the plasma membrane was permeabilized at the low concentration of digitonin treatment (10 μM - 20 μM), revealing the posititve immunostaining of Golgi apparatus using anti-GM130 antibodies. The signals of anti-GalT and anti-GFP antibodies could be detected in the Golgi apparatus upon the addition of the elevated digitonin concentration at 120 μM - 250 μM; however, when the Golgi membranes remained intact at the lower digitonin concentration (10-20 μM), no signals from the immunostaining of anti-GalT and anti-GFP antibodies were found in the images. These results indicate that both proteins of GalT and GFP were expressed in the lumen of Golgi apparatus, as what we have designed for CRISPR/Cas9 strategies.

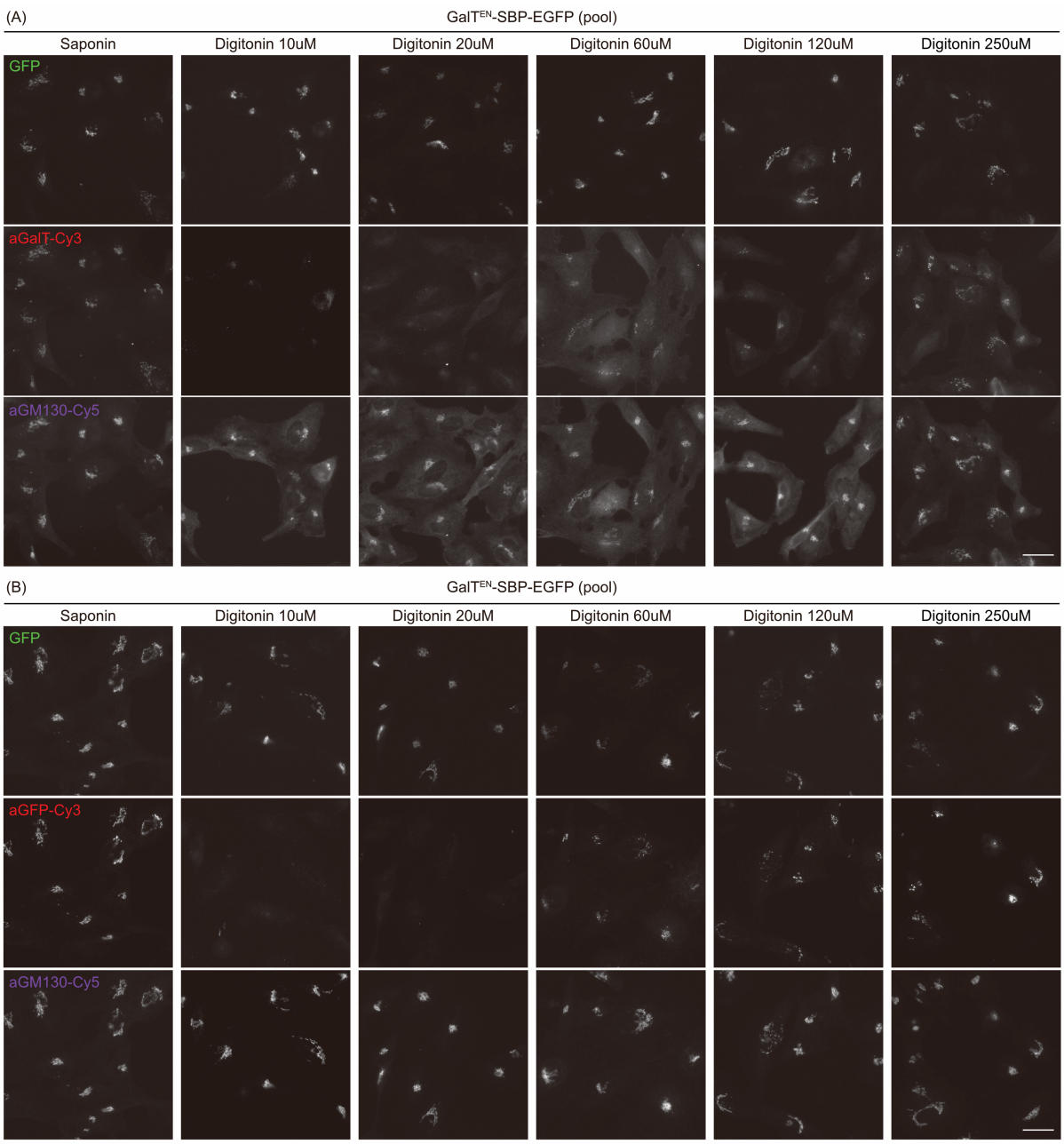

Fig. 7. Validation of protein topology of SBP-EGFP insert in the genome-edited cells through digitonin treatment. (A-B) CRISPR/Cas9 knock-in cell lines in SUM159 cells (pool), expressing GalT^{EN}-SBP-EGFP, were fixed with 3% PFA for 10 mins and then treated with either saponin, or digitonin (from 10 µM - 250 µM) for 10 mins. Cells were then washed with PBS for 3 times and incubated with anti-GalT, anti-GFP, and anti-GM130 antibodies for 30 mins, followed by the secondary antibodies as indicated. Scale bar: 20 µm.

Aside from validation of the protein topology of SBP-EGFP insert, the correlated transmission electron microscopy was performed to examine the localization of endogenous GalT and the insertion of EGFP in the genome-edited cells. Thanks to Severine Divoux, the immunogold staining of anti-GalT antibodies and PAG10 were found in the *trans*- and post-Golgi vesicles, co-localized with anti-EGFP antibodies and PAG15. These results indicated that the protein expression of the knock-in SBP-EGFP cassette does not show ectopic localization.

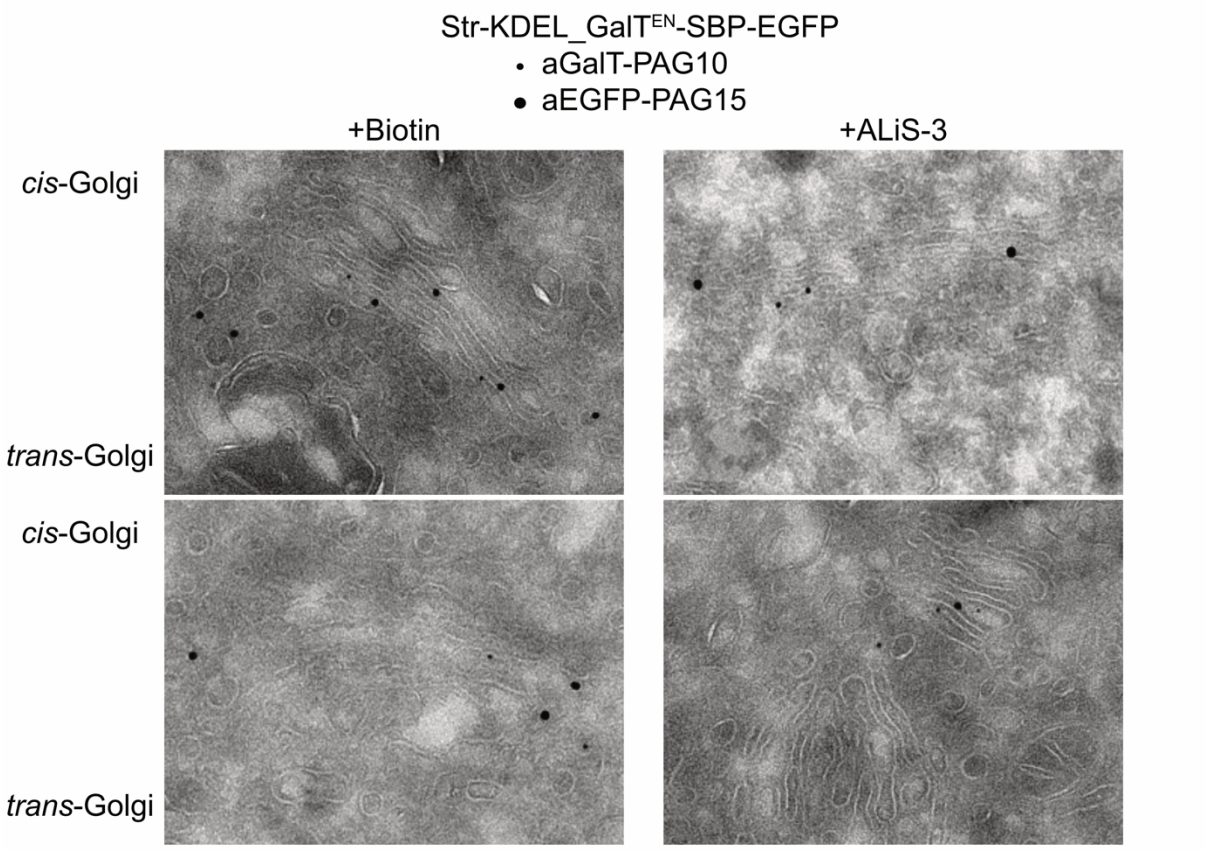

Fig. 8. Localization of GalT^{EN}-SBP-EGFP through electron microscopy. CRISPR/Cas9 knock-in cell lines in SUM159 cells (pool), expressing GalT^{EN}-SBP-EGFP and Str-KDEL, were treated with biotin (400 μM) and ALiS-3 (40 μM) for 1.5 hr. Cells were then fixed with 3% PFA for 10 mins and immunogold labeled with anti-GalT and protein A gold conjugate (PAG10, 10 nm), together with anti-EGFP antibodies and protein A gold conjugate (PAG15, 15 nm).

Discussion

Glycosylation serves as a critical feature of proteins and lipids in all living cells. The large variety of carbohydrate structures are produced in the cells, owing to over hundreds of different Golgi-resident glycosylation enzymes. It is known that these glycosylation enzymes have the non-uniform distribution in the Golgi cisternae. The relative position of the enzymes at steady state often reflects a set of sequential manners of glycan synthesis. Of note, an aberrant glycosylation pattern represents a hallmark of cancer. Studies have revealed that dysregulation of Golgi localization of the glycosylation enzymes, such as as GalNAc transferases and T-synthase (also known as C1GalT1) contribute to several types of cancers (Egea et al., 1993; Ju et al., 2008). These findings bring up the importance of glycosylation enzymes positioning in the Golgi apparatus, the transport and recycling mechanisms between ER and Golgi apparatus.

Among the seven members of β-1, 4-galactosyltransferase gene (B4GalT) family, B4GalT1 is the first enzyme to be identified and characterized, residing in the trans-Golgi cisternae and TGN (Roth and Berger, 1982; Rabouille et al., 1995). The mechanisms of glycosyltransferase retention have been proposed — bilayer thickness model and protein aggregation (or kin-recognition), based on the observation of homo-/hetero-/oligomerization of Golgi-resident enzymes, which prevented their entry into vesicle trafficking and could be in turn retained in the certain Golgi cisternae (Nilsson et al. 1994; Banfield, 2011). Studies have proposed the kin recognition model of the enzyme heteromers GalNT1-ManII and B4GalT1-ST6Gal1 in the Golgi apparatus (de Graffenried and Bertozzi, 2004). This may explain why our attempts to observe the Golgi-to-ER retrograde transport of endogenous B4GalT1 did not reach to our expectation. It is possible that the endogenous B4GalT1 aggregates to form heteromers with ST6Gal1 or oligomers, which prevents the streptavidin from accessing SBP, and thus avoids the retrograde transport from Golgi back to ER.

Localization of KDEL receptors

We have observed that endogenous B4GalT1 in both genome-edited HeLa and SUM159 cell lines do not recycle from Golgi apparatus back to ER, through KDEL-mediated retrograde transport. KDEL receptors were found predominantly localized to the intermediate compartment, colocalizing with Rab1 in the cell periphery during interphase, or close to Golgi during metaphase (Saraste and Marie, 2018). In addition, KDEL receptors can

distribute further to the distal end of *trans*-Golgi region and even plasma membranes (Jia et al., 2021; Miesenböck and Rothman, 1995). Through CRISPR-cas9 knock-in strategy, the endogenous KDEL receptors were detected on the cell surface, capturing and internalizing the fluorescent KDEL peptide (Jia et al., 2021). Hence, stochastic optical reconstruction microscopy (STORM) can be used to visualize the detailed insights of KDEL receptor positioning on different Golgi cisternae in high-resolution, which may in turn interfere with the ER-retrieval of some glycosylation enzymes. This model may explain how the spatial distribution of 3 KDEL receptors serves an important role in the KDEL-mediated retrograde transport.

RUSH assay with ER-stable hooks

Studies in crystal structures have revealed that one tetrameric streptavidin is essential to capture two SBP tags (Barrette-Ng et al., 2013). It indicates that RUSH assay requires 2 times more expression of the hooks than that of the reporter proteins inside cells. However, invariant chain (Ii) forms as a trimer to enable the localization in the ER (Dixon et al., 2006). With these findings, we can hardly imagine the protein structure of an invariant chain fused to streptavidin (Ii-Str) in the ER. Therefore, some targets, such as STIM1 or TRAM, could be tested as alternative ER-localized hooks, as these proteins were shown to have the stable expression in the ER (Gorlich, 1993; Tamborero et al., 2011). Or one may propose to test on monomeric or dimeric form of Streptavidin to improve the ER retrieval (Lim et al., 2011).

Other regulators in Golgi-to-ER retrograde transport

Studies have revealed that different glycosylation enzymes were recycled through COPI-dependent or Rab6-dependent pathways, as mentioned in the introduction parts. To identify some regulatory factors in Golgi-ER retrograde transport, siRNA knockdown experiments, targeting to known regulators, such as Golgi phosphoprotein 3 (GOLPH3), Conserved Oligomeric Golgi (COG) complex and Rab6, were performed in the above-mentioned stable cell lines. High-throughput screening can be performed for the future projects to identify more interesting regulatory factors in these cell lines. Another member of the golgin family, GORAB, was previously identified at *trans*-Golgi in the COPI-mediated retrieval machinery and caused the mislocation of ST6Gal1 (Witkos et al., 2019). We expect to highlight different regulators, some involved in the KDEL-mediated pathway and others in the ER recycling of glycosylation enzymes. A kinetics analysis of two retrograde pathways in the siRNA depleted cells can together be conducted.

In summary, we have developed a novel quantitative assay to monitor the anterograde and retrograde transport between ER and Golgi apparatus in real-time. However, the detailed mechanisms of re-translocation of glycosylation enzymes from Golgi back to ER still remain elusive. Using our modified RUSH assay, we are able to 1) describe the kinetics and modes of transport between Golgi and ER and 2) to identify common and specific regulators involved in the Golgi-to-ER retrograde transport. Our current results confirm the existence of two distinct Golgi-to-ER retrograde transport routes, including KDEL-mediated and glycosylation enzymes recycling pathways.

Reference

Abdul Kadir, L., Stacey, M. and Barrett-Jolley, R. (2018). Emerging Roles of the Membrane Potential: Action Beyond the Action Potential. *Front. Physiol.* **9**, 1661.

Aebi, M. (2013). N-linked protein glycosylation in the ER. *Biochimica et Biophysica Acta (BBA) - Molecular Cell Research* **1833**, 2430–2437.

Almanza, A., Carlesso, A., Chintha, C., Creedican, S., Doultsinos, D., Leuzzi, B., Luís, A., McCarthy, N., Montibeller, L., More, S., et al. (2019). Endoplasmic reticulum stress signalling - from basic mechanisms to clinical applications. *FEBS J* **286**, 241–278.

Appenzeller, C., Andersson, H., Kappeler, F. and Hauri, H.-P. (1999). The lectin ERGIC-53 is a cargo transport receptor for glycoproteins. *Nat Cell Biol* **1**, 330–334.

Apweiler, R. (1999). On the frequency of protein glycosylation, as deduced from analysis of the SWISS-PROT database. *Biochimica et Biophysica Acta (BBA) - General Subjects* **1473**, 4–8.

Arakel, E. C. and Schwappach, B. (2018). Formation of COPI-coated vesicles at a glance. *Journal of Cell Science* **131**, jcs209890.

Bailey Blackburn, J., Pokrovskaya, I., Fisher, P., Ungar, D. and Lupashin, V. V. (2016). COG Complex Complexities: Detailed Characterization of a Complete Set of HEK293T Cells Lacking Individual COG Subunits. *Front. Cell Dev. Biol.* **4**,.

Balch, W. E., Dunphy, W. G., Braell, W. A. and Rothman, J. E. (1984). Reconstitution of the transport of protein between successive compartments of the golgi measured by the coupled incorporation of N-acetylglucosamine. *Cell* **39**, 405–416.

Banfield, D. K. (2011). Mechanisms of protein retention in the Golgi. *Cold Spring Harb Perspect Biol* **3**, a005264.

Bard, F., Mazelin, L., Péchoux-Longin, C., Malhotra, V. and Jurdic, P. (2003). Src Regulates Golgi Structure and KDEL Receptor-dependent Retrograde Transport to the Endoplasmic Reticulum. *Journal of Biological Chemistry* **278**, 46601–46606.

Barr, F. A., Puype, M., Vandekerckhove, J. and Warren, G. (1997). GRASP65, a Protein Involved in the Stacking of Golgi Cisternae. *Cell* **91**, 253–262.

Barrette-Ng, I. H., Wu, S.-C., Tjia, W.-M., Wong, S.-L. and Ng, K. K. S. (2013). The structure of the SBP-Tag–streptavidin complex reveals a novel helical scaffold bridging binding pockets on separate subunits. *Acta Crystallogr D Biol Crystallogr* **69**, 879–887.

Beck, R., Ravet, M., Wieland, F. T. and Cassel, D. (2009). The COPI system: Molecular mechanisms and function. *FEBS Letters* **583**, 2701–2709.

Becker, B., Shaebani, M. R., Rammo, D., Bubel, T., Santen, L. and Schmitt, M. J. (2016). Cargo binding promotes KDEL receptor clustering at the mammalian cell surface. *Sci Rep* **6**, 28940.

Belden, W. J. and Barlowe, C. (2001). Role of Erv29p in collecting soluble secretory proteins into ER-derived transport vesicles. *Science* **294**, 1528–1531.

Bell, A. W., Ward, M. A., Blackstock, W. P., Freeman, H. N. M., Choudhary, J. S., Lewis, A. P., Chotai, D., Fazel, A., Gushue, J. N., Paiement, J., et al. (2001). Proteomics Characterization of Abundant Golgi Membrane Proteins. *Journal of Biological Chemistry* **276**, 5152–5165.

Bergmann, J. E. (1989). Chapter 4 Using Temperature-Sensitive Mutants of VSV to Study Membrane Protein Biogenesis. In *Methods in Cell Biology*, pp. 85–110. Elsevier.

Béthune, J. and Wieland, F. T. (2018). Assembly of COPI and COPII Vesicular Coat Proteins on Membranes. *Annu. Rev. Biophys.* **47**, 63–83.

Beznoussenko, G. V., Parashuraman, S., Rizzo, R., Polishchuk, R., Martella, O., Di Giandomenico, D., Fusella, A., Spaar, A., Sallese, M., Capestrano, M. G., et al. (2014). Transport of soluble proteins through the Golgi occurs by diffusion via continuities across cisternae. *eLife* **3**, e02009.

Blackburn, J. B. and Lupashin, V. V. (2016). Creating Knockouts of Conserved Oligomeric Golgi Complex Subunits Using CRISPR-Mediated Gene Editing Paired with a Selection Strategy Based on Glycosylation Defects Associated with Impaired COG Complex Function. In *The Golgi Complex* (ed. Brown, W. J.), pp. 145–161. New York, NY: Springer New York.

Blackburn, J. B., D'Souza, Z. and Lupashin, V. V. (2019). Maintaining order: COG complex controls Golgi trafficking, processing, and sorting. *FEBS Lett* **593**, 2466–2487.

Blagoveshchenskaya, A., Cheong, F. Y., Rohde, H. M., Glover, G., Knödler, A., Nicolson, T., Boehmelt, G. and Mayinger, P. (2008). Integration of Golgi trafficking and growth factor signaling by the lipid phosphatase SAC1. *Journal of Cell Biology* **180**, 803–812.

Boncompain, G., Divoux, S., Gareil, N., de Forges, H., Lescure, A., Latreche, L., Mercanti, V., Jollivet, F., Raposo, G. and Perez, F. (2012). Synchronization of secretory protein traffic in populations of cells. *Nat Methods* **9**, 493–498.

Boncompain, G., Herit, F., Tessier, S., Lescure, A., Del Nery, E., Gestraud, P., Staropoli, I., Fukata, Y., Fukata, M., Brelot, A., et al. (2019). Targeting CCR5 trafficking to inhibit HIV-1 infection. *Sci. Adv.* **5**, eaax0821.

Boncompain, G. and Perez, F. (2013). The many routes of Golgi-dependent trafficking. *Histochem Cell Biol* **140**, 251–260.

Bonfanti, L., Mironov, A. A., Martínez-Menárguez, J. A., Martella, O., Fusella, A., Baldassarre, M., Buccione, R., Geuze, H. J., Mironov, A. A. and Luini, A. (1998). Procollagen Traverses the Golgi Stack without Leaving the Lumen of Cisternae. *Cell* **95**, 993–1003.

Bottanelli, F., Kilian, N., Ernst, A. M., Rivera-Molina, F., Schroeder, L. K., Kromann, E. B., Lessard, M. D., Erdmann, R. S., Schepartz, A., Baddeley, D., et al. (2017). A novel physiological role for ARF1 in the formation of bidirectional tubules from the Golgi. *MBoC* **28**, 1676–1687.

Bräuer, P., Parker, J. L., Gerondopoulos, A., Zimmermann, I., Seeger, M. A., Barr, F. A. and Newstead, S. (2019). Structural basis for pH-dependent retrieval of ER proteins from the Golgi by the KDEL receptor. *Science* **363**, 1103–1107.

Britain, C. M., Holdbrooks, A. T., Anderson, J. C., Willey, C. D. and Bellis, S. L. (2018). Sialylation of EGFR by the ST6Gal-I sialyltransferase promotes EGFR activation and resistance to gefitinib-mediated cell death. *J Ovarian Res* **11**, 12.

Brockhausen, I., Wandall, H. H., Hagen, K. G. T. and Stanley, P. (2022). O-GalNAc Glycans. In *Essentials of Glycobiology* (ed. Varki, A.), Cummings, R. D.), Esko, J. D.), Stanley, P.), Hart, G. W.), Aebi, M.), Mohnen, D.), Kinoshita, T.), Packer, N. H.), Prestegard, J. H.), et al.), p. Cold Spring Harbor (NY): Cold Spring Harbor Laboratory Press.

Budnik, A. and Stephens, D. J. (2009). ER exit sites - Localization and control of COPII vesicle formation. *FEBS Letters* **583**, 3796–3803.

Cancino, J., Capalbo, A., Di Campli, A., Giannotta, M., Rizzo, R., Jung, J. E., Di Martino, R., Persico, M., Heinklein, P., Sallese, M., et al. (2014). Control Systems of Membrane Transport at the Interface between the Endoplasmic Reticulum and the Golgi. *Developmental Cell* **30**, 280–294.

Cao, X., Surma, M. A. and Simons, K. (2012). Polarized sorting and trafficking in epithelial cells. *Cell Res* **22**, 793–805.

Cavalier-Smith, T. (1988). Origin of the cell nucleus. *Bioessays* **9**, 72–78.

Chabin-Brion, K., Marceiller, J., Perez, F., Settegrana, C., Drechou, A., Durand, G. and Poüs, C. (2001). The Golgi Complex Is a Microtubule-organizing Organelle. *MBoC* **12**, 2047–2060.

Chao, M. P., Jaiswal, S., Weissman-Tsukamoto, R., Alizadeh, A. A., Gentles, A. J., Volkmer, J., Weiskopf, K., Willingham, S. B., Raveh, T., Park, C. Y., et al. (2010). Calreticulin Is the Dominant Pro-Phagocytic Signal on Multiple Human Cancers and Is Counterbalanced by CD47. *Sci. Transl. Med.* **2**,.

Chen, X. and Cubillos-Ruiz, J. R. (2021). Endoplasmic reticulum stress signals in the tumour and its microenvironment. *Nat Rev Cancer* **21**, 71–88.

Chen, I. and Lui, F. (2022). Physiology, Active Transport. In *StatPearls*, p. Treasure Island (FL): StatPearls Publishing.

Chen, Y., Gershlick, D. C., Park, S. Y. and Bonifacino, J. S. (2017a). Segregation in the Golgi complex precedes export of endolysosomal proteins in distinct transport carriers. *Journal of Cell Biology* **216**, 4141–4151.

Chen, Y., Gershlick, D. C., Park, S. Y. and Bonifacino, J. S. (2017b). Segregation in the Golgi complex precedes export of endolysosomal proteins in distinct transport carriers. *Journal of Cell Biology* **216**, 4141–4151.

Chia, J., Tay, F. and Bard, F. (2019). The GalNAc-T Activation (GALA) Pathway: Drivers and markers. *PLoS ONE* **14**, e0214118.

Chia, J., Wang, S.-C., Wee, S., Gill, D. J., Tay, F., Kannan, S., Verma, C. S., Gunaratne, J. and Bard, F. A. (2021). Src activates retrograde membrane traffic through phosphorylation of GBF1. *eLife* **10**, e68678.

Climer, L. K., Dobretsov, M. and Lupashin, V. (2015). Defects in the COG complex and COG-related trafficking regulators affect neuronal Golgi function. *Front. Neurosci.* **9**,.

Cluett, E. B. and Brown, W. J. (1992). Adhesion of Golgi cisternae by proteinaceous interactions: intercisternal bridges as putative adhesive structures. *Journal of Cell Science* **103**, 773–784.

Cole, N. B., Sciaky, N., Marotta, A., Song, J. and Lippincott-Schwartz, J. (1996). Golgi dispersal during microtubule disruption: regeneration of Golgi stacks at peripheral endoplasmic reticulum exit sites. *MBoC* **7**, 631–650.

Cole, N. B., Ellenberg, J., Song, J., DiEuliis, D. and Lippincott-Schwartz, J. (1998). Retrograde transport of Golgi-localized proteins to the ER. *J Cell Biol* **140**, 1–15.

Corbett, E. F. and Michalak, M. (2000). Calcium, a signaling molecule in the endoplasmic reticulum? *Trends in Biochemical Sciences* **25**, 307–311.

Crick, F. H. (1958). On protein synthesis. *Symp Soc Exp Biol* **12**, 138–163.

Cummings, R. D. and Etzler, M. E. (2009). Antibodies and Lectins in Glycan Analysis. In *Essentials of Glycobiology* (ed. Varki, A.), Cummings, R. D.), Esko, J. D.), Freeze, H. H.), Stanley, P.), Bertozzi, C. R.), Hart, G. W.), and Etzler, M. E.), p. Cold Spring Harbor (NY): Cold Spring Harbor Laboratory Press.

Cummings, R. D., Schnaar, R. L. and Ozeki, Y. (2022). R-Type Lectins. In *Essentials of Glycobiology* (ed. Varki, A.), Cummings, R. D.), Esko, J. D.), Stanley, P.), Hart, G. W.), Aebi, M.), Mohnen, D.), Kinoshita, T.), Packer, N. H.), Prestegard, J. H.), et al.), p. Cold Spring Harbor (NY): Cold Spring Harbor Laboratory Press.

de Graffenried, C. L. and Bertozzi, C. R. (2004). The roles of enzyme localisation and complex formation in glycan assembly within the Golgi apparatus. *Current Opinion in Cell Biology* **16**, 356–363.

De Matteis, M. A., Wilson, C. and D'Angelo, G. (2013). Phosphatidylinositol-4-phosphate: The Golgi and beyond: Prospects & Overviews. *BioEssays* **35**, 612–622.

Dell, A., Galadari, A., Sastre, F. and Hitchen, P. (2010). Similarities and Differences in the Glycosylation Mechanisms in Prokaryotes and Eukaryotes. *International Journal of Microbiology* **2010**, 1–14.

Demaretz, S., Seaayfan, E., Bakhos-Douaihy, D., Frachon, N., Kömhoff, M. and Laghmani, K. (2021). Golgi Alpha1,2-Mannosidase IA Promotes Efficient Endoplasmic Reticulum-Associated Degradation of NKCC2. *Cells* **11**, 101.

Devireddy, S. and Ferguson, S. M. (2021). *Surf4 Promotes Endoplasmic Reticulum Exit of the Lysosomal Prosaposin-Progranulin Complex*. Cell Biology.

Dewald, B., Touster, O., and With the technical assistance of Vera Coleman (1973). A New α-d-Mannosidase Occurring in Golgi Membranes. *Journal of Biological Chemistry* **248**, 7223–7233.

Di Martino, R., Sticco, L. and Luini, A. (2019). Regulation of cargo export and sorting at the trans-Golgi network. *FEBS Lett* **593**, 2306–2318.

Dixon, A. M., Stanley, B. J., Matthews, E. E., Dawson, J. P. and Engelman, D. M. (2006). Invariant Chain Transmembrane Domain Trimerization: A Step in MHC Class II Assembly. *Biochemistry* **45**, 5228–5234.

D'Souza, Z., Taher, F. S. and Lupashin, V. V. (2020). Golgi inCOGnito: From vesicle tethering to human disease. *Biochimica et Biophysica Acta (BBA) - General Subjects* **1864**, 129694.

D'Souza-Schorey, C. and Chavrier, P. (2006). ARF proteins: roles in membrane traffic and beyond. *Nat Rev Mol Cell Biol* **7**, 347–358.

Durán, J. M., Valderrama, F., Castel, S., Magdalena, J., Tomás, M., Hosoya, H., Renau-Piqueras, J., Malhotra, V. and Egea, G. (2003). Myosin Motors and Not Actin Comets Are Mediators of the Actin-based Golgi-to-Endoplasmic Reticulum Protein Transport. *MBoC* **14**, 445–459.

Echard, A., Opdam, F. J. M., de Leeuw, H. J. P. C., Jollivet, F., Savelkoul, P., Hendriks, W., Voorberg, J., Goud, B. and Fransen, J. A. M. (2000). Alternative Splicing of the Human *Rab6A* Gene Generates Two Close but Functionally Different Isoforms. *MBoC* **11**, 3819–3833.

Eckert, E. S. P., Reckmann, I., Hellwig, A., Röhling, S., El-Battari, A., Wieland, F. T. and Popoff, V. (2014). Golgi phosphoprotein 3 triggers signal-mediated incorporation of glycosyltransferases into coatomer-coated (COPI) vesicles. *J Biol Chem* **289**, 31319–31329.

Efimov, A., Kharitonov, A., Efimova, N., Loncarek, J., Miller, P. M., Andreyeva, N., Gleeson, P., Galjart, N., Maia, A. R. R., McLeod, I. X., et al. (2007). Asymmetric CLASP-Dependent Nucleation of Noncentrosomal Microtubules at the trans-Golgi Network. *Developmental Cell* **12**, 917–930.

Egea, G., Franci, C., Gambus, G., Lesuffleur, T., Zweibaum, A. and Real, F. X. (1993). cis-Golgi resident proteins and O-glycans are abnormally compartmentalized in the RER of colon cancer cells. *Journal of Cell Science* **105**, 819–830.

Emmer, B. T., Hesketh, G. G., Kotnik, E., Tang, V. T., Lascuna, P. J., Xiang, J., Gingras, A.-C., Chen, X.-W. and Ginsburg, D. (2018). The cargo receptor SURF4 promotes the efficient cellular secretion of PCSK9. *eLife* **7**, e38839.

Foulquier, F. (2009). COG defects, birth and rise! *Biochimica et Biophysica Acta (BBA) - Molecular Basis of Disease* **1792**, 896–902.

Fourriere, L., Divoux, S., Roceri, M., Perez, F. and Boncompain, G. (2016a). Microtubule-independent secretion requires functional maturation of Golgi elements. *Journal of Cell Science* jcs.188870.

Fourriere, L., Divoux, S., Roceri, M., Perez, F. and Boncompain, G. (2016b). Microtubule-independent secretion requires functional maturation of Golgi elements. *Journal of Cell Science* jcs.188870.

Franke, W. W., Kartenbeck, J., Krien, S., Woude, W. J., Scheer, U. and Morré, D. J. (1972). Inter- and intracisternal elements of the Golgi apparatus: A system of membrane-to-membrane cross-links. *Z.Zellforsch* **132**, 365–380.

Friedman, J. R., Webster, B. M., Mastronarde, D. N., Verhey, K. J. and Voeltz, G. K. (2010). ER sliding dynamics and ER–mitochondrial contacts occur on acetylated microtubules. *Journal of Cell Biology* **190**, 363–375.

Friedman, J. R., Lackner, L. L., West, M., DiBenedetto, J. R., Nunnari, J. and Voeltz, G. K. (2011). ER tubules mark sites of mitochondrial division. *Science* **334**, 358–362.

Fries, E. and Rothman, J. E. (1980). Transport of vesicular stomatitis virus glycoprotein in a cell-free extract. *Proc. Natl. Acad. Sci. U.S.A.* **77**, 3870–3874.

Fritzler, M. J., Hamel, J. C., Ochs, R. L. and Chan, E. K. (1993). Molecular characterization of two human autoantigens: unique cDNAs encoding 95- and 160-kD proteins of a putative family in the Golgi complex. *Journal of Experimental Medicine* **178**, 49–62.

Fromme, J. C. and Schekman, R. (2005). COPII-coated vesicles: flexible enough for large cargo? *Current Opinion in Cell Biology* **17**, 345–352.

Fuchs, E., Haas, A. K., Spooner, R. A., Yoshimura, S., Lord, J. M. and Barr, F. A. (2007). Specific Rab GTPase-activating proteins define the Shiga toxin and epidermal growth factor uptake pathways. *Journal of Cell Biology* **177**, 1133–1143.

Fujiwara, T., Oda, K., Yokota, S., Takatsuki, A. and Ikehara, Y. (1988). Brefeldin A causes disassembly of the Golgi complex and accumulation of secretory proteins in the endoplasmic reticulum. *J Biol Chem* **263**, 18545–18552.

Futerman, A. H., Stieger, B., Hubbard, A. L. and Pagano, R. E. (1990). Sphingomyelin synthesis in rat liver occurs predominantly at the cis and medial cisternae of the Golgi apparatus. *J Biol Chem* **265**, 8650–8657.

Gassmann, M., Haller, C., Stoll, Y., Aziz, S. A., Biermann, B., Mosbacher, J., Kaupmann, K. and Bettler, B. (2005). The RXR-Type Endoplasmic Reticulum-Retention/Retrieval Signal of $GABA_{B1}$ Requires Distant Spacing from the Membrane to Function. *Mol Pharmacol* **68**, 137–144.

Gaynor, E. C., Graham, T. R. and Emr, S. D. (1998). COPI in ER/Golgi and intra-Golgi transport: do yeast COPI mutants point the way? *Biochimica et Biophysica Acta (BBA) - Molecular Cell Research* **1404**, 33–51.

Ghosh, P., Dahms, N. M. and Kornfeld, S. (2003). Mannose 6-phosphate receptors: new twists in the tale. *Nat Rev Mol Cell Biol* **4**, 202–212.

Giannotta, M., Ruggiero, C., Grossi, M., Cancino, J., Capitani, M., Pulvirenti, T., Consoli, G. M. L., Geraci, C., Fanelli, F., Luini, A., et al. (2012). The KDEL receptor

couples to Gα $_{q/11}$ to activate Src kinases and regulate transport through the Golgi: The KDEL receptor acts as a novel GPCR. *The EMBO Journal* **31**, 2869–2881.

Gill, D. J., Chia, J., Senewiratne, J. and Bard, F. (2010). Regulation of O-glycosylation through Golgi-to-ER relocation of initiation enzymes. *Journal of Cell Biology* **189**, 843–858.

Gillingham, A. K. and Munro, S. (2016). Finding the Golgi: Golgin Coiled-Coil Proteins Show the Way. *Trends in Cell Biology* **26**, 399–408.

Giraudo, C. G. and Maccioni, H. J. F. (2003). Ganglioside Glycosyltransferases Organize in Distinct Multienzyme Complexes in CHO-K1 Cells. *Journal of Biological Chemistry* **278**, 40262–40271.

Girod, A., Storrie, B., Simpson, J. C., Johannes, L., Goud, B., Roberts, L. M., Lord, J. M., Nilsson, T. and Pepperkok, R. (1999). Evidence for a COP-I-independent transport route from the Golgi complex to the endoplasmic reticulum. *Nat Cell Biol* **1**, 423–430.

Glick, B. S. and Luini, A. (2011). Models for Golgi Traffic: A Critical Assessment. *Cold Spring Harbor Perspectives in Biology* **3**, a005215–a005215.

Godi, A., Pertile, P., Meyers, R., Marra, P., Di Tullio, G., Iurisci, C., Luini, A., Corda, D. and De Matteis, M. A. (1999). ARF mediates recruitment of PtdIns-4-OH kinase-beta and stimulates synthesis of PtdIns(4,5)P2 on the Golgi complex. *Nat Cell Biol* **1**, 280–287.

Gommel, D. U. (2001). Recruitment to Golgi membranes of ADP-ribosylation factor 1 is mediated by the cytoplasmic domain of p23. *The EMBO Journal* **20**, 6751–6760.

Gonzalez, A. and Rodriguez-Boulan, E. (2009). Clathrin and AP1B: key roles in basolateral trafficking through trans-endosomal routes. *FEBS Lett* **583**, 3784–3795.

Gorlich, D. (1993). Protein translocation into proteoliposomes reconstituted from purified components of the endoplasmic reticulum membrane. *Cell* **75**, 615–630.

Goud, B., Liu, S. and Storrie, B. (2018). Rab proteins as major determinants of the Golgi complex structure. *Small GTPases* **9**, 66–75.

Grasse, P. P. (1957). [Ultrastructure, polarity and reproduction of Golgi apparatus]. *C R Hebd Seances Acad Sci* **245**, 1278–1281.

Grigoriev, I., Gouveia, S. M., van der Vaart, B., Demmers, J., Smyth, J. T., Honnappa, S., Splinter, D., Steinmetz, M. O., Putney, J. W., Hoogenraad, C. C., et al. (2008). STIM1 Is a MT-Plus-End-Tracking Protein Involved in Remodeling of the ER. *Current Biology* **18**, 177–182.

Halperin, L., Jung, J. and Michalak, M. (2014). The many functions of the endoplasmic reticulum chaperones and folding enzymes: Functions of ER Chaperones and Folding Enzymes. *IUBMB Life* **66**, 318–326.

Hang, H. C. and Bertozzi, C. R. (2005). The chemistry and biology of mucin-type O-linked glycosylation. *Bioorganic & Medicinal Chemistry* **13**, 5021–5034.

Hara-Kuge, S. (1994). En bloc incorporation of coatomer subunits during the assembly of COP- coated vesicles [published erratum appears in J Cell Biol 1994 Jul;126(2):589]. *The Journal of Cell Biology* **124**, 883–892.

Hardwick, K. G., Lewis, M. J., Semenza, J., Dean, N. and Pelham, H. R. (1990). ERD1, a yeast gene required for the retention of luminal endoplasmic reticulum proteins, affects glycoprotein processing in the Golgi apparatus. *EMBO J* **9**, 623–630.

Hathaway, H. J., Evans, S. C., Dubois, D. H., Foote, C. I., Elder, B. H. and Shur, B. D. (2003). Mutational analysis of the cytoplasmic domain of beta1,4-galactosyltransferase I: influence of phosphorylation on cell surface expression. *J Cell Sci* **116**, 4319–4330.

Heffernan, L. F. and Simpson, J. C. (2014). The trials and tubule-ations of Rab6 involvement in Golgi-to-ER retrograde transport. *Biochemical Society Transactions* **42**, 1453–1459.

Hetz, C. (2012). The unfolded protein response: controlling cell fate decisions under ER stress and beyond. *Nat Rev Mol Cell Biol* **13**, 89–102.

Hobohm, L., Koudelka, T., Bahr, F. H., Truberg, J., Kapell, S., Schacht, S.-S., Meisinger, D., Mengel, M., Jochimsen, A., Hofmann, A., et al. (2022). N-terminome analyses underscore the prevalence of SPPL3-mediated intramembrane proteolysis among Golgi-resident enzymes and its role in Golgi enzyme secretion. *Cell. Mol. Life Sci.* **79**, 185.

Holthuis, J. C. M., Pomorski, T., Raggers, R. J., Sprong, H. and Van Meer, G. (2001). The Organizing Potential of Sphingolipids in Intracellular Membrane Transport. *Physiological Reviews* **81**, 1689–1723.

Homma, Y., Hiragi, S. and Fukuda, M. (2021). Rab family of small GTPases: an updated view on their regulation and functions. *FEBS J* **288**, 36–55.

Hoogenraad, C. C. (2001). Mammalian Golgi-associated Bicaudal-D2 functions in the dynein-dynactin pathway by interacting with these complexes. *The EMBO Journal* **20**, 4041–4054.

Hooke, R. and Jo. Martyn and Ja. Allestry. (1665). *Micrographia, or, Some physiological descriptions of minute bodies made by magnifying glasses :with observations and inquiries thereupon /by R. Hooke ...* London : Printed by Jo. Martyn and Ja. Allestry, printers to the Royal Society.

Huang, Y., Ma, T., Lau, P. K., Wang, J., Zhao, T., Du, S., Loy, M. M. T. and Guo, Y. (2019). Visualization of Protein Sorting at the Trans-Golgi Network and Endosomes Through Super-Resolution Imaging. *Front. Cell Dev. Biol.* **7**, 181.

Huitema, K., van den Dikkenberg, J., Brouwers, J. F. H. M. and Holthuis, J. C. M. (2004). Identification of a family of animal sphingomyelin synthases. *EMBO J* **23**, 33–44.

Hutagalung, A. H. and Novick, P. J. (2011). Role of Rab GTPases in Membrane Traffic and Cell Physiology. *Physiological Reviews* **91**, 119–149.

Iida, H. and Shibata, Y. (1991). Functional Golgi units in microtubule-disrupted cultured atrial myocytes. *J Histochem Cytochem.* **39**, 1349–1355.

Isaji, T., Im, S., Gu, W., Wang, Y., Hang, Q., Lu, J., Fukuda, T., Hashii, N., Takakura, D., Kawasaki, N., et al. (2014). An Oncogenic Protein Golgi Phosphoprotein 3 Up-regulates Cell Migration via Sialylation. *Journal of Biological Chemistry* **289**, 20694–20705.

Ishikawa, Y., Ito, S., Nagata, K., Sakai, L. Y. and Bächinger, H. P. (2016). Intracellular mechanisms of molecular recognition and sorting for transport of large extracellular matrix molecules. *Proc. Natl. Acad. Sci. U.S.A.* **113**,.

Jackson, M. R., Nilsson, T. and Peterson, P. A. (1990). Identification of a consensus motif for retention of transmembrane proteins in the endoplasmic reticulum. *The EMBO Journal* **9**, 3153–3162.

Jamieson, J. D. and Palade, G. E. (1966). Role of the Golgi complex in the intracellular transport of secretory proteins. *Proc. Natl. Acad. Sci. U.S.A.* **55**, 424–431.

Jamieson, J. D. and Palade, G. E. (1967). Intracellular transport of secretory proteins in the pancreatic exocrine cell. *Journal of Cell Biology* **34**, 577–596.

Janvier, K., Kato, Y., Boehm, M., Rose, J. R., Martina, J. A., Kim, B.-Y., Venkatesan, S. and Bonifacino, J. S. (2003). Recognition of dileucine-based sorting signals from HIV-1 Nef and LIMP-II by the AP-1 gamma-sigma1 and AP-3 delta-sigma3 hemicomplexes. *J Cell Biol* **163**, 1281–1290.

Jia, J., Yue, X., Zhu, L., Jing, S., Wang, Y., Gim, B., Qian, Y. and Lee, I. (2021). KDEL receptor is a cell surface receptor that cycles between the plasma membrane and the Golgi via clathrin-mediated transport carriers. *Cell. Mol. Life Sci.* **78**, 1085–1100.

Jiang, S. and Storrie, B. (2005). Cisternal rab proteins regulate Golgi apparatus redistribution in response to hypotonic stress. *Mol Biol Cell* **16**, 2586–2596.

Jiang, K., Hua, S., Mohan, R., Grigoriev, I., Yau, K. W., Liu, Q., Katrukha, E. A., Altelaar, A. F. M., Heck, A. J. R., Hoogenraad, C. C., et al. (2014). Microtubule Minus-End Stabilization by Polymerization-Driven CAMSAP Deposition. *Developmental Cell* **28**, 295–309.

Jin, L., Pahuja, K. B., Wickliffe, K. E., Gorur, A., Baumgärtel, C., Schekman, R. and Rape, M. (2012). Ubiquitin-dependent regulation of COPII coat size and function. *Nature* **482**, 495–500.

Jin, J., Momboisse, F., Boncompain, G., Koensgen, F., Zhou, Z., Cordeiro, N., Arenzana-Seisdedos, F., Perez, F., Lagane, B., Kellenberger, E., et al. (2018a). CCR5 adopts three homodimeric conformations that control cell surface delivery. *Sci. Signal.* **11**, eaal2869.

Jordan, M., Schallhorn, A. and Wurm, F. M. (1996). Transfecting mammalian cells: optimization of critical parameters affecting calcium-phosphate precipitate formation. *Nucleic Acids Res* **24**, 596–601.

Ju, T. and Cummings, R. D. (2002). A unique molecular chaperone Cosmc required for activity of the mammalian core 1 β3-galactosyltransferase. *Proc. Natl. Acad. Sci. U.S.A.* **99**, 16613–16618.

Ju, T., Aryal, R. P., Stowell, C. J. and Cummings, R. D. (2008). Regulation of protein O-glycosylation by the endoplasmic reticulum–localized molecular chaperone Cosmc. *Journal of Cell Biology* **182**, 531–542.

Katayama, K., Sasaki, T., Goto, S., Ogasawara, K., Maru, H., Suzuki, K. and Suzuki, H. (2011). Insertional mutation in the Golgb1 gene is associated with osteochondrodysplasia and systemic edema in the OCD rat. *Bone* **49**, 1027–1036.

Kawamoto, K., Yoshida, Y., Tamaki, H., Torii, S., Shinotsuka, C., Yamashina, S. and Nakayama, K. (2002). GBF1, a Guanine Nucleotide Exchange Factor for ADP-Ribosylation Factors, is Localized to the *cis* -Golgi and Involved in Membrane Association of the COPI Coat: **GBF1 Regulates COPI Membrane Association**. *Traffic* **3**, 483–495.

Klöpper, T. H., Kienle, N., Fasshauer, D. and Munro, S. (2012). Untangling the evolution of Rab G proteins: implications of a comprehensive genomic analysis. *BMC Biol* **10**, 71.

Koga, D. and Ushiki, T. (2006). Three-dimensional ultrastructure of the Golgi apparatus in different cells: high-resolution scanning electron microscopy of osmium-macerated tissues. *Arch Histol Cytol* **69**, 357–374.

Koreishi, M., Gniadek, T. J., Yu, S., Masuda, J., Honjo, Y. and Satoh, A. (2013). The Golgin Tether Giantin Regulates the Secretory Pathway by Controlling Stack Organization within Golgi Apparatus. *PLoS ONE* **8**, e59821.

Kornberg, R. D. (2007). The molecular basis of eukaryotic transcription. *Proc. Natl. Acad. Sci. U.S.A.* **104**, 12955–12961.

Krahn, M. P. and Wodarz, A. (2012). Phosphoinositide lipids and cell polarity: linking the plasma membrane to the cytocortex. *Essays in Biochemistry* **53**, 15–27.

Kreis, T. E. and Lodish, H. F. (1986). Oligomerization is essential for transport of vesicular stomatitis viral glycoprotein to the cell surface. *Cell* **46**, 929–937.

Kremers, G.-J., Gilbert, S. G., Cranfill, P. J., Davidson, M. W. and Piston, D. W. (2011). Fluorescent proteins at a glance. *Journal of Cell Science* **124**, 157–160.

Ladinsky, M. S., Wu, C. C., McIntosh, S., McIntosh, J. R. and Howell, K. E. (2002). Structure of the Golgi and distribution of reporter molecules at 20 degrees C reveals the complexity of the exit compartments. *Mol Biol Cell* **13**, 2810–2825.

Lewis, M. J. and Pelham, H. R. (1990). A human homologue of the yeast HDEL receptor. *Nature* **348**, 162–163.

Lewis, M. J. and Pelham, H. R. B. (1992). Sequence of a second human KDEL receptor. *Journal of Molecular Biology* **226**, 913–916.

Li, A., Song, N.-J., Riesenberg, B. P. and Li, Z. (2020). The Emerging Roles of Endoplasmic Reticulum Stress in Balancing Immunity and Tolerance in Health and Diseases: Mechanisms and Opportunities. *Front. Immunol.* **10**, 3154.

Lim, K. H., Huang, H., Pralle, A. and Park, S. (2011). Engineered Streptavidin Monomer and Dimer with Improved Stability and Function. *Biochemistry* **50**, 8682–8691.

Lin, H.-H. and Tang, M.-J. (1997). Thyroid hormone upregulates Na,K-ATPase α and β mRNA in primary cultures of proximal tubule cells. *Life Sciences* **60**, 375–382.

Linstedt, A. D., Jesch, S. A., Mehta, A., Lee, T. H., Garcia-Mata, R., Nelson, D. S. and Sztul, E. (2000). Binding Relationships of Membrane Tethering Components. *Journal of Biological Chemistry* **275**, 10196–10201.

Lippincott-Schwartz, J., Yuan, L. C., Bonifacino, J. S. and Klausner, R. D. (1989). Rapid redistribution of Golgi proteins into the ER in cells treated with brefeldin A: evidence for membrane cycling from Golgi to ER. *Cell* **56**, 801–813.

Liu, L., Doray, B. and Kornfeld, S. (2018). Recycling of Golgi glycosyltransferases requires direct binding to coatomer. *Proc. Natl. Acad. Sci. U.S.A.* **115**, 8984–8989.

Liu, P., Zhao, L., Kroemer, G. and Kepp, O. (2020). Secreted calreticulin mutants subvert anticancer immunosurveillance. *OncoImmunology* **9**, 1708126.

Loo, D. D. F., Hirayama, B. A., Gallardo, E. M., Lam, J. T., Turk, E. and Wright, E. M. (1998). Conformational changes couple Na^+ and glucose transport. *Proc. Natl. Acad. Sci. U.S.A.* **95**, 7789–7794.

Lopez, L. C., Youakim, A., Evans, S. C. and Shur, B. D. (1991). Evidence for a molecular distinction between Golgi and cell surface forms of beta 1,4-galactosyltransferase. *J Biol Chem* **266**, 15984–15991.

Lowery, J., Szul, T., Styers, M., Holloway, Z., Oorschot, V., Klumperman, J. and Sztul, E. (2013). The Sec7 Guanine Nucleotide Exchange Factor GBF1 Regulates Membrane Recruitment of BIG1 and BIG2 Guanine Nucleotide Exchange Factors to the Trans-Golgi Network (TGN). *Journal of Biological Chemistry* **288**, 11532–11545.

Lujan, P. and Campelo, F. (2021). Should I stay or should I go? Golgi membrane spatial organization for protein sorting and retention. *Archives of Biochemistry and Biophysics* **707**, 108921.

Ma, W. and Goldberg, J. (2013). Rules for the recognition of dilysine retrieval motifs by coatomer. *EMBO J* **32**, 926–937.

Ma, W. and Goldberg, J. (2016). TANGO1/cTAGE5 receptor as a polyvalent template for assembly of large COPII coats. *Proc. Natl. Acad. Sci. U.S.A.* **113**, 10061–10066.

Mach, J. M. and Lehmann, R. (1997). An Egalitarian-BicaudalD complex is essential for oocyte specification and axis determination in Drosophila. *Genes Dev* **11**, 423–435.

Machamer, C. E. (1991). Golgi retention signals: do membranes hold the key? *Trends in Cell Biology* **1**, 141–144.

Malhotra, V., Serafini, T., Orci, L., Shepherd, J. C. and Rothman, J. E. (1989). Purification of a novel class of coated vesicles mediating biosynthetic protein transport through the Golgi stack. *Cell* **58**, 329–336.

Mali, P., Yang, L., Esvelt, K. M., Aach, J., Guell, M., DiCarlo, J. E., Norville, J. E. and Church, G. M. (2013). RNA-Guided Human Genome Engineering via Cas9. *Science* **339**, 823–826.

Mallard, F., Tang, B. L., Galli, T., Tenza, D., Saint-Pol, A., Yue, X., Antony, C., Hong, W., Goud, B. and Johannes, L. (2002). Early/recycling endosomes-to-TGN transport involves two SNARE complexes and a Rab6 isoform. *Journal of Cell Biology* **156**, 653–664.

Malsam, J., Satoh, A., Pelletier, L. and Warren, G. (2005). Golgin Tethers Define Subpopulations of COPI Vesicles. *Science* **307**, 1095–1098.

Marsh, B. J., Mastronarde, D. N., Buttle, K. F., Howell, K. E. and McIntosh, J. R. (2001). Organellar relationships in the Golgi region of the pancreatic beta cell line, HIT-T15, visualized by high resolution electron tomography. *Proc. Natl. Acad. Sci. U.S.A.* **98**, 2399–2406.

Martin, W. F., Garg, S. and Zimorski, V. (2015). Endosymbiotic theories for eukaryote origin. *Phil. Trans. R. Soc. B* **370**, 20140330.

Martinez, O., Schmidt, A., Salaméro, J., Hoflack, B., Roa, M. and Goud, B. (1994). The small GTP-binding protein rab6 functions in intra-Golgi transport. *Journal of Cell Biology* **127**, 1575–1588.

Matanis, T., Akhmanova, A., Wulf, P., Del Nery, E., Weide, T., Stepanova, T., Galjart, N., Grosveld, F., Goud, B., De Zeeuw, C. I., et al. (2002). Bicaudal-D regulates COPI-independent Golgi–ER transport by recruiting the dynein–dynactin motor complex. *Nat Cell Biol* **4**, 986–992.

Matsuto, M., Kano, F. and Murata, M. (2015). Reconstitution of the targeting of Rab6A to the Golgi apparatus in semi-intact HeLa cells: A role of BICD2 in stabilizing Rab6A on Golgi membranes and a concerted role of Rab6A/BICD2 interactions in Golgi-to-ER retrograde transport. *Biochimica et Biophysica Acta (BBA) - Molecular Cell Research* **1853**, 2592–2609.

Mayinger, P. (2011). Signaling at the Golgi. *Cold Spring Harbor Perspectives in Biology* **3**, a005314–a005314.

Melançon, P., Glick, B. S., Malhotra, V., Weidman, P. J., Serafini, T., Gleason, M. L., Orci, L. and Rothman, J. E. (1987). Involvement of GTP-binding "G" proteins in transport through the Golgi stack. *Cell* **51**, 1053–1062.

Meusser, B., Hirsch, C., Jarosch, E. and Sommer, T. (2005). ERAD: the long road to destruction. *Nat Cell Biol* **7**, 766–772.

Miesenböck, G. and Rothman, J. E. (1995). The capacity to retrieve escaped ER proteins extends to the trans-most cisterna of the Golgi stack. *Journal of Cell Biology* **129**, 309–319.

Milland, J., Russell, S. M., Dodson, H. C., McKenzie, I. F. C. and Sandrin, M. S. (2002). The Cytoplasmic Tail of α1,3-Galactosyltransferase Inhibits Golgi Localization of the Full-length Enzyme. *Journal of Biological Chemistry* **277**, 10374–10378.

Miserey-Lenkei, S., Chalancon, G., Bardin, S., Formstecher, E., Goud, B. and Echard, A. (2010). Rab and actomyosin-dependent fission of transport vesicles at the Golgi complex. *Nat Cell Biol* **12**, 645–654.

Misra, S., Puertollano, R., Kato, Y., Bonifacino, J. S. and Hurley, J. H. (2002). Structural basis for acidic-cluster-dileucine sorting-signal recognition by VHS domains. *Nature* **415**, 933–937.

Mitra, K., Ubarretxena-Belandia, I., Taguchi, T., Warren, G. and Engelman, D. M. (2004). Modulation of the bilayer thickness of exocytic pathway membranes by membrane proteins rather than cholesterol. *Proc. Natl. Acad. Sci. U.S.A.* **101**, 4083–4088.

Monetta, P., Slavin, I., Romero, N. and Alvarez, C. (2007). Rab1b interacts with GBF1 and modulates both ARF1 dynamics and COPI association. *Mol Biol Cell* **18**, 2400–2410.

Morgan, G. W., Kail, M., Hollinshead, M. and Vaux, D. J. (2013). Combined biochemical and cytological analysis of membrane trafficking using lectins. *Analytical Biochemistry* **441**, 21–31.

Moyer, B. D., Allan, B. B. and Balch, W. E. (2001). Rab1 Interaction with a GM130 Effector Complex Regulates COPII Vesicle *cis* -Golgi Tethering: Rab1-GM130 Complex Regulates COPII-Golgi Transport. *Traffic* **2**, 268–276.

Munro, S. (1991). Sequences within and adjacent to the transmembrane segment of alpha-2,6-sialyltransferase specify Golgi retention. *EMBO J* **10**, 3577–3588.

Munro, S. (1995). An investigation of the role of transmembrane domains in Golgi protein retention. *The EMBO Journal* **14**, 4695–4704.

Murphy, E. J., Anderson, D. K. and Horrocks, L. A. (1993). Phospholipid and phospholipid fatty acid composition of mixed murine spinal cord neuronal cultures. *J. Neurosci. Res.* **34**, 472–477.

Nakamura, N., Lowe, M., Levine, T. P., Rabouille, C. and Warren, G. (1997). The Vesicle Docking Protein p115 Binds GM130, a cis-Golgi Matrix Protein, in a Mitotically Regulated Manner. *Cell* **89**, 445–455.

Nangalia, J., Massie, C. E., Baxter, E. J., Nice, F. L., Gundem, G., Wedge, D. C., Avezov, E., Li, J., Kollmann, K., Kent, D. G., et al. (2013). Somatic *CALR* Mutations in Myeloproliferative Neoplasms with Nonmutated *JAK2*. *N Engl J Med* **369**, 2391–2405.

Nguyen, A. T., Chia, J., Ros, M., Hui, K. M., Saltel, F. and Bard, F. (2017). Organelle Specific O-Glycosylation Drives MMP14 Activation, Tumor Growth, and Metastasis. *Cancer Cell* **32**, 639-653.e6.

Nichols, W. C., Seligsohn, U., Zivelin, A., Terry, V. H., Hertel, C. E., Wheatley, M. A., Moussalli, M. J., Hauri, H.-P., Ciavarella, N., Kaufman, R. J., et al. (1998). Mutations in the ER–Golgi Intermediate Compartment Protein ERGIC-53 Cause Combined Deficiency of Coagulation Factors V and VIII. *Cell* **93**, 61–70.

Nilsson, T., Jackson, M. and Peterson, P. A. (1989). Short cytoplasmic sequences serve as retention signals for transmembrane proteins in the endoplasmic reticulum. *Cell* **58**, 707–718.

Nilsson, T., Lucocq, J. M., Mackay, D. and Warren, G. (1991). The membrane spanning domain of beta-1,4-galactosyltransferase specifies trans Golgi localization. *EMBO J* **10**, 3567–3575.

Nilsson, T., Pypaert, M., Hoe, M. H., Slusarewicz, P., Berger, E. G. and Warren, G. (1993). Overlapping distribution of two glycosyltransferases in the Golgi apparatus of HeLa cells. *J Cell Biol* **120**, 5–13.

Nilsson, T., Hoe, M. H., Slusarewicz, P., Rabouille, C., Watson, R., Hunte, F., Watzele, G., Berger, E. G. and Warren, G. (1994). Kin recognition between medial Golgi enzymes in HeLa cells. *The EMBO Journal* **13**, 562–574.

Niu, T.-K., Pfeifer, A. C., Lippincott-Schwartz, J. and Jackson, C. L. (2005). Dynamics of GBF1, a Brefeldin A-Sensitive Arf1 Exchange Factor at the Golgi. *MBoC* **16**, 1213–1222.

Nixon-Abell, J., Obara, C. J., Weigel, A. V., Li, D., Legant, W. R., Xu, C. S., Pasolli, H. A., Harvey, K., Hess, H. F., Betzig, E., et al. (2016). Increased spatiotemporal resolution reveals highly dynamic dense tubular matrices in the peripheral ER. *Science* **354**, aaf3928.

Novick, P. and Schekman, R. (1979). Secretion and cell-surface growth are blocked in a temperature-sensitive mutant of *Saccharomyces cerevisiae*. *Proc. Natl. Acad. Sci. U.S.A.* **76**, 1858–1862.

Nyfeler, B., Reiterer, V., Wendeler, M. W., Stefan, E., Zhang, B., Michnick, S. W. and Hauri, H.-P. (2008). Identification of ERGIC-53 as an intracellular transport receptor of α1-antitrypsin. *Journal of Cell Biology* **180**, 705–712.

Ohno, H., Stewart, J., Fournier, M. C., Bosshart, H., Rhee, I., Miyatake, S., Saito, T., Gallusser, A., Kirchhausen, T. and Bonifacino, J. S. (1995). Interaction of tyrosine-based sorting signals with clathrin-associated proteins. *Science* **269**, 1872–1875.

Olson, L. J., Hindsgaul, O., Dahms, N. M. and Kim, J.-J. P. (2008). Structural insights into the mechanism of pH-dependent ligand binding and release by the cation-dependent mannose 6-phosphate receptor. *J Biol Chem* **283**, 10124–10134.

Ondruskova, N., Cechova, A., Hansikova, H., Honzik, T. and Jaeken, J. (2021). Congenital disorders of glycosylation: Still "hot" in 2020. *Biochimica et Biophysica Acta (BBA) - General Subjects* **1865**, 129751.

Orci, L., Montesano, R., Meda, P., Malaisse-Lagae, F., Brown, D., Perrelet, A. and Vassalli, P. (1981). Heterogeneous distribution of filipin--cholesterol complexes across the cisternae of the Golgi apparatus. *Proc. Natl. Acad. Sci. U.S.A.* **78**, 293–297.

Palade, G. E. (1955). A SMALL PARTICULATE COMPONENT OF THE CYTOPLASM. *The Journal of Biophysical and Biochemical Cytology* **1**, 59–68.

Palade, G. E. and Siekevitz, P. (1956a). LIVER MICROSOMES. *The Journal of Biophysical and Biochemical Cytology* **2**, 171–200.

Palade, G. E. and Siekevitz, P. (1956b). PANCREATIC MICROSOMES. *The Journal of Biophysical and Biochemical Cytology* **2**, 671–690.

Patterson, G. H., Hirschberg, K., Polishchuk, R. S., Gerlich, D., Phair, R. D. and Lippincott-Schwartz, J. (2008). Transport through the Golgi Apparatus by Rapid Partitioning within a Two-Phase Membrane System. *Cell* **133**, 1055–1067.

Pecot, M. Y. and Malhotra, V. (2006). The Golgi Apparatus Maintains Its Organization Independent of the Endoplasmic Reticulum. *MBoC* **17**, 5372–5380.

Pelletier, L., Stern, C. A., Pypaert, M., Sheff, D., Ngô, H. M., Roper, N., He, C. Y., Hu, K., Toomre, D., Coppens, I., et al. (2002). Golgi biogenesis in Toxoplasma gondii. *Nature* **418**, 548–552.

Pfeffer, S. (2005). A model for Rab GTPase localization. *Biochem Soc Trans* **33**, 627–630.

Plutner, H., Cox, A. D., Pind, S., Khosravi-Far, R., Bourne, J. R., Schwaninger, R., Der, C. J. and Balch, W. E. (1991). Rab1b regulates vesicular transport between the endoplasmic reticulum and successive Golgi compartments. *Journal of Cell Biology* **115**, 31–43.

Polishchuk, R. S., Polishchuk, E. V., Marra, P., Alberti, S., Buccione, R., Luini, A. and Mironov, A. A. (2000). Correlative light-electron microscopy reveals the tubular-saccular ultrastructure of carriers operating between Golgi apparatus and plasma membrane. *J Cell Biol* **148**, 45–58.

Presley, J. F., Cole, N. B., Schroer, T. A., Hirschberg, K., Zaal, K. J. M. and Lippincott-Schwartz, J. (1997a). ER-to-Golgi transport visualized in living cells. *Nature* **389**, 81–85.

Presley, J. F., Cole, N. B., Schroer, T. A., Hirschberg, K., Zaal, K. J. M. and Lippincott-Schwartz, J. (1997b). ER-to-Golgi transport visualized in living cells. *Nature* **389**, 81–85.

Pulvirenti, T., Giannotta, M., Capestrano, M., Capitani, M., Pisanu, A., Polishchuk, R. S., Pietro, E. S., Beznoussenko, G. V., Mironov, A. A., Turacchio, G., et al. (2008). A traffic-activated Golgi-based signalling circuit coordinates the secretory pathway. *Nat Cell Biol* **10**, 912–922.

Puthenveedu, M. A., Bachert, C., Puri, S., Lanni, F. and Linstedt, A. D. (2006). GM130 and GRASP65-dependent lateral cisternal fusion allows uniform Golgi-enzyme distribution. *Nat Cell Biol* **8**, 238–248.

Qiao, Y., Molina, H., Pandey, A., Zhang, J. and Cole, P. A. (2006). Chemical rescue of a mutant enzyme in living cells. *Science* **311**, 1293–1297.

Quental, R., Azevedo, L., Matthiesen, R. and Amorim, A. (2010). Comparative analyses of the Conserved Oligomeric Golgi (COG) complex in vertebrates. *BMC Evol Biol* **10**, 212.

Rabouille, C. and Linstedt, A. D. (2016). GRASP: A Multitasking Tether. *Front Cell Dev Biol* **4**, 1.

Rabouille, C., Hui, N., Hunte, F., Kieckbusch, R., Berger, E. G., Warren, G. and Nilsson, T. (1995). Mapping the distribution of Golgi enzymes involved in the construction of complex oligosaccharides. *Journal of Cell Science* **108**, 1617–1627.

Raote, I., Ortega-Bellido, M., Santos, A. J., Foresti, O., Zhang, C., Garcia-Parajo, M. F., Campelo, F. and Malhotra, V. (2018). TANGO1 builds a machine for collagen export by recruiting and spatially organizing COPII, tethers and membranes. *eLife* **7**, e32723.

Raykhel, I., Alanen, H., Salo, K., Jurvansuu, J., Nguyen, V. D., Latva-Ranta, M. and Ruddock, L. (2007). A molecular specificity code for the three mammalian KDEL receptors. *Journal of Cell Biology* **179**, 1193–1204.

Reily, C., Stewart, T. J., Renfrow, M. B. and Novak, J. (2019). Glycosylation in health and disease. *Nat Rev Nephrol* **15**, 346–366.

Rhee, S. W., Starr, T., Forsten-Williams, K. and Storrie, B. (2005). The Steady-State Distribution of Glycosyltransferases Between the Golgi Apparatus and the Endoplasmic Reticulum is Approximately 90:10: Golgi Glycosyltransferase Distribution. *Traffic* **6**, 978–990.

Rios, R. M. (2014). The centrosome–Golgi apparatus nexus. *Phil. Trans. R. Soc. B* **369**, 20130462.

Rivero, S., Cardenas, J., Bornens, M. and Rios, R. M. (2009). Microtubule nucleation at the cis-side of the Golgi apparatus requires AKAP450 and GM130. *EMBO J* **28**, 1016–1028.

Rizzo, R., Russo, D., Kurokawa, K., Sahu, P., Lombardi, B., Supino, D., Zhukovsky, M. A., Vocat, A., Pothukuchi, P., Kunnathully, V., et al. (2021). Golgi maturation-dependent glycoenzyme recycling controls glycosphingolipid biosynthesis and cell growth via GOLPH3. *EMBO J* **40**,.

Robertson, J. D. (1960). A molecular theory of cell membrane structure. In *Verhandlungen Band II / Biologisch-Medizinischer Teil* (ed. Bargmann, W.), Peters, D.), and Wolpers, C.), pp. 159–171. Berlin, Heidelberg: Springer Berlin Heidelberg.

Roboti, P., Sato, K. and Lowe, M. (2015). The golgin GMAP-210 is required for efficient membrane trafficking in the early secretory pathway. *Journal of Cell Science* jcs.166710.

Roeder, R. G. (2019). 50+ years of eukaryotic transcription: an expanding universe of factors and mechanisms. *Nat Struct Mol Biol* **26**, 783–791.

Ros, M., Nguyen, A. T., Chia, J., Le Tran, S., Le Guezennec, X., McDowall, R., Vakhrushev, S., Clausen, H., Humphries, M. J., Saltel, F., et al. (2020). ER-resident oxidoreductases are glycosylated and trafficked to the cell surface to promote matrix degradation by tumour cells. *Nat Cell Biol* **22**, 1371–1381.

Roth, J. and Berger, E. G. (1982). Immunocytochemical localization of galactosyltransferase in HeLa cells: codistribution with thiamine pyrophosphatase in trans-Golgi cisternae. *J Cell Biol* **93**, 223–229.

Roth, J., Taatjes, D. J., Weinstein, J., Paulson, J. C., Greenwell, P. and Watkins, W. M. (1986). Differential subcompartmentation of terminal glycosylation in the Golgi apparatus of intestinal absorptive and goblet cells. *Journal of Biological Chemistry* **261**, 14307–14312.

Roubin, R., Acquaviva, C., Chevrier, V., Sedjaï, F., Zyss, D., Birnbaum, D. and Rosnet, O. (2013). Myomegalin is necessary for the formation of centrosomal and Golgi-derived microtubules. *Biology Open* **2**, 238–250.

Rowland, A. A., Chitwood, P. J., Phillips, M. J. and Voeltz, G. K. (2014). ER contact sites define the position and timing of endosome fission. *Cell* **159**, 1027–1041.

Russo, R. N., Shaper, N. L., Taatjes, D. J. and Shaper, J. H. (1992). Beta 1,4-galactosyltransferase: a short NH2-terminal fragment that includes the cytoplasmic and transmembrane domain is sufficient for Golgi retention. *Journal of Biological Chemistry* **267**, 9241–9247.

Sabatini, D. D. (2010). Philip Siekevitz: Bridging biochemistry and cell biology. *Journal of Cell Biology* **189**, 3–5.

Saegusa, K., Sato, M., Morooka, N., Hara, T. and Sato, K. (2018). SFT-4/Surf4 control ER export of soluble cargo proteins and participate in ER exit site organization. *J Cell Biol* **217**, 2073–2085.

Saegusa, K., Matsunaga, K., Maeda, M., Saito, K., Izumi, T. and Sato, K. (2022). Cargo receptor Surf4 regulates endoplasmic reticulum export of proinsulin in pancreatic β-cells. *Commun Biol* **5**, 458.

Saito, K., Chen, M., Bard, F., Chen, S., Zhou, H., Woodley, D., Polischuk, R., Schekman, R. and Malhotra, V. (2009). TANGO1 Facilitates Cargo Loading at Endoplasmic Reticulum Exit Sites. *Cell* **136**, 891–902.

Saito, K., Yamashiro, K., Ichikawa, Y., Erlmann, P., Kontani, K., Malhotra, V. and Katada, T. (2011). cTAGE5 mediates collagen secretion through interaction with TANGO1 at endoplasmic reticulum exit sites. *MBoC* **22**, 2301–2308.

Saito, K., Yamashiro, K., Shimazu, N., Tanabe, T., Kontani, K. and Katada, T. (2014). Concentration of Sec12 at ER exit sites via interaction with cTAGE5 is required for collagen export. *Journal of Cell Biology* **206**, 751–762.

Saraste, J. (2016). Spatial and Functional Aspects of ER-Golgi Rabs and Tethers. *Front. Cell Dev. Biol.* **4**,.

Saraste, J., Lahtinen, U. and Goud, B. (1995). Localization of the small GTP-binding protein rab1p to early compartments of the secretory pathway. *J Cell Sci* **108 (Pt 4)**, 1541–1552.

Saraste, J. and Marie, M. (2018). Intermediate compartment (IC): from pre-Golgi vacuoles to a semi-autonomous membrane system. *Histochem Cell Biol* **150**, 407–430.

Sato, Y., Hayashi, K., Amano, Y., Takahashi, M., Yonemura, S., Hayashi, I., Hirose, H., Ohno, S. and Suzuki, A. (2014). MTCL1 crosslinks and stabilizes non-centrosomal microtubules on the Golgi membrane. *Nat Commun* **5**, 5266.

Satoh, A., Hayashi-Nishino, M., Shakuno, T., Masuda, J., Koreishi, M., Murakami, R., Nakamura, Y., Nakamura, T., Abe-Kanoh, N., Honjo, Y., et al. (2019). The Golgin Protein Giantin Regulates Interconnections Between Golgi Stacks. *Front. Cell Dev. Biol.* **7**, 160.

Schjoldager, K. T., Narimatsu, Y., Joshi, H. J. and Clausen, H. (2020). Global view of human protein glycosylation pathways and functions. *Nat Rev Mol Cell Biol* **21**, 729–749.

Schleiden, M. J. (1838). *Beiträge zur Phytogenesis*. Arch. Anat. Physiol. Wiss. Med.

Schmid-Burgk, J. L., Höning, K., Ebert, T. S. and Hornung, V. (2016). CRISPaint allows modular base-specific gene tagging using a ligase-4-dependent mechanism. *Nat Commun* **7**, 12338.

Schutze, M. P., Peterson, P. A. and Jackson, M. R. (1994). An N-terminal double-arginine motif maintains type II membrane proteins in the endoplasmic reticulum. *EMBO J* **13**, 1696–1705.

Schwann, T. and Hünseler, F. (1839). *Mikroskopische Untersuchungen über die Ubereinstimmung in der Struktur und dem Wachstume der Tiere und Pflanzen*. (ed. Berlin, Verlag der Sand schen Buchhandlung (G. E. Reimer) Neue Not Geb Nat Heil.

Semenza, J. C., Hardwick, K. G., Dean, N. and Pelham, H. R. B. (1990). ERD2, a yeast gene required for the receptor-mediated retrieval of luminal ER proteins from the secretory pathway. *Cell* **61**, 1349–1357.

Sengupta, P. and Lippincott-Schwartz, J. (2013). Photohighlighting Approaches to Access Membrane Dynamics of the Golgi Apparatus. In *Methods in Cell Biology*, pp. 217–234. Elsevier.

Sengupta, P., Satpute-Krishnan, P., Seo, A. Y., Burnette, D. T., Patterson, G. H. and Lippincott-Schwartz, J. (2015). ER trapping reveals Golgi enzymes continually revisit the ER through a recycling pathway that controls Golgi organization. *Proc. Natl. Acad. Sci. U.S.A.* **112**,.

Shah, N., Kuntz, D. A. and Rose, D. R. (2008). Golgi α-mannosidase II cleaves two sugars sequentially in the same catalytic site. *Proc. Natl. Acad. Sci. U.S.A.* **105**, 9570–9575.

Sharpe, H. J., Stevens, T. J. and Munro, S. (2010). A comprehensive comparison of transmembrane domains reveals organelle-specific properties. *Cell* **142**, 158–169.

Shestakova, A., Suvorova, E., Pavliv, O., Khaidakova, G. and Lupashin, V. (2007). Interaction of the conserved oligomeric Golgi complex with t-SNARE Syntaxin5a/Sed5 enhances intra-Golgi SNARE complex stability. *Journal of Cell Biology* **179**, 1179–1192.

Shikano, S. and Li, M. (2003). Membrane receptor trafficking: Evidence of proximal and distal zones conferred by two independent endoplasmic reticulum localization signals. *Proc. Natl. Acad. Sci. U.S.A.* **100**, 5783–5788.

Shima, D. T., Cabrera-Poch, N., Pepperkok, R. and Warren, G. (1998). An Ordered Inheritance Strategy for the Golgi Apparatus: Visualization of Mitotic Disassembly Reveals a Role for the Mitotic Spindle. *Journal of Cell Biology* **141**, 955–966.

Shin, J. J. H., Crook, O. M., Borgeaud, A. C., Cattin-Ortolá, J., Peak-Chew, S. Y., Breckels, L. M., Gillingham, A. K., Chadwick, J., Lilley, K. S. and Munro, S. (2020). Spatial proteomics defines the content of trafficking vesicles captured by golgin tethers. *Nat Commun* **11**, 5987.

Short, B., Preisinger, C., Körner, R., Kopajtich, R., Byron, O. and Barr, F. A. (2001). A GRASP55-rab2 effector complex linking Golgi structure to membrane traffic. *Journal of Cell Biology* **155**, 877–884.

Short, B., Preisinger, C., Schaletzky, J., Kopajtich, R. and Barr, F. A. (2002). The Rab6 GTPase Regulates Recruitment of the Dynactin Complex to Golgi Membranes. *Current Biology* **12**, 1792–1795.

Shur, B. D. and Hall, N. G. (1982). A role for mouse sperm surface galactosyltransferase in sperm binding to the egg zona pellucida. *Journal of Cell Biology* **95**, 574–579.

Simons, K. and Fuller, S. D. (1985). Cell surface polarity in epithelia. *Annu Rev Cell Biol* **1**, 243–288.

Singer, S. J. and Nicolson, G. L. (1972). The Fluid Mosaic Model of the Structure of Cell Membranes: Cell membranes are viewed as two-dimensional solutions of oriented globular proteins and lipids. *Science* **175**, 720–731.

Sjöstrand, F. S. and Hanzon, V. (1954). Ultrastructure of golgi apparatus of exocrinecells of mouse pancreas. *Experimental Cell Research* **7**, 415–429.

Sönnichsen, B., Lowe, M., Levine, T., Jämsä, E., Dirac-Svejstrup, B. and Warren, G. (1998). A Role for Giantin in Docking COPI Vesicles to Golgi Membranes. *Journal of Cell Biology* **140**, 1013–1021.

Stanley, P. (2011). Golgi Glycosylation. *Cold Spring Harbor Perspectives in Biology* **3**, a005199–a005199.

Stevenson, N. L., Bergen, D. J. M., Lu, Y., Prada-Sanchez, M. E., Kadler, K. E., Hammond, C. L. and Stephens, D. J. (2021). Giantin is required for intracellular N-terminal processing of type I procollagen. *J Cell Biol* **220**, e202005166.

Storrie, B., White, J., Röttger, S., Stelzer, E. H., Suganuma, T. and Nilsson, T. (1998). Recycling of golgi-resident glycosyltransferases through the ER reveals a novel pathway and provides an explanation for nocodazole-induced Golgi scattering. *J Cell Biol* **143**, 1505–1521.

Stow, J. L., Fath, K. R. and Burgess, D. R. (1998). Budding roles for myosin II on the Golgi. *Trends Cell Biol* **8**, 138–141.

Subathra, M., Qureshi, A. and Luberto, C. (2011). Sphingomyelin Synthases Regulate Protein Trafficking and Secretion. *PLoS ONE* **6**, e23644.

Sumya, F. T., Pokrovskaya, I. D., D'Souza, Z. and Lupashin, V. V. (2022). *Acute COG inactivation unveiled its immediate impact on Golgi and illuminated the nature of intra-Golgi recycling vesicles*. Cell Biology.

Sun, X., Zhan, M., Sun, X., Liu, W. and Meng, X. (2021a). C1GALT1 in health and disease (Review). *Oncol Lett* **22**, 589.

Sun, X., Mahajan, D., Chen, B., Song, Z. and Lu, L. (2021b). A quantitative study of the Golgi retention of glycosyltransferases. *Journal of Cell Science* **134**, jcs258564.

Swindall, A. F. and Bellis, S. L. (2011). Sialylation of the Fas death receptor by ST6Gal-I provides protection against Fas-mediated apoptosis in colon carcinoma cells. *J Biol Chem* **286**, 22982–22990.

Tachibana, R., Terai, T., Boncompain, G., Sugiyama, S., Saito, N., Perez, F. and Urano, Y. (2017). Improving the Solubility of Artificial Ligands of Streptavidin to Enable More Practical Reversible Switching of Protein Localization in Cells. *ChemBioChem* **18**, 358–362.

Tafesse, F. G., Sanyal, S., Ashour, J., Guimaraes, C. P., Hermansson, M., Somerharju, P. and Ploegh, H. L. (2013). Intact sphingomyelin biosynthetic pathway is essential for intracellular transport of influenza virus glycoproteins. *Proc. Natl. Acad. Sci. U.S.A.* **110**, 6406–6411.

Tamborero, S., Vilar, M., Martínez-Gil, L., Johnson, A. E. and Mingarro, I. (2011). Membrane Insertion and Topology of the Translocating Chain-Associating Membrane Protein (TRAM). *Journal of Molecular Biology* **406**, 571–582.

Tan, J. Z. A., Fourriere, L., Wang, J., Perez, F., Boncompain, G. and Gleeson, P. A. (2020). Distinct anterograde trafficking pathways of BACE1 and amyloid precursor protein from the TGN and the regulation of amyloid-β production. *MBoC* **31**, 27–44.

Tang, X., Chen, R., Mesias, V. S. D., Wang, T., Wang, Y., Poljak, K., Fan, X., Miao, H., Hu, J., Zhang, L., et al. (2022). A SURF4-to-proteoglycan relay mechanism that mediates the sorting and secretion of a tagged variant of sonic hedgehog. *Proc. Natl. Acad. Sci. U.S.A.* **119**, e2113991119.

Terai, T., Kohno, M., Boncompain, G., Sugiyama, S., Saito, N., Fujikake, R., Ueno, T., Komatsu, T., Hanaoka, K., Okabe, T., et al. (2015). Artificial Ligands of Streptavidin (ALiS): Discovery, Characterization, and Application for Reversible Control of Intracellular Protein Transport. *J. Am. Chem. Soc.* **137**, 10464–10467.

Thomas, S. M. and Brugge, J. S. (1997). CELLULAR FUNCTIONS REGULATED BY SRC FAMILY KINASES. *Annu. Rev. Cell Dev. Biol.* **13**, 513–609.

Tisdale, E. J. (2003). Rab2 Interacts Directly with Atypical Protein Kinase C (aPKC) ι/λ and Inhibits aPKCι/λ-dependent Glyceraldehyde-3-phosphate Dehydrogenase Phosphorylation. *Journal of Biological Chemistry* **278**, 52524–52530.

Trucco, A., Polishchuk, R. S., Martella, O., Pentima, A. D., Fusella, A., Giandomenico, D. D., Pietro, E. S., Beznoussenko, G. V., Polishchuk, E. V., Baldassarre, M., et al. (2004). Secretory traffic triggers the formation of tubular continuities across Golgi sub-compartments. *Nat Cell Biol* **6**, 1071–1081.

Tu, L., Tai, W. C. S., Chen, L. and Banfield, D. K. (2008). Signal-Mediated Dynamic Retention of Glycosyltransferases in the Golgi. *Science* **321**, 404–407.

Tuccillo, F. M., de Laurentiis, A., Palmieri, C., Fiume, G., Bonelli, P., Borrelli, A., Tassone, P., Scala, I., Buonaguro, F. M., Quinto, I., et al. (2014). Aberrant Glycosylation as Biomarker for Cancer: Focus on CD43. *BioMed Research International* **2014**, 1–13.

Tulsiani, D. R. and Touster, O. (1985). Characterization of a novel alpha-D-mannosidase from rat brain microsomes. *Journal of Biological Chemistry* **260**, 13081–13087.

Uhlén, M., Karlsson, M. J., Hober, A., Svensson, A.-S., Scheffel, J., Kotol, D., Zhong, W., Tebani, A., Strandberg, L., Edfors, F., et al. (2019). The human secretome. *Sci. Signal.* **12**, eaaz0274.

Ungar, D., Oka, T., Brittle, E. E., Vasile, E., Lupashin, V. V., Chatterton, J. E., Heuser, J. E., Krieger, M. and Waters, M. G. (2002). Characterization of a mammalian Golgi-localized protein complex, COG, that is required for normal Golgi morphology and function. *Journal of Cell Biology* **157**, 405–415.

Utskarpen, A., Slagsvold, H. H., Iversen, T.-G., Wälchli, S. and Sandvig, K. (2006). Transport of Ricin from Endosomes to the Golgi Apparatus is Regulated by Rab6A and Rab6A′: Ricin Transport Following Rab6a/A′ Depletion. *Traffic* **7**, 663–672.

Valderrama, F., M. Durán, J., Babià, T., Barth, H., Renau-Piqueras, J. and Egea, G. (2001). Actin Microfilaments Facilitate the Retrograde Transport from the Golgi Complex to the Endoplasmic Reticulum in Mammalian Cells: Actin in the ER/Golgi Interface. *Traffic* **2**, 717–726.

Valente, C., Turacchio, G., Mariggiò, S., Pagliuso, A., Gaibisso, R., Di Tullio, G., Santoro, M., Formiggini, F., Spanò, S., Piccini, D., et al. (2012). A 14-3-3γ dimer-based scaffold bridges CtBP1-S/BARS to PI(4)KIIIβ to regulate post-Golgi carrier formation. *Nat Cell Biol* **14**, 343–354.

Valm, A. M., Cohen, S., Legant, W. R., Melunis, J., Hershberg, U., Wait, E., Cohen, A. R., Davidson, M. W., Betzig, E. and Lippincott-Schwartz, J. (2017). Applying systems-level spectral imaging and analysis to reveal the organelle interactome. *Nature* **546**, 162–167.

Van Damme, E. J. M. (2022). 35 years in plant lectin research: a journey from basic science to applications in agriculture and medicine. *Glycoconj J* **39**, 83–97.

van Galen, J., Campelo, F., Martínez-Alonso, E., Scarpa, M., Martínez-Menárguez, J. Á. and Malhotra, V. (2014). Sphingomyelin homeostasis is required to form functional enzymatic domains at the trans-Golgi network. *Journal of Cell Biology* **206**, 609–618.

van Meer, G. (1998). Lipids of the Golgi membrane. *Trends in Cell Biology* **8**, 29–33.

Vance, J. E. (2008). Thematic Review Series: Glycerolipids. Phosphatidylserine and phosphatidylethanolamine in mammalian cells: two metabolically related aminophospholipids. *Journal of Lipid Research* **49**, 1377–1387.

Vedrenne, C., Klopfenstein, D. R. and Hauri, H.-P. (2005). Phosphorylation Controls CLIMP-63–mediated Anchoring of the Endoplasmic Reticulum to Microtubules. *MBoC* **16**, 1928–1937.

Verchère, A., Cowton, A., Jenni, A., Rauch, M., Häner, R., Graumann, J., Bütikofer, P. and Menon, A. K. (2020). *Complexity of the eukaryotic dolichol-linked oligosaccharide scramblase suggested by activity correlation profiling mass spectrometry*. Biochemistry.

Villani, M., Subathra, M., Im, Y.-B., Choi, Y., Signorelli, P., Del Poeta, M. and Luberto, C. (2008). Sphingomyelin synthases regulate production of diacylglycerol at the Golgi. *Biochemical Journal* **414**, 31–41.

Vollenweider, F., Kappeler, F., Itin, C. and Hauri, H.-P. (1998). Mistargeting of the Lectin ERGIC-53 to the Endoplasmic Reticulum of HeLa Cells Impairs the Secretion of a Lysosomal Enzyme. *Journal of Cell Biology* **142**, 377–389.

Wanschers, B., van de Vorstenbosch, R., Wijers, M., Wieringa, B., King, S. M. and Fransen, J. (2008). Rab6 family proteins interact with the dynein light chain protein DYNLRB1. *Cell Motil. Cytoskeleton* **65**, 183–196.

Waterman-Storer, C. M. and Salmon, E. D. (1998). Endoplasmic reticulum membrane tubules are distributed by microtubules in living cells using three distinct mechanisms. *Current Biology* **8**, 798–807.

Weigel, A. V., Chang, C.-L., Shtengel, G., Xu, C. S., Hoffman, D. P., Freeman, M., Iyer, N., Aaron, J., Khuon, S., Bogovic, J., et al. (2021). ER-to-Golgi protein delivery through an interwoven, tubular network extending from ER. *Cell* **184**, 2412-2429.e16.

Weisz, O. A. and Rodriguez-Boulan, E. (2009). Apical trafficking in epithelial cells: signals, clusters and motors. *J Cell Sci* **122**, 4253–4266.

Welch, L. G. and Munro, S. (2019). A tale of short tails, through thick and thin: investigating the sorting mechanisms of Golgi enzymes. *FEBS Lett* **593**, 2452–2465.

Welch, L. G., Peak-Chew, S.-Y., Begum, F., Stevens, T. J. and Munro, S. (2021). GOLPH3 and GOLPH3L are broad-spectrum COPI adaptors for sorting into intra-Golgi transport vesicles. *Journal of Cell Biology* **220**, e202106115.

Weller, S. G., Capitani, M., Cao, H., Micaroni, M., Luini, A., Sallese, M. and McNiven, M. A. (2010). Src kinase regulates the integrity and function of the Golgi apparatus via activation of dynamin 2. *Proc. Natl. Acad. Sci. U.S.A.* **107**, 5863–5868.

Wells, W. A. (2005). Ribosomes, or the particles of Palade. *Journal of Cell Biology* **168**, 12–12.

White, J., Johannes, L., Mallard, F., Girod, A., Grill, S., Reinsch, S., Keller, P., Tzschaschel, B., Echard, A., Goud, B., et al. (1999). Rab6 Coordinates a Novel Golgi to ER Retrograde Transport Pathway in Live Cells. *Journal of Cell Biology* **147**, 743–760.

Wilkinson, H. and Saldova, R. (2020). Current Methods for the Characterization of *O* -Glycans. *J. Proteome Res.* **19**, 3890–3905.

Willett, R., Ungar, D. and Lupashin, V. (2013). The Golgi puppet master: COG complex at center stage of membrane trafficking interactions. *Histochem Cell Biol* **140**, 271–283.

Willett, R., Pokrovskaya, I., Kudlyk, T. and Lupashin, V. (2014). Multipronged interaction of the COG complex with intracellular membranes. *Cellular Logistics* **4**, e27888.

Willett, R., Blackburn, J. B., Climer, L., Pokrovskaya, I., Kudlyk, T., Wang, W. and Lupashin, V. (2016). COG lobe B sub-complex engages v-SNARE GS15 and functions via regulated interaction with lobe A sub-complex. *Sci Rep* **6**, 29139.

Wilson, D. W., Lewis, M. J. and Pelham, H. R. (1993). pH-dependent binding of KDEL to its receptor in vitro. *J Biol Chem* **268**, 7465–7468.

Witkos, T. M. and Lowe, M. (2017). Recognition and tethering of transport vesicles at the Golgi apparatus. *Current Opinion in Cell Biology* **47**, 16–23.

Wong, M. and Munro, S. (2014). The specificity of vesicle traffic to the Golgi is encoded in the golgin coiled-coil proteins. *Science* **346**, 1256898–1256898.

Woźniak, M. J., Bola, B., Brownhill, K., Yang, Y.-C., Levakova, V. and Allan, V. J. (2009). Role of kinesin-1 and cytoplasmic dynein in endoplasmic reticulum movement in VERO cells. *Journal of Cell Science* **122**, 1979–1989.

Wu, X., Steet, R. A., Bohorov, O., Bakker, J., Newell, J., Krieger, M., Spaapen, L., Kornfeld, S. and Freeze, H. H. (2004). Mutation of the COG complex subunit gene COG7 causes a lethal congenital disorder. *Nat Med* **10**, 518–523.

Wu, Z., Newstead, S. and Biggin, P. C. (2020). The KDEL trafficking receptor exploits pH to tune the strength of an unusual short hydrogen bond. *Sci Rep* **10**, 16903.

Yang, J.-S., Valente, C., Polishchuk, R. S., Turacchio, G., Layre, E., Branch Moody, D., Leslie, C. C., Gelb, M. H., Brown, W. J., Corda, D., et al. (2011). COPI acts in both vesicular and tubular transport. *Nat Cell Biol* **13**, 996–1003.

Yates, J. R., Gilchrist, A., Howell, K. E. and Bergeron, J. J. M. (2005). Proteomics of organelles and large cellular structures. *Nat Rev Mol Cell Biol* **6**, 702–714.

Yin, Y., Garcia, M. R., Novak, A. J., Saunders, A. M., Ank, R. S., Nam, A. S. and Fisher, L. W. (2018). Surf4 (Erv29p) binds amino-terminal tripeptide motifs of soluble cargo proteins with different affinities, enabling prioritization of their exit from the endoplasmic reticulum. *PLoS Biol* **16**, e2005140.

Youakim, A., Dubois, D. H. and Shur, B. D. (1994). Localization of the long form of beta-1,4-galactosyltransferase to the plasma membrane and Golgi complex of 3T3 and F9 cells by immunofluorescence confocal microscopy. *Proc Natl Acad Sci U S A* **91**, 10913–10917.

Young, J., Stauber, T., del Nery, E., Vernos, I., Pepperkok, R. and Nilsson, T. (2005). Regulation of microtubule-dependent recycling at the trans-Golgi network by Rab6A and Rab6A'. *Mol Biol Cell* **16**, 162–177.

Zerangue, N., Schwappach, B., Jan, Y. N. and Jan, L. Y. (1999). A New ER Trafficking Signal Regulates the Subunit Stoichiometry of Plasma Membrane KATP Channels. *Neuron* **22**, 537–548.

Zhang, L., Luo, S. and Zhang, B. (2016a). Glycan analysis of therapeutic glycoproteins. *mAbs* **8**, 205–215.

Zhang, L., Luo, S. and Zhang, B. (2016b). The use of lectin microarray for assessing glycosylation of therapeutic proteins. *mAbs* **8**, 524–535.

Zhao, L., Liu, P., Boncompain, G., Loos, F., Lachkar, S., Bezu, L., Chen, G., Zhou, H., Perez, F., Kepp, O., et al. (2018). Identification of pharmacological inhibitors of conventional protein secretion. *Sci Rep* **8**, 14966.

Zhen, Y. and Stenmark, H. (2015). Cellular functions of Rab GTPases at a glance. *Journal of Cell Science* jcs.166074.

Zheng, P., Obara, C. J., Szczesna, E., Nixon-Abell, J., Mahalingan, K. K., Roll-Mecak, A., Lippincott-Schwartz, J. and Blackstone, C. (2022). ER proteins decipher the tubulin code to regulate organelle distribution. *Nature* **601**, 132–138.

Zielinska, D. F., Gnad, F., Wiśniewski, J. R. and Mann, M. (2010). Precision mapping of an in vivo N-glycoproteome reveals rigid topological and sequence constraints. *Cell* **141**, 897–907.

Zolov, S. N. and Lupashin, V. V. (2005). Cog3p depletion blocks vesicle-mediated Golgi retrograde trafficking in HeLa cells. *Journal of Cell Biology* **168**, 747–759.

RÉSUMÉ

Les cellules de mammifères sont caractérisées par la coexistence de plusieurs voies de transport, dont le transport antérograde et rétrograde. L'appareil de Golgi joue un rôle central dans le traitement et le tri des protéines dans le trafic bidirectionnel. Le système Retention Using Selective Hooks (RUSH) permet de synchroniser le transport des protéines depuis le RE et d'analyser systématiquement les voies sécrétoires. Grâce à l'interaction entre la streptavidine (Str) et un peptide de liaison à la streptavidine (SBP), la protéine rapporteur peut être retenue dans le RE et ensuite libérée par l'ajout de biotine. Cependant, la biotine a une grande affinité pour la streptavidine, ce qui nuit à la réversibilité du test RUSH. Grâce aux ligands artificiels de la streptavidine (ALiS), le transport rétrograde du Golgi vers le RE peut être analysé à l'aide de l'outil RUSH après lab-vage de ALiS. Le test RUSH réversible a d'abord été mis en place pour étudier deux mécanismes de transport rétrograde depuis Golgi vers le RE, notamment la voie médiée par le motif KDEL et la voie de recyclage des enzymes de glycosylation. Str-KDEL ou Ii-Str ont été utilisées comme protéines d'ancrage et les enzymes golgiennes ManII* (Mannosidase II)-SBP-EGFP ou ST* (Sialyltransférase)-SBP-GFP ont été utilisées comme rapporteurs RUSH. Notre analyse cinétique a montré que le transport de l'appareil de Golgi vers le RE de ManII* et de ST* est plus lent par la voie de recyclage des enzymes de glycosylation que par la voie induite par le motif KDEL. Pour caractériser le rôle des facteurs de régulation dans le transport rétrograde médié par le motif KDEL, nous avons réalisé des expériences d'ARNi ciblant COG3 et Rab6. Nos données montrent que la déplétion de COG3 entraîne un retard dans le transport rétrograde de ManII* et ST* et que la déplétion de Rab6 entraîne une altération du trafic de ST*, ce qui est cohérent avec les études précédentes. Nos données confirment l'existence et la différence de cinétique du transport rétrograde Golgi-RE dépendant du motif KDEL et le recyclage des enzymes golgiennes de glycosylation.

Enfin, nous avons synchronisé le transport des enzymes golgiennes de glycosylation endogènes en utilisant des approches de knock-in CRISPR-Cas9 ou CRISPaint et l'outil RUSH. La distribution subcellulaire de ManII^{EN}-SBP-mNeonGreen, GalNAc-T1^{EN}-SBP-mNeonGreen et B4GalT1^{EN}-SBP-EGFP a été détectée dans le Golgi, et nous avons pu synchroniser leur transport bidirectionnel grâce à l'expression de Str-KDEL.

MOTS CLÉS

Transport intracellulaire des protéines; L'appareil de Golgi; CRISPR-Cas9

ABSTRACT

Mammalian cells are characterized by the co-existence of multiple membrane trafficking pathways and connecting the different membrane organelles. The Golgi apparatus has a central role in processing and sorting cargos in the bi-directional trafficking. The Retention Using Selective Hooks (RUSH) system allows to synchronize the transport of cargos from the ER to the Golgi apparatus and other downstream compartments and to systematically analyze the secretory routes. Owing to the interaction of streptavidin (Str) and streptavidin-binding peptide (SBP), the reporter protein can be retained in the ER and then released by the addition of biotin. However, biotin has a high affinity to streptavidin, impairing reversibility of the RUSH assay. With the Artificial Ligands of Streptavidin (ALiS), Golgi-to-ER retrograde transport can be monitored using RUSH upon their washout. The reversible RUSH assay was firstly set up to study two mechanisms of Golgi-to-ER retrograde transport, including the KDEL-mediated retrieval pathway and the glycosylation enzyme recycling pathway. Core streptavidin fused with the ER-retention signal (Str-KDEL), or with the invariant chain (Ii-Str) were used as hooks. Golgi-resident enzymes, ManII* (Mannosidase II)-SBP-EGFP or ST* (Sialyltransferase)-SBP-GFP served as Golgi-targeted RUSH reporters. Our kinetic analysis showed that the Golgi-to-ER transport of ManII* and ST* are both slower through the glycosylation enzyme recycling pathway than the KDEL-meditated retrieval pathway. To characterize the role of putative regulatory factors in KDEL-mediated retrograde transport, we performed RNAi experiments targeting to COG3 and Rab6. Our data showed that knockdown of COG3 resulted in delayed retrograde transport of ManII* and ST*, and the depletion of Rab6 led to impaired trafficking of ST*, consistent with the previous studies. Our data indicated that there are two distinct pathways regulating the retrograde transport of Golgi cargos, including KDEL-mediated ER retrieval and ER recycling of Golgi glycosylation enzymes.

Lastly, we have generated endogenous tagged Golgi glycosylation enzymes using CRISPR-Cas9 or CRISPaint knock-in approaches and applied the reversible RUSH assays in the selected clones. The subcellular distribution of endogenous ManII^{EN}-SBP-mNeonGreen, GalNAc-T1^{EN}-SBP-mNeonGreen and B4GalT1^{EN}-SBP-EGFP were detected in Golgi, and we were able to synchronize the bidirectional transport through the expression of Str-KDEL.

KEYWORDS

Intracellular protein transport; Golgi apparatus; CRISPR-Cas9